THE DETERMINATION OF RAINFALL VOLUMES USING A CONVENTIONAL S-BAND WEATHER RADAR

Sean O'Beirne

A Dissertation Submitted to the Faculty of Science,
University of the Witwatersrand, Johannesburg,
for the Degree of Master of Science

Johannesburg, 1992

ABSTRACT

Two aspects of radar-based measurement of convective rainfall over the Transvaal Highveld are examined. Drop size distributions (DSDs) are studied in order to quantify the effects of drop size distribution variability on the Z-R relationship, and the area-time integral (ATI) method is investigated as a possible means of radar rainfall measurement. Drop sorting effects are clearly evident in convective rain with resultant DSDs having higher numbers of large drops and causing Z-R derived rain rates to be overestimated. In the absence of updraughts DSDs appear to represent equilibrium between drop growth and drop disintegration effects. These patterns are generally evident in stratiform rain and lead to the Z-R relationship underestimating the rain rate. N_0 'jumps' are evident in the DSD data and appear to be related to the transition between convective and stratiform rain. Patterns described in DSDs elsewhere in the world are evident in DSDs measured in convective rain on the Transvaal Highveld. These patterns include the tendency for the DSD slope, Λ to become constant as rain rates approach 100 mm.h^{-1} in the $\Lambda - R$ relationship and to become constant as liquid water content exceeds 1,2 g.m^{-3} in the $\Lambda - W$ relationship. A quadratic Z-R relationship of $Z = 2{,}35 + 1{,}36(\log R) + 0{,}09(\log R)^2$ appears to generate the best estimates of average rain rate when used to derive the V-ATI relationship. As V-ATI derived rain rates continued to overestimate rain rates measured at the ground using rain gauges a gauge-derived rain rate probability weighting scheme has been used to optimise the V-ATI relationship. The ATI method appears to be a useful way of measuring seasonal volumetric rainfall totals but operational application in measuring daily rainfall amounts could not be properly assessed due to inadequate ground-based rain rate data.

I declare that this dissertation is my own unaided work.
It has not been submitted before for any other degree
or examination at any other University.

University of the Witwatersrand, 1992

PREFACE

The accurate measurement of rainfall in space and time has remained a problematic issue in spite of advances in rainfall measurement technologies. Of these technologies, weather radar remains the only source of adequate information on the areal coverage of rainfall, thereby enabling volumetric rainfall totals to be calculated. Weather radars have been used over the last few decades as a rainfall measurement tool and considerable scientific effort has been expended in accurately defining the relationship between the return signal received by the radar and rain rate over the area of the radar coverage. The so-called *Z-R* relationship has been identified as the most practical method of radar rainfall measurement (Wilson and Brandes, 1989). Several factors introduce inaccuracies in the standard *Z-R* approach, of which one is variability in the drop-size distribution. The variability in drop size distributions is in turn brought about by a variety of kinematic and microphysical processes occurring in the storm.

Drop size variability generates only one of several sources of error, however, and over the last few years the emphasis has shifted towards establishing ways of nullifying other sources of measurement error such as partial beam filling and advection of precipitation (Zawadski, 1984; Joss and Waldvogel, 1989; Rosenfeld, 1991). A radar rainfall measurement technique developed in response to these problems is the area-time integral (ATI). The ATI technique is based on the relationship between storm area and duration, and the rain volume produced by that storm. The technique has recently received considerable attention and forms the basis of the radar rainfall approach that will be used with a spaceborne radar in the Tropical Rain Measuring Mission (TRMM) (Rosenfeld, *et al.*, 1990). In developing the radar rainfall approach to be used in TRMM a problem was identified in that rain volume versus area-time integral (V-ATI) relationships are likely to vary considerably from one convective regime to the next. The derivation of a V-ATI relationship for the Transvaal Highveld, therefore, may contribute to TRMM. More important is the fact that the ability to measure rainfall volumes accurately using radar will contribute significantly to the fields of hydrology, agronomy, meteorology and climatology.

In this dissertation two important aspects of radar rainfall measurement are investigated for convective rain storms occurring over the Transvaal Highveld.

Specific aims are :

(i) to study the effect of drop-size distributions on the average *Z-R* relationship, identifying in the process a suitable *Z-R* relationship for radar rainfall measurement of Transvaal storms; and

(ii) to derive a suitable V-ATI relationship for the Transvaal Highveld.

The intention is to identify whether the ATI technique can be used to supplant the conventional *Z-R* technique in terms of both accuracy and operational applicability. Literature pertinent to radar rainfall measurement, drop size distribution studies and the ATI technique is reviewed in **Chapter 1. Chapter 2** describes the data sources and the methods of analysis utilised in the study. The drop size distribution study and derivation of the average *Z-R* relationship is contained in **Chapter 3.** The ATI technique is examined in **Chapter 4** and an optimised V-ATI relationship derived for the Transvaal Highveld in **Chapter 5.** Results of the study of drop-size distributions contained in Chapter 3 were presented at the 6th Annual Conference of the South African Society for Atmospheric Scientists held at the Geological Survey in October 1991.

The idea of undertaking an ATI study was generated by Ana Maria Gomes, Ematek, CSIR. Supervision of the study was provided by Dr Janette Lindesay of the University of the Witwatersrand and Dr Gerhard Held, Ematek, CSIR Valuable comments were added by Ronald C. Grosh, Ematek, CSIR and statistics help proffered by Chris Gilfillan, Datatek, CSIR. Eleonore Jacobs, Datatek, CSIR, developed the area integration software. All are thanked for their inputs. The bulk of this work was conducted under contract to the Water Research Commission in the Precipitation and Airflow project (PRAI).

CONTENTS

SECTION I

BACKGROUND

CHAPTER 1

INTRODUCTION AND LITERATURE REVIEW

Introduction

Despite the importance of precipitation data in the fields of hydrology, agronomy, meteorology and climatology, accurate measurement of rainfall in space and time has remained an elusive problem. Operational forecasting of river flows and flash flood potential requires accurate descriptions of rain fields in real time (Austin, 1981). Similarly, a high degree of accuracy is crucial to weather modification exercises in discriminating between effective and ineffective seeding operations (Woodley *et al.*, 1975; Heimbach and Super, 1980). Data obtained from rain gauge networks seldom reflects adequately the characteristics of the rain field and logistics often prohibit real-time data assimilation (Neff, 1977). In an area such as the Transvaal Highveld where convective rain storms produce precipitation highly variable in space and time the problem of areal and temporal resolution is acutely felt and compounded by an inadequate rain gauge network.

From its earliest application as a meteorological tool in the 1940s, weather radar has been seen as a possible solution to the problem of rainfall measurement (Wys *et al.*, 1989). Not only can a single radar be used to scan a large area in real time but, in mapping the areal extent of the rainfall field, the radar echo pattern becomes the equivalent of an infinitely dense rain gauge network. Radar rainfall measurement is based upon the relationship between radar echo and rain rate. Attenuation of the return signal can be measured and statistically related to rain rate (Wexler and Atlas, 1963; Atlas, 1964) or a polarised radar can be used in which rain rate is measured as a function of the ratios of the return signals on vertically (Z_v) and horizontally (Z_h) polarised pulses (Seliga and Bringi, 1976; Seliga *et al.*, 1981; Goddard *et al.*, 1982). Most radar rainfall measurement techniques, however, use the so-called *Z-R* relationship which simply relates radar reflectivity factor (Z) to rain rate (R). It is the *Z-R* approach that is considered most practical for operational measurement of rainfall (Wilson and Brandes, 1979).

The Z-R relationship can only be determined empirically, however, and this has lead to a wide variety of relationships being documented from all over the world. Z-R relationships have been seen to differ widely for different geographic locations, from storm to storm in the same location and indeed for different stages in the lifecycles of individual storms. Z-R variability is directly related to changing drop size distributions and these changing drop-size distributions are in turn a function of various microphysical and kinematic processes within the storm. A study of drop-size distributions over the Transvaal Highveld with specific reference to Z-R relationships thus forms the first part of this dissertation.

The second part of the dissertation is aimed at investigating the area-time integral (ATI) of radar rainfall measurement. In broad terms the technique is based on establishing a relationship between storm area and duration and rainfall volume. Although first proposed over a decade ago the ATI technique has only recently begun to receive concentrated research attention (Atlas, *et al.*, 1990; Rosenfeld, *et al.*, 1990; Geotis, 1991). The ATI technique has several advantages over conventional methods of radar rainfall measurement. The first of these is that remotely-sited or spaceborne radars, which cannot be regularly calibrated, can provide accurate rainfall volume estimates because only the area of the storm need be measured. Secondly, storm area can be measured by satellite and thus related to rainfall volumes using a rain volume versus ATI relationship (Doneaud *et al.*, 1987; Atlas and Bell, 1991). Thirdly, problems of partial beam filling, cited as an even greater potential source of error than Z-R variability (Joss and Waldvogel, 1989), can be overcome to some extent using the ATI technique. Finally the technique is of academic interest in identifying factors that may cause changes in the relationship between storm area and rain flux, an aspect particularly pertinent to weather modification experiments.

In this chapter radar rainfall measurement theory, including derivation of radar reflectivity factor (Z) and rainfall rate (R), is discussed. Literature pertaining to Z-R relationships, drop size distribution studies and the area-time integral method of radar rainfall measurement is reviewed. The chapter is concluded by detailing the hypotheses that will be tested in the course of the dissertation.

Radar Reflectivity Factor

Radar reflectivity factor (Z) is a term used to describe the strength of the return signal received by the radar. Derivation of Z is based on an approximate form of the radar equation and is thus fairly lengthy. For this reason only the important components of the derivation are highlighted here.

The strength of the returned signal received by the radar is a function of characteristics of both the radar and the target. Characteristics of the radar that influence the return signal are the strength of the transmitted signal, P_t, which may be several orders of magnitude greater than the return signal, the wavelength, λ, the effective cross-section of the radar antenna, A_e, and a factor referred to as 'antenna gain', G. Antenna gain refers to the magnification of the signal brought about by the fact that the antenna concentrates both the transmitted and returned signals into a narrow beam.

The pulse transmitted by the radar imparts energy to the target, some of which is lost as heat and the rest of which is reradiated as a scattered electro-magnetic field. If this power were to be reradiated isotropically, the power of the return signal received by the radar would be given by

$$P_r = \frac{P_t G A_t A_e}{(4\pi)^2 r^4} \tag{1.1}$$

where A_t is the cross-sectional area of the target at range, r.

Were the radar beam to be directed at a single object and were that object to scatter the incident pulse isotropically the effect of the size of the target could be incorporated into the equation as a single term in the form of the cross section of the target. The radar beam of a weather radar illuminates many hundreds of targets simultaneously, however, and these targets seldom scatter isotropically. For this reason a function known as the back scattering cross section is introduced. The back-scattering cross-section (σ) is defined as "the area which, when multiplied by the incident energy, gives the total power radiated by an isotropic source which radiates the same power in the backward direction as the scatterer" (Battan, 1973, p.30). In other words σ is the area that would isotropically scatter the same signal as the signal actually received.

As the signal received by the radar is a signal scattered by a multitude of scatterers the return signal is described as the sum of the return signals received from individual scatterers, with each scatterer contributing proportionally to the back scattering cross section (Joss and Waldvogel, 1988). Due to the continual movement of the scatterers signal phases differ from one reflected pulse to the next. Received power is thus given by averaging over a large number of independent arrays of scatterers, *viz.*

$$\overline{P_r} = \frac{P_t G^2 \lambda^2}{(4\pi)^3 r^4} \sum_{i=0}^{n} \sigma_i \tag{1.2}$$

The effect of the target in scattering the pulse transmitted by the radar is incorporated by introducing the Rayleigh approximation (considered most appropriate for a wavelength of 10 cm) of the scattering of a plane wave, *viz.*

$$\sigma_i = \frac{\pi^5}{\lambda^4} |K|^2 D_i^6 \tag{1.3}$$

where D_i is the diameter of the sphere and $|K|^2$ is a function of the dielectric property of the sphere.

The fully derived radar equation, including the effect of the Rayleigh approximation of the back-scattering cross-section is then

$$\overline{P_r} = \left(\frac{\pi^3 P_t G^2 \theta \phi h}{16x64\lambda^2 \ln 2} \right) \frac{|K|^2}{r^2} \sum_{Vol} D_i^6 \tag{1.4}$$

Equation (1.4) can be rewritten

$$\overline{P_r} = \frac{C |K|^2 Z}{r^2} \tag{1.5}$$

As all the terms within the parentheses of equation (1.4) are fixed characteristics of the radar or are numerical constants they can be summarised by C. Z is referred to as radar reflectivity and is given by the quantity $\sum_{Vol} D_i^6$. If the radar is being used to measure rainfall, then the scatterers would be raindrops which can be described by a drop-size distribution. The drop-size distribution in turn is described in terms of the number of drops (N_D) per size interval (D_i). Thus radar reflectivity factor is given by

$$Z = \int_0^\infty N_D D^6 dD \tag{1.6}$$

and is expressed in units of mm^6 .m^{-3} (Battan, 1973).

Rain rate (R) can be calculated from a given drop size distribution in a similar way using the following equation

$$R = \frac{\pi}{6} \int_0^\infty N_D D^3 Vt_D dD \tag{1.7}$$

where Vt_D is the terminal velocity of the drop by diameter (Doviak and Zrnic, 1984).

Z-R Relationships

Relationships between Z and R can only be determined empirically. Either Z and R can be calculated from the same set of drop-size distributions using equations 1.6 and 1.7, or Z can be measured aloft using radar and compared to R measured at the ground using a rain gauge. This latter approach is not strictly a Z-R relationship because it may include errors in the radar calibration and evaporation of rain between the height of the radar beam and the ground. Z is thus labelled equivalent radar reflectivity factor, Z_e (Joss and Waldvogel, 1988). Z-R relationships are expressed in a general relationship of the form

$$Z = aR^b \tag{1.8}$$

Many Z-R relationships have been documented from around the world. Values of the coefficients a and b differ widely for different geographic locations, in different rain systems in the same location and even for different stages in the lifecycles of individual storms. Z-R variability is directly related to changes in drop size distribution and is thus to a large degree dependant on the various microphysical and kinematic processes that shape drop size distributions. Understanding the influence of these processes on the drop size distribution and resultant changes in the Z-R relationship is thus essential in effecting accurate radar rainfall measurement (Hodson, 1986).

Much of the work described in the literature on Z-R relationships has involved descriptions of drop size distributions. The two are addressed in this chapter as separate topics but it should be appreciated that Z-R relationships and drop size distributions are closely related. Although the discussion that follows focuses on drop size distributions specifically, reference is made on several occasions to associated Z-R relationships.

Drop Size Distributions (DSDs)

Although drop-size distributions were first measured in the late nineteenth century (Wiesner, 1895), Marshall and Palmer (1948) (hereafter referred to as M-P) have received widest acclaim for seminal work in the field. Using dyed filter paper to measure DSDs, they proposed a general relation of the form

$$N_D = N_0 e^{-\Lambda D} \tag{1.9}$$

where D is the raindrop diameter, N_D is the number of drops of diameter between D and $D + dD$, N_0 is the value of N_D for $D =$ [illegible] and Λ is an empirically determined coefficient of rain intensity (Fig. 1.1). In addition they found that N_0 was a constant equal to 0,08 cm^{-4} and that

$$\Lambda = 4{,}1R^{-0{,}21} \tag{1.10}$$

where R is rainfall rate in $mm.hr^{-1}$ and Λ in mm^{-1}. They also proposed a Z-R relationship of the form $Z = 200R^{1.6}$.

Within a relatively short space of time it was realised that while the M-P distribution was suitably representative of DSDs in warm frontal rain, coalescence showers had DSDs that were entirely different (Mason and Andrews, 1960). It was similarly apparent that DSDs measured at the ground did not necessarily reflect those at cloud base. The importance of DSDs aloft, besides being in the area likely to be measured by radar, had the potential to offer valuable clues as to factors influencing the evolution of raindrop spectra. A initial exponential DSD with a large negative slope for example, would be

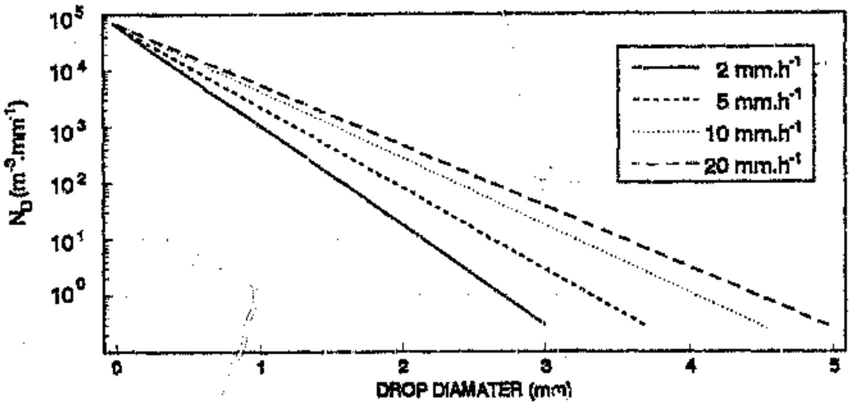

Figure 1.1: Drop-size distributions for different rain rates computed from the Marshall-Palmer (1948) relationship of $N_D = N_0 e^{-\Lambda D}$.

substantially modified by the effects of coalescence, accretion and evaporation, whereas only small changes would be evident in an initial DSD of relatively small negative slope. This implied that spectra observed at the ground must develop from a distribution aloft having fewer smaller drops and more larger drops than indicated by an M-P distribution (Hardy, 1963).

A theory that followed on from this argument was that an M-P distribution would change only slowly during fall and that narrow distributions would rapidly tend towards an exponential distribution (Srivastava, 1967). This appeared to suggest that the exponential shape of a DSD is due to the coalescence process. The effects of drop break-up were included in subsequent work in which equilibrium distributions were shown to be the result of a balance between drop growth and drop disintegration processes. Equilibrium distributions would be realised more rapidly in situations of higher liquid water content, but it was unlikely that they would be realised in natural conditions of liquid water content and fall distance (Srivastava, 1971). Furthermore, observed distributions were limited to smaller sizes and were distinctly steeper than computed distributions. This implied that other processes besides break-up and coalescence were responsible for shaping DSDs such as collisional break-up effects and condensation.

Drop-size distributions measured at heights just below the 0°C level with a vertically-pointing Doppler radar were found to be well approximated by an

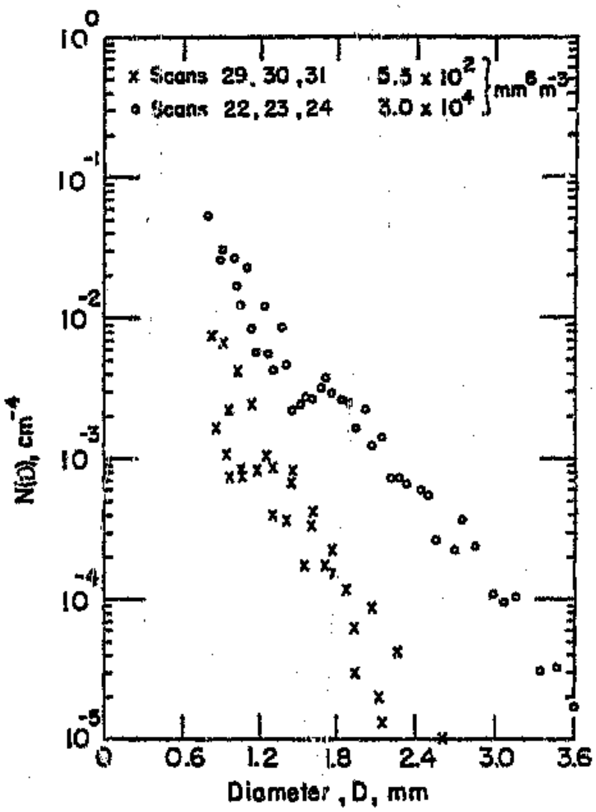

Figure 1.2: Typical drop-size distributions which have been computed from six Doppler spectra. Circles indicate Doppler spectra with radar reflectivity values of 2,7, 3,0 and 3,2 mm^6 m^{-3} while crosses indicate Doppler spectra with radar reflectivity factors of 5,0, 5,8 and 8,8 mm^6 .m^{-3} (after Sekhon and Srivastava, 1971).

exponential distribution but with steeper curves than M-P (Sekhon and Srivastava, 1971) (Fig. 1.2). Also N_0 was not constant as suggested by Marshall and Palmer (1948) but in fact increased with increasing rain rate. Ground-based disdrometer measurements confirmed this finding when 'jumps' in the temporal N_0 pattern were identified. These 'jumps' were subsequently ascribed to changes in rainfall regime from continuous to convective rain or *vice versa* (Joss and Waldvogel, 1974).

The condensation and break-up computations were improved and the activation of cloud condensation nuclei (CCN) included in two models aimed at improving understanding of processes affecting DSDs (Young, 1975). Two different models, namely 'collisional break-up' and 'spontaneous disintegration', were developed. The spontaneous disintegration model generated an even flatter curve than that produced by Srivastava (1971) indicating that spontaneous break-up is unlikely to be the sole agent in shaping DSDs. The collisional break-up model, on the other hand, produced a 'steady state' spectrum, exponential in form and in fair agreement with M-P (Fig. 1.3). DSD evolution in still air was modelled assuming warm rain processes (List and Gillespie, 1976). Using only collisional break-up data the model produced spectra which had virtually no drops larger than 2,5 mm in diameter but with high concentrations of smaller drops. The existence of large drops appeared solely attributable to ice-phase precipitation mechanisms. Collisional break-up dominated over spontaneous break-up when the initial number concentrations (N_0) of small drops is within the commonly observed range. When N_0 was some two orders of magnitude lower, spontaneous break-up played a significant role in shaping the observed DSDs (Srivastava, 1978).

Data from airborne optical spectrometer measurements together with 3 and 10 cm radar measurements showed that the temporal evolution of DSDs at cloud base is dominated by updraught sorting (sedimentation) effects where smaller drops have insufficient terminal velocity to fall through cloud base (Carbone and Nelson, 1978). Sedimentation leads to higher numbers of large drops and fewer small drops during the cloud-growth stage (Fig. 1.4). During this stage drop numbers are typically one order of magnitude lower than M-P at the 1 mm diameter size. During dissipation, drop spectra assume M-P characteristics but rarely achieve comparably high concentrations of small drops or comparably low concentrations of large drops. Also, spontaneous break-up processes may be important for rainfall rates in excess of 30 $mm.h^{-1}$ when liquid water content values are greater than 1 $g.m^{-3}$. Conventional Z-R estimation techniques, it was argued, were precluded by high drop size variability unless allowance was made for spatial and temporal change. On storm days when large quantities of precipitation were produced, early radar echoes resulted from both liquid and ice-phase processes. The concept of an ensemble of drops evolving to a unique equilibrium appeared unlikely in the presence of strong vertical air motions (Carbone and Nelson, 1978).

The M-P Z-R relationship was also shown to be inappropriate in measuring rain rates exceeding 25 $mm.h^{-1}$ (Hodson, 1986). Data obtained from a vertically-pointing Doppler radar (Pasqualucci, 1982a, 1982b) was used to show that at rain rates exceeding 25 $mm.h^{-1}$ the slope of the DSD, Λ, will tend towards

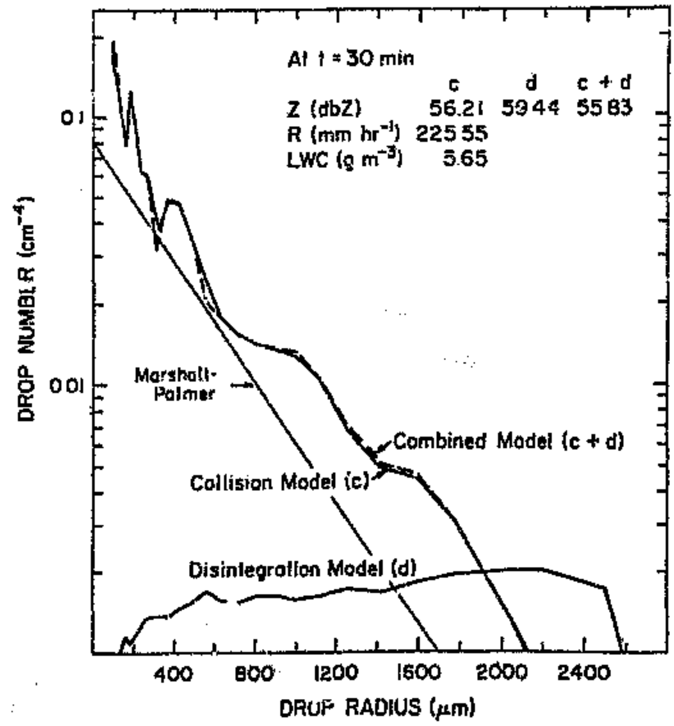

Figure 1.3: Drop spectra at 30 minutes resulting from collision and disintegration models separately and combined. Initial conditions assume a cloud base temperature of 15°C, an updraught of 3 m.s^{-1} and a maritime CCN spectrum (after Young, 1975).

a constant value between 2,1 and 2,3 mm^{-1}. A *Z-R* relationship computed from these values gives $Z = 939R$ and indicates that attenuation is also proportional to rain rate when the vertical wind velocity is nil. When rain rate is greater than 25 mm.h^{-1} the M-P distribution applies for drops greater than 3,0 to 3,5 mm in diameter, but larger drops have decreasing values of Λ arising from drop break-up. Drop break-up data indicate that a large number of drops in the 3,0 to 3,5 mm size range are generated by drop break-up effects (Low and List, 1982).

The idea of equilibrium drop-size distributions, in which drop growth effects were balanced out by drop disintegration effects, received considerable attention in the 1980s. It was argued that natural levels of liquid water content would not allow realisation of equilibrium in the time or fall distance normally available. Model results supported this claim showing modelled equilibrium DSDs to be trimodal with peaks at drop diameters of 0,268, 0,790 and 1,760 mm (List *et al.*, 1987). Equilibrium distributions were shown to take time to evolve especially at

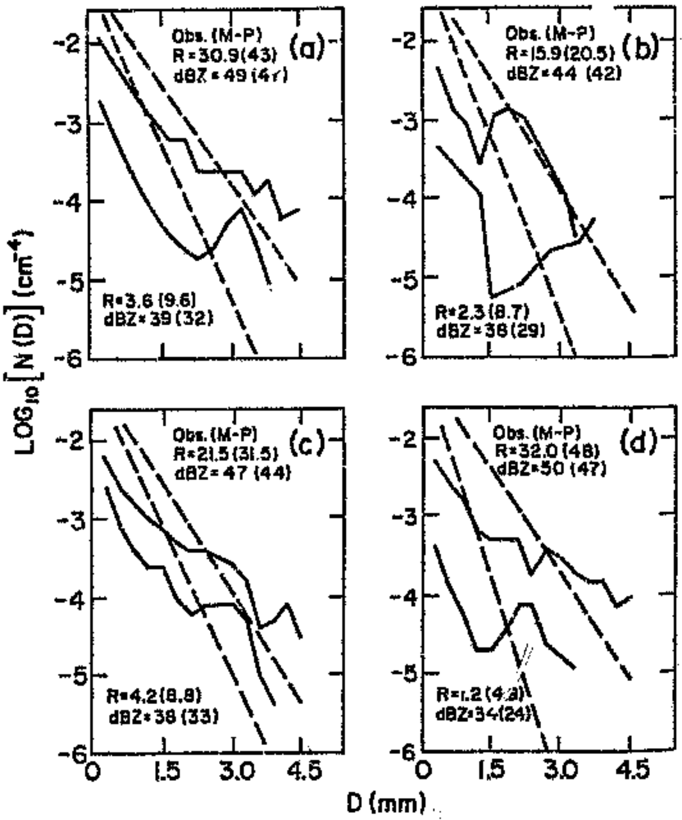

Figure 1.4: Drop spectra for high and low rainfall rate regions of storms. Note the large deficit of small drops and excess of large drops compared to Marshall-Palmer (dashed) which have been plotted for equivalent rain rates (after Carbone and Nelson, 1978).

rain rates of less than 10 mm.h⁻¹. In natural steady rain spectra deviations from equilibria are indicative of a number of features, including changes in rain processes with height and whether rain originated from warm or cold cloud processes (List *et al.*, 1987).

A time-dependent rain shaft model assuming an M-P distribution with a rain rate of 50 mm.h⁻¹ showed that the largest drops would reach the ground first with the onset of rain (List *et al.*, 1988). As more drops appear the drop spectrum widens rapidly as a result of collisional drop break-up. At high rain rates equilibrium is reached after some 3 km of fall. Results of the model runs showed that small drops measured at the ground do not originate at cloud base but occur rather as a result of collisional break-up effects amongst the larger drops during their fall. Although this specific work was based on assumptions pertaining to warm rain processes it was argued that the results may also represent cold cloud processes where warm rain develops parallel to the ice particles (List *et al.*, 1987). Any DSD will develop with time into an equilibrium DSD regardless of the initial spectrum. All equilibrium distributions have the same shape with observed differences being related to a factor proportional to rain rate (List, 1988).

The Area-Time Integral

The measurement of rainfall using radar was pioneered by Byers (1948) who summed rainfall totals from rain gauges in the area covered by radar echo. Several subsequent studies refined radar rainfall measurement by relating radar reflectivity Z to rain rate R (Twomey, 1953). The development and introduction of radar signal processing techniques in the late 1960s and early 1970s further contributed to enhancing the accuracy of radar rainfall measurement. Analog and digital integrators reduced radar measurement error by approximately 1.5 dB (Stout and Mueller, 1968). Nevertheless radar rainfall measurement techniques were not accurate enough to become entirely independent of a rain gauge network and good results began to be achieved by combining the two measurement sources. Data from the rain gauges were used to calibrate the radar, reducing error by about 40 per cent in an area of a thousand square miles (Wilson, 1970). Most subsequent radar rainfall measurement exercises have utilised a combined radar rain gauge measurement approach (Harrold *et al.*, 1974; Hill *et al.*, 1981; Xue *et al.*, 1989).

Alternative methods have been attempted in an effort to effect more accurate radar measurement of rainfall. Two of these approaches have yielded results comparable to and in some instances better than the standard Z-R approach. The first of these is monitoring attenuation of the radar signal by rain. As signal attenuation is proportional to rain rate the use of two signals of different wavelengths, one of which is attenuated, allows appraisal of the radar rainfall measurement accuracy and its modification as appropriate (Kozu and Nakamura, 1991). Signals with wavelengths short enough to be attenuated, however, may sometimes be absorbed entirely by intense precipitation (Austin, 1981). The second approach is in using differential reflectivities from orthogonally polarised radar signals (Seliga and Bringi, 1976; Seliga *et al.*, 1981). As falling drops have an oblate spheroidal shape the return signal on a vertically polarised pulse will be different to that received from a horizontally polarised pulse (Goddard *et al.*, 1982). The ratios of the reflectivities Z_h and Z_v is a direct measure of rainfall rate (Doviak and Zrnic, 1984). In spite of the development of alternative methods the standard *Z-R* approach remains the most practical for operational measurement of rainfall (Wilson and Brandes, 1979).

The equivocal nature of *Z-R* relationships has already been highlighted, but while it is important, DSD variability is only one of several sources of error in radar rainfall measurement. Variations in the DSD and resultant *Z-R* errors are even less severe when considering rain over a large area or of extended duration (Doviak and Zrnic, 1984). Other sources of error may occur at random, such as advection of precipitation or errors in radar calibration, or systematically such as attenuation effects (Zawadski, 1984). A far more serious problem than DSD variations is range-related measurement errors such as horizontal and vertical reflectivity gradients (Joss and Waldvogel, 1989) and partial beam filling. As a result it is virtually impossible *deterministically* to relate actual measured radar reflectivity (Z_e) to rain rate (R) (Rosenfeld, 1991).

The area-time integral (ATI) method of radar rainfall measurement is based on the observed relationship between storm area and duration and the rain volume produced by that storm. In fact rain volume is dependant on storm area to a greater degree than on rain rate because the distribution of rainfall rates from one convective storm to the next is quite similar (Lopez *et al.*, 1988), i.e. the probability density function (p.d.f.) of rainfall rates from one storm to the next is essentially constant (Atlas *et al.*, 1990a). Thus only storm area, which is easily measured using radar, need be known before an estimate can be made of the rainfall volume. In addition the ATI method can be used on radars that cannot be maintained and kept calibrated, such as remotely-sited or spaceborne radars (Geotis, 1991). The ATI method has also been favourably reviewed as a possible means of enhancing satellite-estimated rainfall (*inter alia* Doneaud *et al.*, 1987; Atlas and Bell, 1991). The height-area rain threshold (HART) technique, which is based to some extent on the ATI method, was specifically developed for use by spaceborne radar in TRMM (Tropical Rain Measuring Mission) (Rosenfeld *et al.*, 1990).

Pioneering work on the ATI method is attributed to Doneaud *et al.* (1981) who proposed the technique as a means of measuring rainfall by radar without using a Z-R relationship. Doneaud *et al.* made use of two data sets from the northern Great Plains cloud seeding experiments, one of which contained radar and rain gauge data while the other contained radar data only. An array was constructed with columns representing hours and rows representing 22 automatic rain gauge locations. Rain events were then described in terms of the array (Fig. 1.5). It can be seen from the figure that a rain event could be described by several gauges recording rain for one time period (A), or one gauge recording rain over different time periods (B), or seperate gauges recording rain at different times (C). The area and duration of rain events (referred to as the integrated rainfall coverage or IRC) were calculated accordingly. Rainfall volume was then determined from radar and standard rain gauge data. Logarithms of the rainfall volume and the IRC were found to be well correlated with a correlation coefficient of 0,89.

The second data set, consisting of radar data only, was evaluated in a slightly different way in that both the IRC and the rainfall volume were estimated from the radar data. The IRC in turn was estimated in one of two ways:

1. Using the maximum radar echo area in any one scan during one hour (Maximum Hourly Echo Area, MHEA)
2. Using the average radar echo area during the hour (Average Hourly Echo Area, AHEA).

MHEA gave a better correlation coefficient than AHEA when regressed against radar estimated rainfall volume prompting Doneaud *et al.* to conclude that MHEA was the better predictor of rainfall volume.

The concept of the area-time integral was introduced in subsequent work (Doneaud *et al.*, 1984a). Rain volume V over an area A during time t is given by

$$V = \int_t^{\infty} \int_A^{\infty} R \, da \, dt \tag{1.11}$$

Assuming rainfall rate R to be constant equation 1.11 could be rewritten as

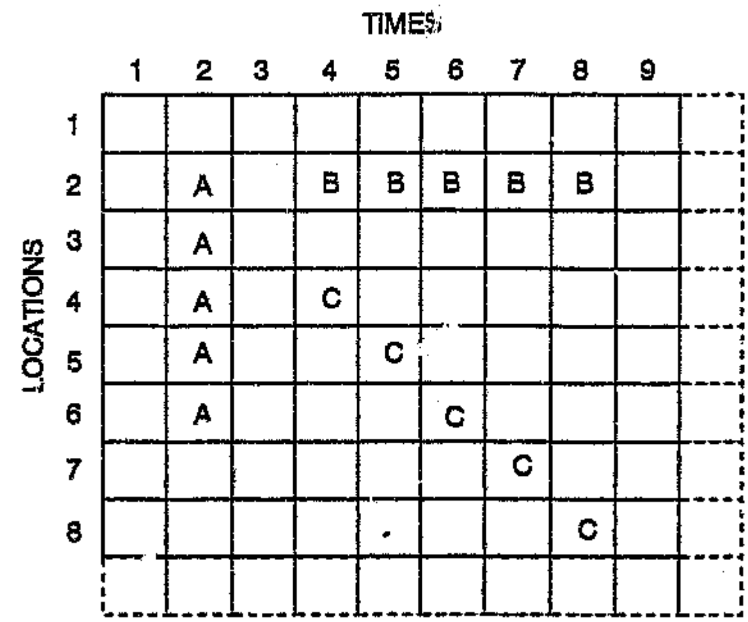

Figure 1.5: Schematic illustration of the array of possible rain locations and time intervals involved in determining the integrated rainfall coverage (IRC). The A's, B's and C's represent distinct rain occurrences that contribute equally to the IRC (After Doneaud *et al.*, 1981)

$$V = R\int_{t}^{\infty}\int_{A}^{\infty} da\, dt \tag{1.12}$$

It is the double integral that is referred to as ATI, a value which may be approximated by summation, i.e.

$$ATI = \int_{t}^{\infty}\int_{A}^{\infty} da\, dt \approx \sum_{i=1}^{\infty} A_i \Delta t_i \tag{1.13}$$

An important part of the calculation of the ATI is determining an appropriate reflectivity threshold. Echo below this threshold is then not included in the ATI. There are a number of factors that need to be considered in selecting an appropriate threshold value. A threshold value set too high would exclude echo area producing significant precipitation. On the other hand, a threshold set too low would include echo area unlikely to produce significant amounts of precipitation (Doneaud *et al.*, 1984a). This latter point is also important in reducing the need for an evaporation correction between the height of the radar beam and the ground (Doneaud *et al.*, 1981).

Radar estimated rain volume can be related to ATI in a power-law of the general form

$$V = K(ATI)^b \qquad (1.14)$$

where K and b are coefficients determined by the regression analysis (Doneaud *et al.*, 1984a). The ratio of the ATI in km^2.h to the rain volume in km^2.mm gives the average rain rate R in mm.h^{-1}, *viz.*

$$\overline{R} = \frac{V}{(ATI)} \qquad (1.15)$$

By substituting equation 1.14 into equation 1.15 the equation is defined as

$$\overline{R} = K(ATI)^{b-1} \qquad (1.16)$$

A slope value, $b - 1$, of less than one implies an improbable situation, that larger, sustained storms produce lower average rain rates, whereas a slope value exceeding 1 suggests rain rate increases with increasing ATI. A slope value of 1 indicates rain rate to be independent of the ATI. In investigating the evolution of rain rates in storms in the semiarid climate of North Dakota average rain rates were found to depend on the reflectivity threshold used in the V-ATI calculation and a threshold value of 25 dBZ was considered most suitable. This threshold value gave average rain rates of 4,0 mm.h^{-1} and 4,8 mm.h^{-1} for a dry and subsequent wetter season respectively. An average rain rate 2,5 times larger was found for Florida (Doneaud *et al.*, 1984b).

The V-ATI relationship is clearly useful in estimating the amount of rain from a storm over the storm lifetime. To be operationally practical, however, it is necessary to determine whether the V-ATI relationship can be used at intermediate stages of a storm's lifetime providing estimates of the rain volume in real time. A comparison of V-ATI relationships computed from different stages of storm development showed that the predictive power of the V-ATI relationship increases as the time increment used in the ATI approaches the total storm duration. Nevertheless multiple linear regression, which included the maximum radar estimated rain volume, the maximum area, the maximum reflectivity and the maximum echo height, showed radar estimated rain volume to be well correlated with the maximum single-scan rain volume. This implies that the total rain volume could in fact be estimated by simply identifying the maximum stage of development of the storm (Doneaud *et al.*, 1984b).

The possibility of using V-ATI relationships in enhancing satellite rainfall estimation has already been mentioned with several provisos. Differences between radar reflectivity features and satellite features make area delineation difficult and accurately identifying the starting and ending times of the convective events is crucial. Starting times are easily identified but cirrus debris renders identification of the ending time extremely difficult. The fact that total rain volume can be estimated by identifying the maximum stage of storm development, however, implies that the ending time of the convective storm can be taken as the time of maximum development. Satellite data definition of maximum development could be based on the maximum count value (i.e. minimum temperature) (Doneaud *et al.*, 1987). Further investigations were conducted of calculating radar ATI using maximum area, maximum reflectivity and maximum echo height of the convective event as the ending time of the analysis. Rainfall volume was computed for the lifetime of the storm. Results demonstrated that the ATI method can be applied only for the growth portion of a convective event using the maximum echo area as the ending time of the analysis giving rainfall estimates comparable to those obtained using conventional *Z-R* techniques with space and time integration. As such the ATI technique could be used to nowcast total rain volume (Doneaud *et al.*, 1988).

Premises and Hypotheses

In this study two major aspects of radar rainfall volume measurements will be considered. The first of these will be a study of drop-size distribution patterns in rain from convective storms over the Transvaal Highveld. Specific objectives of this first section are to

a. determine an appropriate *Z-R* relationship for use in radar rainfall estimation techniques;
b. document likely effects of microphysical and kinematic processes on drop-size distributions and how these differ between convective and stratiform rain as evidenced in DSDs measured on the ground; and

c. consider the significance of drop-size distribution variability on the *Z-R* relationship and resultant changes in radar rainfall measurement accuracy.

In the second part of the dissertation a specific radar rainfall measurement technique known as the area-time integral (ATI) will be considered in order to:

a. determine an optimal method of determining volume versus area-time integral (V-ATI) relationships;
b. select an appropriate minimum reflectivity threshold;
c. assess the sensitivity of the V-ATI relationship to changes in the *Z-R* relationship; and
d. assess the accuracy of the area-time integral method in measuring convective rainfall over the Transvaal Highveld.

****

Literature pertaining to radar rainfall measurement, including drop-size distribution (DSD) studies and the area-time integral (ATI) technique, has been reviewed. Radar reflectivity factor *(Z)* and rain rate *(R)* computational formulae have been derived. The importance of kinematic and microphysical cloud processes on evolving drop-size distributions have been highlighted with specific reference to concomitant changes in the *Z-R* relationship. Promising results obtained from the area-time integral (ATI) approach to radar rainfall measurement have been reviewed. It has been proposed that the ATI technique be investigated as a means of improving radar rainfall measurement in storm systems over the Transvaal Highveld. In the following chapter the various data sources used in the study will be discussed.

CHAPTER 2

DATA AND METHODS

Several data sources have been utilised during the course of this study. The primary data source is an S-band weather radar situated at Houtkoppen to the north north-west of the Johannesburg city centre (Fig. 2.1). The radar has a radial range of 300 km, a beam width of 1,1° and a wavelength of 10,6 cm (Gomes and Held, 1991). The radar was modified to operate in Doppler mode in 1986. Data obtained from the radar are stored on magnetic tape before being transferred to the CSIR mainframe computer for further processing.

The first step in processing the data for the ATI study was the development of software capable of integrating the area of reflectivity with respect to time within the confines of a fixed geographical region. Only radar data in plan-position-indicator (PPI) format at minimum elevation angles (approximately 2°) were used. Initially a 1° latitude by 1° longitude grid square was chosen as the area in which radar echo was to be integrated. The area of radar echo was integrated over an hour. Unsatisfactory results were obtained using this approach so a second approach was developed whereby all radar echo within a 75 km radius of the radar was integrated. Not only is radar rainfall measurement considered tenuous at ranges exceeding 75 km but this is also the maximum range at which data are recorded when the radar is operated in Doppler mode. The second approach was further refined by integrating echo area for each scan and multiplying the area by the time between that and the following scan. This second approach had several advantages over the first. Echo area was not truncated at the limits of the grid square and integrations for individual scans simplified the analysis considerably. V-ATI computations were based on data from the 1987/88 rainfall season.

Raindrop-size distributions were measured using a Joss-Waldvogel raindrop disdrometer (Joss and Waldvogel, 1967). The disdrometer was operated on the roof of a building within the CSIR campus (Fig. 2.1). The principle of operation of the disdrometer is that a voltage is induced into a sensing coil by the downward displacement of a styrofoam body (Fig. 2.2). This signal is amplified and applied to another coil within the transducer to counteract the movement

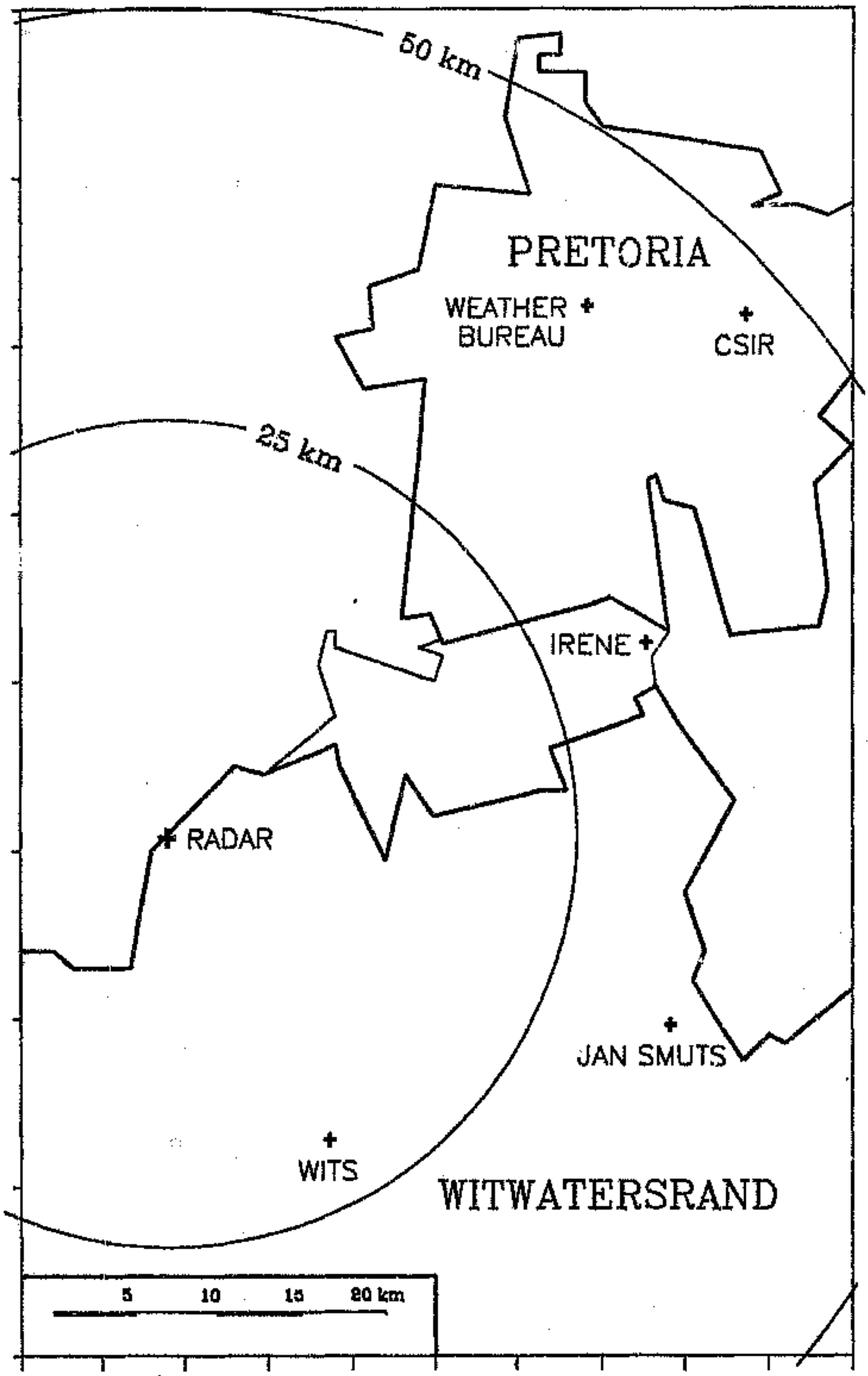

Figure 2.1: Schematised map of the disdrometer site (CSIR), the autographic rain recorder stations (Forum Building (SAWB), Irene weather station, Jan Smuts and the University of the Witwatersrand (WITS), and the radar. Circular lines are radar range rings.

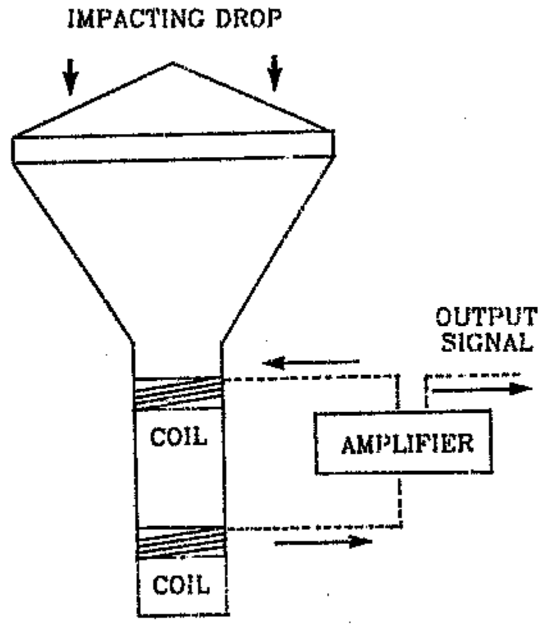

Figure 2.2: Schematic illustration of the principle of operation of the raindrop disdrometer.

of the body and return it to its rest position. Thus the instrument retains a high recovery rate and is capable of measuring several hundred drops a second (Waldvogel, 1974; Kinnel, 1976). The disdrometer was housed in a polystyrene-lined box with only the styrofoam plate exposed, to dampen extraneous noise from the drops hitting the roof. The box was covered with foam rubber to prevent splashing effects. The disdrometer was operated approximately 2 m away from a tipping-bucket rain gauge allowing appraisal of the disdrometer in measuring rainfall. Unfortunately some teething troubles with installing the disdrometer meant that continuous measurement was only effected from the end of November 1989. The disdrometer was subsequently operational for the rest of the 1989/90 season and the entire duration of the 1990/91 rainfall season. In total 16 791 minutes of data were collected during which 1006,52 mm of rain were recorded. For the 1989/90 season a sample volume of 11 592 m^3 was recorded and for the 1990/91 season 21 990 m^3. In comparison other ground-based DSD studies had sample volumes of $\pm$ 300 m^3 (Marshall and Palmer, 1948), 4100 m^3 (Austin and Geotis, 1979), 30 000 m^3 (Richards and Crozier, 1983) and 316 000 m^3 (Breuer and Kreuels, 1976). It must be pointed out that DSD studies utilising radar have sample volumes orders of magnitude higher than ground-based

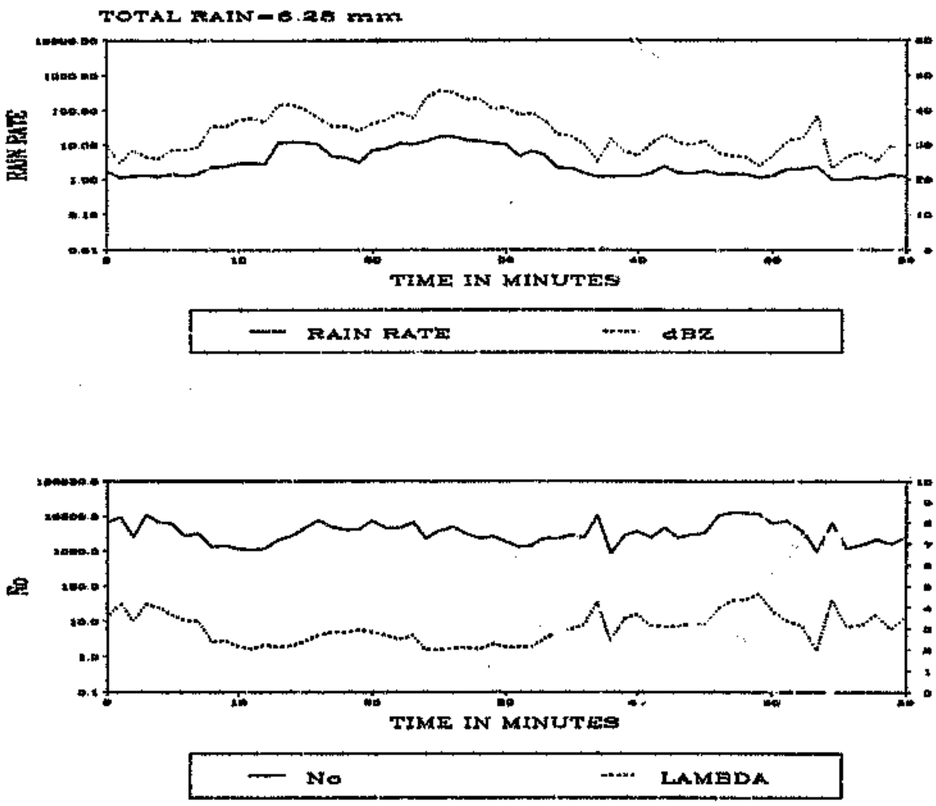

Figure 2.3: An example of plots generated for every hour of disdrometer data which were subsequently analysed.

studies. Sample volumes of 2,5 x 10^6 m^3 (Caton, 1966) and 33,3 x 10^6 m^3 (Richards and Crozier, 1983) are common in radar-based DSD studies.

The data processing software provided with the disdrometer was found to be restrictive, particularly in processing large amounts of data. Disdrometer data were thus transferred to the CSIR VM mainframe and a suite of programs written which plotted rain rate and other DSD characteristics against time (Fig. 2.3). Each hour of disdrometer data was plotted in this way. The plots were analysed and rain episodes identified for further study. *Z-R* relationships and time averaged DSDs were then determined for individual rain episodes and for the season as a whole.

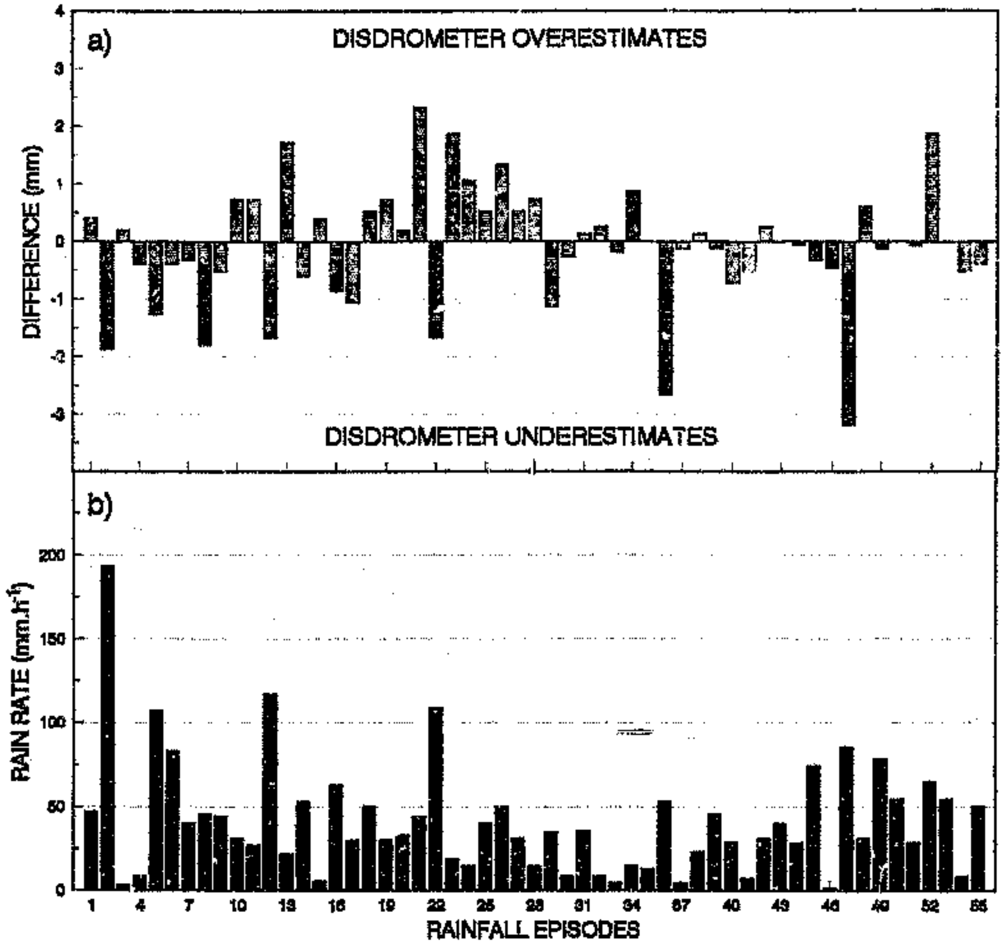

Figure 2.4: a) Differences between rain totals measured by disdrometer and those measured using a tipping-bucket rain gauge for 55 consecutively numbered rain episodes during the 1989/90 and 1990/91 rainfall seasons and b) maximum rainfall rate during the above-mentioned rain episode.

Rainfall totals measured using the disdrometer compared reasonably well with totals measured using the tipping-bucket rain gauge with a mean difference between the two instruments for 55 rain episodes of 0,0914 mm. Significant departures for individual rain episodes are apparent, however, of which underestimates by the disdrometer during periods of high rain rate are most significant (Fig. 2.4). The underestimation appears to be related to an instrument deficiency in that smaller drops are not always registered during high rain rates due to instrument dead-time. Various authors have reported this problem including Joss and Gori (1978) and List (1988). List in particular compared DSDs measured by disdrometer with those measured using a laser spectrometer. Small drops measured by the spectrometer were not recorded by the disdrometer in high rainfall rates. The deficiency should not detract substantially from the usefulness of the instrument. Although rain rates may be underestimated on some occasions, calculation of the reflectivity factor will not be affected significantly by drops of less than 1 mm in diameter.

Autographic rainfall records were obtained from the South African Weather Bureau for stations at the Forum Building (SAWB) in Pretoria, Irene and Jan Smuts Airport (Fig. 2.1). Records from a tipping bucket rain gauge maintained by the Department of Geography and Environmental Studies at the University of the Witwatersrand (Wits) were also used. Average rain rates were then computed at each of the three Weather Bureau stations for the 1986/87, 1987/88, 1988/89 and 1989/90 rainfall seasons. Unfortunately the time resolution on the strip charts used to record the rainfall on the Wits and CSIR rain gauges does not allow rain rates to be calculated with sufficient accuracy. The Wits rainfall record was excluded from the study and rain rates derived from disdrometer measurements used instead of the CSIR rain gauge. Both gauges are described here simply to recognise their existence. The ground-truth rain rate data used in validating and ultimately in optimising the ATI technique, was obtained from the disdrometer, the Forum Building autographic rain gauge, the Irene autographic rain gauge and the Jan Smuts autographic rain gauge.

****

The three sources of data used in this study have been described, *viz.* the weather radar, the raindrop disdrometer and the automatic rain gauge network. In the following chapter, drop-size distributions measured using the disdrometer are analysed in order to assess the effect of drop size distribution variability on the *Z-R* relationship, and to derive an appropriate *Z-R* relationship for convective rain measurement over the Transvaal Highveld.

SECTION II

DROP-SIZE DISTRIBUTIONS AND Z-R RELATIONSHIPS

CHAPTER 3

DROP-SIZE DISTRIBUTIONS AND Z-R RELATIONSHIPS

Introduction

The importance of drop-size distribution information in effecting accurate radar rainfall measurement has already been highlighted. In addition, the theoretical background to DSD studies has been discussed, including the influence of kinematic and microphysical processes in modifying evolving DSDs. In this chapter DSDs measured during the 1989/90 and 1990/91 rainfall seasons and their implications for radar measurement of rainfall on the Transvaal Highveld will be discussed. Both DSDs *per se* and average *Z-R* relationships will be considered in order to identify DSD characteristics relevant to this study and to derive a suitable *Z-R* relationship for convective rainfall measurement over the Transvaal Highveld.

Drop-Size Distributions

Due to the fact that their measurement techniques were rather crude, the drop-size distributions used in Marshall and Palmer's (1948) study were averaged over time. A more sophisticated measurement instrument like the disdrometer allows for better temporal resolution of DSDs, but time averaged DSDs for individual rain episodes make for interesting comparisons with earlier work done in this field. Time averaged DSDs over the Transvaal Highveld measured using the disdrometer tend to be flatter than M-P curves with fewer small drops and more large drops (Fig. 3.1).

The temporal variation of DSDs is not represented in either an average DSD or an average *Z-R* relationship, however. The extent of temporal variability of DSDs is clearly evident in a three-dimensional drop-size distribution field which is representative of a 17 minute period during the lifecycle of an arbitrarily chosen storm (Fig. 3.2). In order to quantify temporal variability in drop size spectra, Waldvogel's (1974) paramaterisation method has been used. Waldvogel based his technique on the assumption that a DSD averaged over one minute would be described adequately by an exponential distribution. The exponential

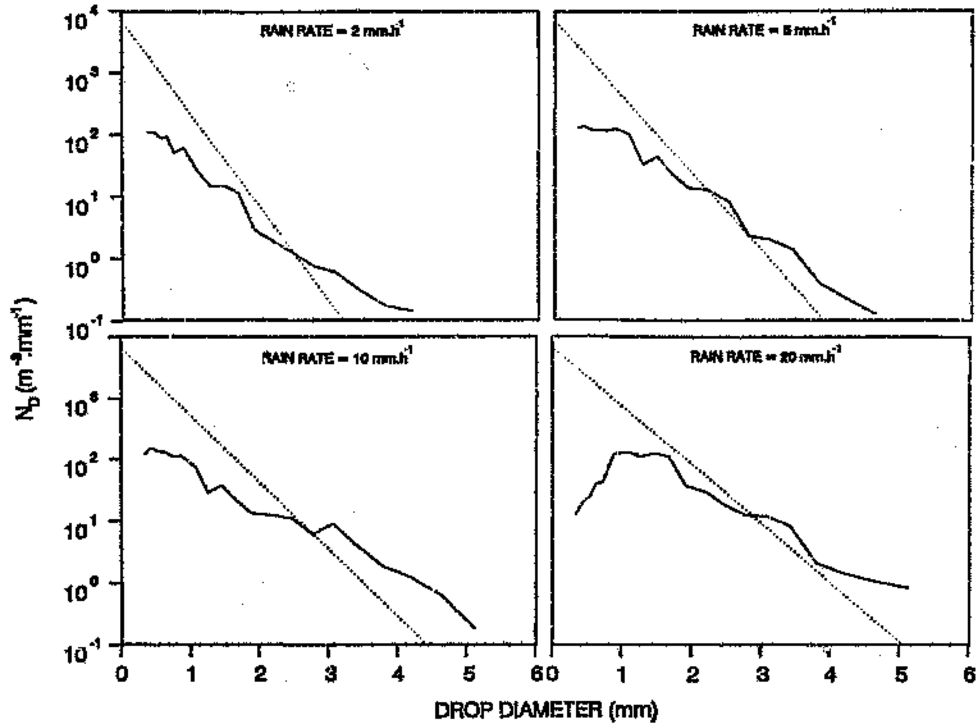

Figure 3.1: Plots of drop-size distributions for rain events with differing average rain rates (solid lines), compared with M-P distributions (dotted lines).

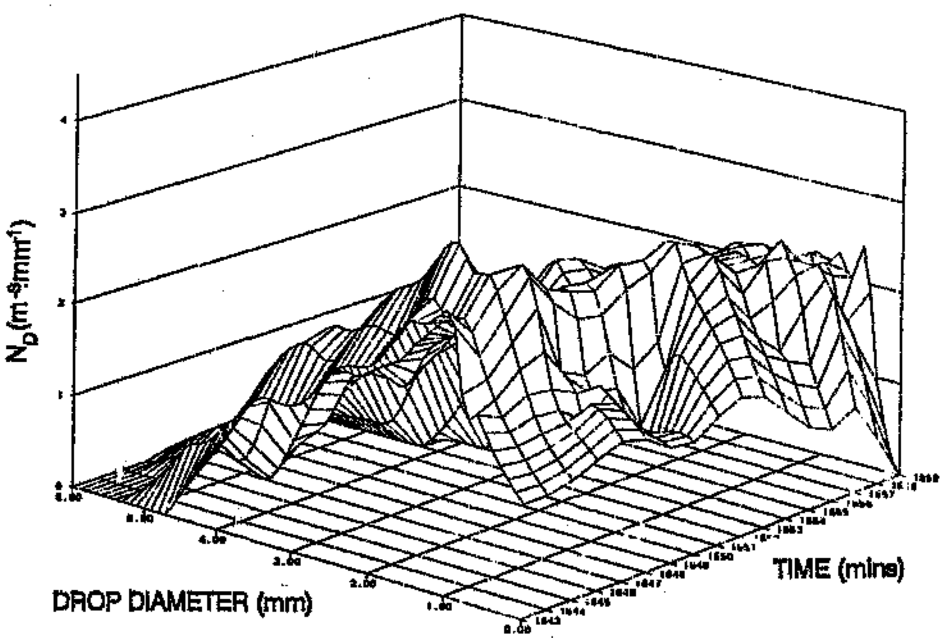

Figure 3.2: Three-dimensional drop-size distribution field from 16:43 to 16:49 on 8 December 1989.

distribution could be described in turn by the intercept value, N_0, and the slope, Λ. N_0 and Λ are obtained by substituting for the number of drops N_D (equation 1.9) in the equations for calculating liquid water content (W) and radar reflectivity factor (Z) as follows:

$$W = \frac{\pi}{6}\int_0^\infty N_D D^3 dD \qquad = \frac{\pi}{6} N_0 \int_0^\infty e^{-\Lambda D} D^3 dD \tag{3.1}$$

$$Z = \int_0^\infty N_D D^6 dD \qquad = N_0 \int_0^\infty e^{-\Lambda D} D^6 dD \tag{3.2}$$

N_0 and Λ can now be calculated from equations 3.1 and 3.2.

$$N_0 = \frac{1}{\pi}\left(\frac{6!}{\pi}\right)^{\frac{4}{3}}\left(\frac{W}{Z}\right)^{\frac{4}{3}} W$$

$$N_0 = 446\left(\frac{W}{Z}\right)^{\frac{4}{3}} W \tag{3.3}$$

$$\Lambda = \left(\frac{6!}{\pi}\right)^{\frac{1}{3}}\left(\frac{W}{Z}\right)^{\frac{1}{3}}$$

$$\Lambda = 6{,}12\left(\frac{W}{Z}\right)^{\frac{1}{3}} \tag{3.4}$$

Changes in rain rate, liquid water content and radar reflectivity factor can then be related to changes in drop size spectra. N_0, Λ and rain rate have been plotted as functions of time for a rainfall event in December 1989 (Fig. 3.3a). At 16:30 (marked (a) in Fig. 3.3A) values of N_0 show a moderate decrease while Λ values decrease sharply. At the same time a significant increase in rain rate is evident. The low values of both N_0 and Λ, i.e. a low intercept value and a relatively flat slope, imply that DSDs are dominated by large drops with relatively few smaller drops. Such a pattern can be related to theoretical studies and in particular to results obtained from a time dependent rain shaft model (List, 1988). Results obtained from the model showed that cloud base DSDs would be significantly modified by drop sorting (sedimentation) effects. Drop sorting is the process by which smaller drops remain suspended due to the presence of strong

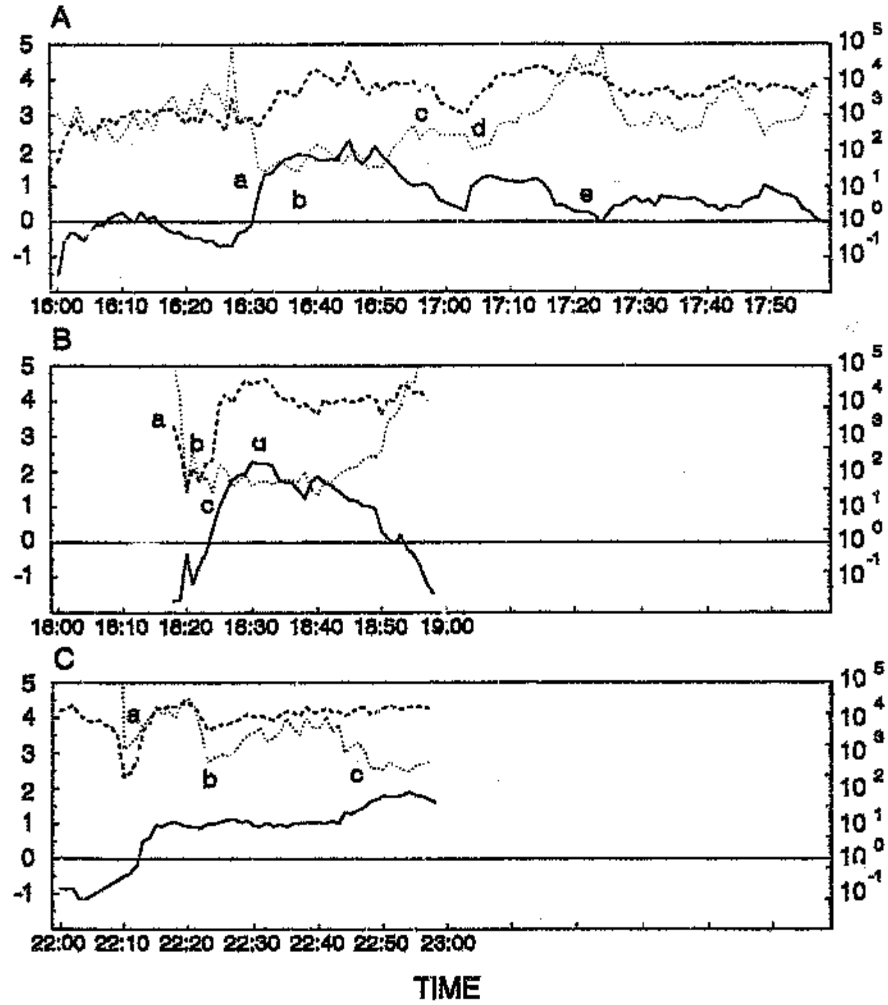

Figure 3.3: N_0, Λ and rain rate plotted as functions of time. N_0 and rain rate are plotted on a log scale on the right hand axis in units of $m^{-3}.mm^{-1}$ and $mm.h^{-1}$ respectively. Λ is plotted on a linear scale on the left hand axis in units of mm^{-1}. Lower case letters are discussed in the text.
A: 8 December 1989, 16:00 to 17:59.
B: 22 December 1989, 18:18 to 18:59.
C: 4 March 1990, 22:00 to 22:59.

updraughts and only the larger drops have sufficient terminal velocity to begin falling. As a result, DSDs at ground level are characterised by an initial scattering of large drops as the rain starts. As the large drop numbers increase, smaller drops begin to appear in the drop size spectra. The model results also suggested that these smaller drops appear in the spectra as a result of break-up effects due to drop collision, rather than having originated at cloud base.

By 16:35 (marked (b) in Fig. 3.3A) N_0 had increased significantly along with a moderate increase in Λ. The increase in the intercept value and slight steepening of the slope indicates greater numbers of small drops in the spectra. The pattern remained reasonably constant for some 15-20 minutes before the rain rate began to decrease. Coincident with the rain rate decrease was a marked steepening of the DSD slope (indicated by increasing Λ values) implying progressively fewer large drops in the spectra. From 16:55 (marked (c) in Fig 3.3A) Λ became constant while N_0 began to decrease, implying decreasing numbers of drops throughout the entire spectrum. Shortly after 17:00 (marked (d) in Fig 3.3a) a short burst of rain is evident which injected some larger drops (indicated by a decrease in Λ). By 17:50 DSDs had no large drops, indicated by high N_0 and high Λ values.

Similar patterns of evolving drop size spectra are evident in other convective storms and were especially pronounced in rain from a storm that traversed the disdrometer site on 22 December 1989 (Fig. 3.3B). From the onset of the rain at 18:18 there was a sharp, parallel decrease in N_0 and Λ (marked (a) in Fig. 3.3B) implying that initial DSDs contained some large drops. The slight decrease in rain rate occurred at the same time as N_0 and Λ increased (marked (b) in Fig 3.3B) suggesting that the slight lull in the rainfall was as a result of the absence of large drops. As the rain rate began to increase again, an influx of large drops is evidenced by a much flatter DSD slope (low Λ values).

Between 18:24 and 18:25 (marked (c) in Fig 3.3B) an N_0 jump occurred of slightly more than one order of magnitude with a concomitant steepening of the DSD slope. N_0 jumps have been identified in disdrometer data records and ascribed to changes in the rainfall regime from convective to continuous rain (Joss and Waldvogel, 1974). The N_0 jump evident in this storm appears indicative of a sudden downpour of small drops. This substantial increase in the number of small drops cannot be easily attributed to collisional breakup effects and would seem to be better accounted for by the rapid collapse of the thunderstorm updraught. The rain peak of 46,5 mm.h^{-1} (marked (d) in Fig 3.3B) coincided with high N_0 and low Λ values implying high numbers of both small and large drops. Rain rate subsequently decreased and from 18:39 (marked (e) in Fig 3.3B) onwards the DSD slope became progressively steeper indicating diminishing numbers of large drops.

If the rainfall pattern seen for this storm is compared to the well-documented lifecycle of an isolated, single-cell storm (Preston-Whyte and Tyson, 1988) interesting similarities are evident. Single-cell storms are characteristically short-lived, typically less than 60 minutes, and show marked temporal changes. Most significant, however, is the fact that in single-cell storms the updraught collapses due to friction created by falling rain (Chisholm and Renick, 1972). The rain rate pattern from the storm that occurred on 22 December 1989 is entirely consistent with the characteristics of a single-cell storm. These similarities suggest that the N_0 jump may well indicate the rapid decay and collapse of the thunderstorm updraught. Verification of this idea would require a comprehensive radar-based analysis of the storm. Such an analysis is beyond the scope of the present study.

Stratiform rain, on the other hand, without significant drop-sorting effects, shows an entirely different pattern. On 4 March 1990, a convective storm system passed over the disdrometer site trailing an extensive region of stratiform rain. Rain fell intermittently for some six hours. After an initial downpour with the passing of the leading edge of the storm, rain had stopped falling by 21:59 and gradually began to fall again after 22:00 (Fig. 3.3C). The parallel increase in N_0 and Λ (marked (a) in Fig 3.3C) implies that the DSDs that contributed to the measured rain rate were entirely devoid of large drops. The pattern prevailed for about 10 minutes before sharp decreases in both N_0 and Λ indicate the influx of large drops (marked (b) in Fig. 3.3C). Whether the influx of large drops is related to processes of rain drop evolution within the thuderstorm updraught or whether they have arisen from drop coalescence effects cannot be resolved in the present analysis. The increase in rain rate from 22:45 (marked (c) in Fig 3.3C) is again associated with a flattening DSD slope, but in that case high N_0 values were maintained. This implies that drop sorting effects were present and that the rain rate increase resulted from an influx of large drops while high numbers of small drops were maintained.

An alternative means of portraying changing DSDs is by plotting rain rate as a function of N_0 and Λ (Fig. 3.4). Wide ranges of possible DSD spectra are evident for each of the four groups of rain rates. The concept of 'equilibrium DSDs', in which drop growth effects and drop disintegration effects are in balance, has been discussed by several authors (Srivastava, 1971; Zawadzki and de Agostinho Antonio, 1986; List, 1988). As median values of N_0 and Λ for the

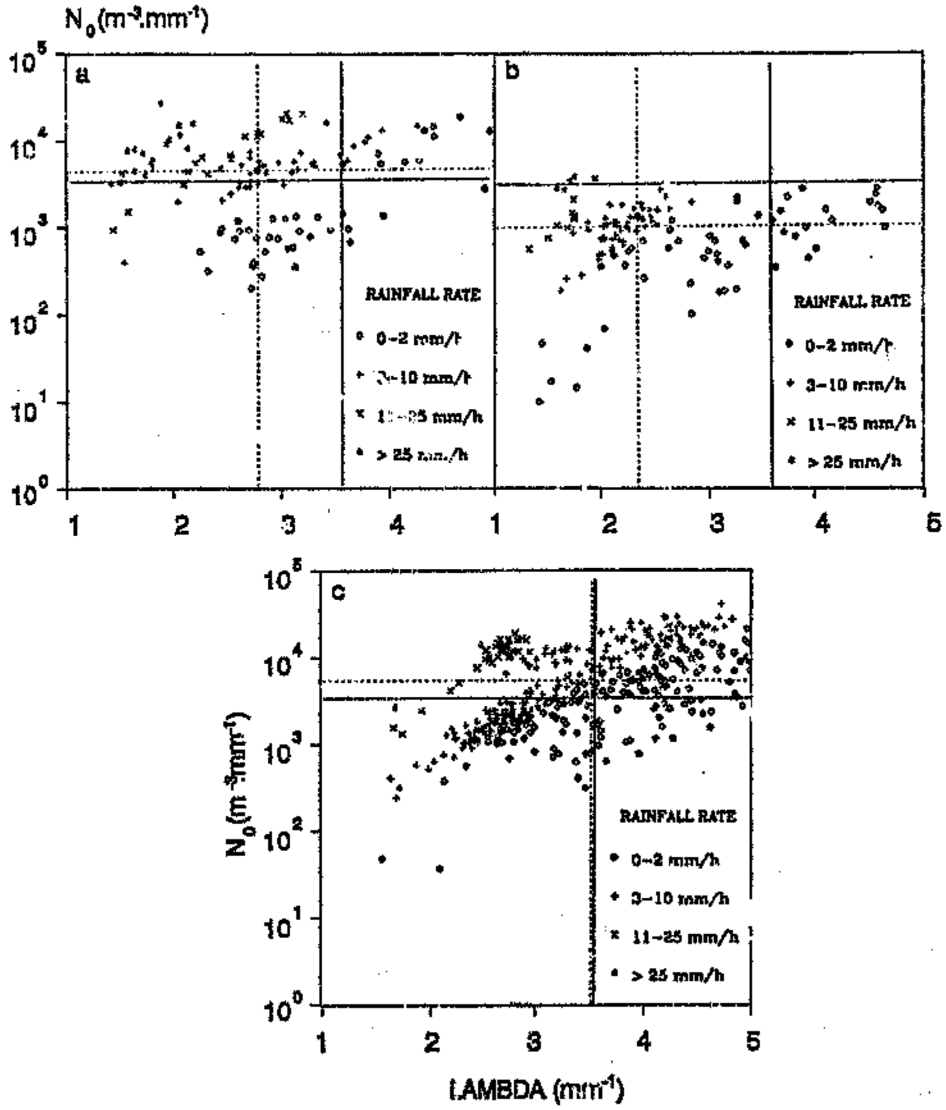

Figure 3.4: Rain rate as a function of N_0 and Λ. Solid lines indicate median values for the entire season, dashed lines median values for the individual rain episode
a) 8 December 1989, 16:00 to 17:59
b) 22 December 1989, 18:06 to 21:20
c) 4 March 1990, 19:14 to 05:21

entire rainfall season appeared to be the most likely representation of equilibrium DSDs, seasonal median values of N_0 and Λ are plotted as solid lines on the graphs. Median values of N_0 and Λ for the individual rain episodes are also plotted on the graphs as dashed lines. For the storm on 8 December 1989, the median Λ value is less than the seasonal Λ median implying that DSDs in the rain from this storm were characterised by significant numbers of large drops.

Both the median Λ and N_0 values for the storm on 22 December 1989 are less than the seasonal median values suggesting that, although there were significant numbers of large drops in the DSDs, there were generally fewer drops than for the storm on 8 December 1989. The median N_0 and Λ values for the storm on 4 March 1990 correspond quite well with the seasonal median N_0 and Λ values suggesting that equilibrium DSDs are a feature of stratiform rain. Equilibrium DSDs have been observed in steady tropical rain in which the absence of updraughts was identified as playing a crucial role in the formation of equilibrium DSDs (Zawadzki and de Agostinho Antonio, 1986).

The importance of quantifying the various kinematic and microphysical processes that influence DSD evolution lies in establishing the effects of these processes on the Z-R relationship. In order to illustrate the effects of changing drop spectra on the Z-R relationship, the radar reflectivity curve has been introduced into the rain rate graph from the storm on 8 December 1989. Implicit in the use of a Z-R relationship is the assumption that Z and R are directly proportional. Thus if the two curves are overlaid (Fig. 3.5B) and plotted against time, deviations in the relationship are easily recognisable. At (a) for example, radar reflectivity significantly exceeds rain rate. Corresponding N_0 and Λ curves (Fig. 3.5A) indicate a flat DSD slope with a moderate intercept value implying high numbers of large drops in the drop size spectrum. On the other hand, radar reflectivity is significantly less than rain rate at (b) and in this case the N_0 and Λ curves indicate N_0 large drops in the drop size spectrum. At (c) radar reflectivity changes from exceeding rain rate to underestimating rain rate. In this instance rain rate remains nearly constant and the deviations are in direct response to changes in the DSD.

Analyses of individual storms provide important insight into the processes that modify evolving DSDs. In addition the analyses highlight the effects of changing DSDs on the Z-R relationship. Where such analyses fail is in assessing the climatological significance of changing DSDs for an entire rainfall season. For this reason the graphs in which rain rate has been plotted as a function of N_0 and Λ have been extended to include data for the entire 1989/90 rainfall season. The graph has been divided into 16 blocks by including divisions at the

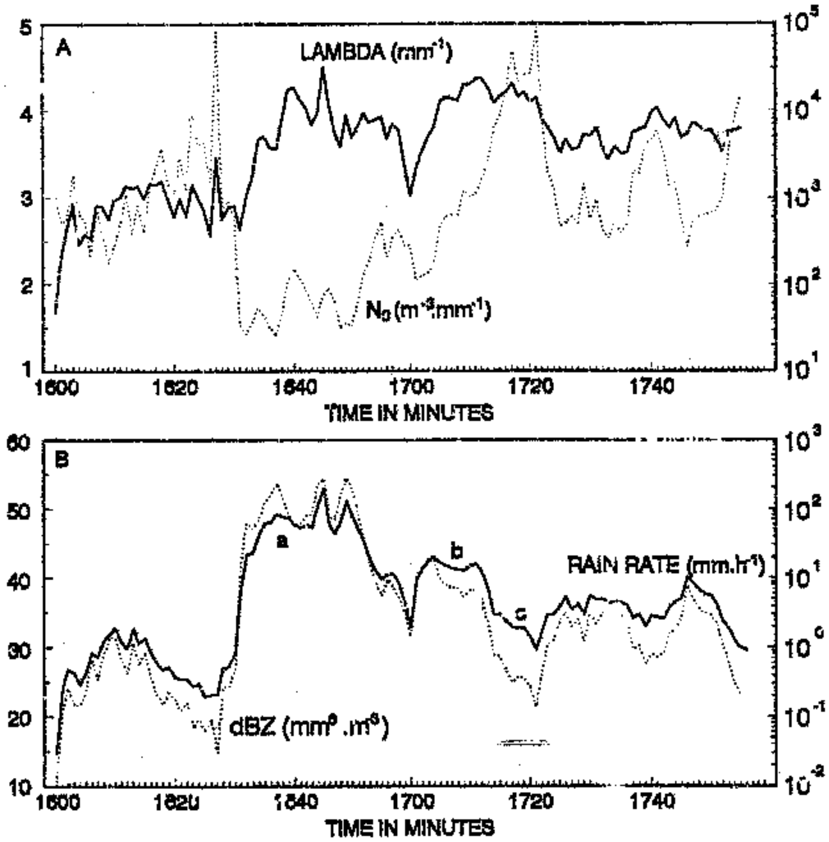

Figure 3.5: A) N_0 and Λ plotted against time for 8 December 1989, 16:00 to 17:59. B) Rain rate and radar reflectivity factor for the same period. The letters a, b and c are discussed in the text.

25 and 75% quartiles of N_0 and Λ. Each block in the $N_0 - \Lambda$ plot thus represents a specific DSD and has been labelled A1 to D4 (Fig. 3.6). Block A1, for example, represents below median values of N_0 and below median values of Λ, whereas block D1 represents above median values of N_0 with below median values of Λ. All possible combinations of N_0 and Λ are listed together with concomitant DSD characteristics, in Table 3.1.

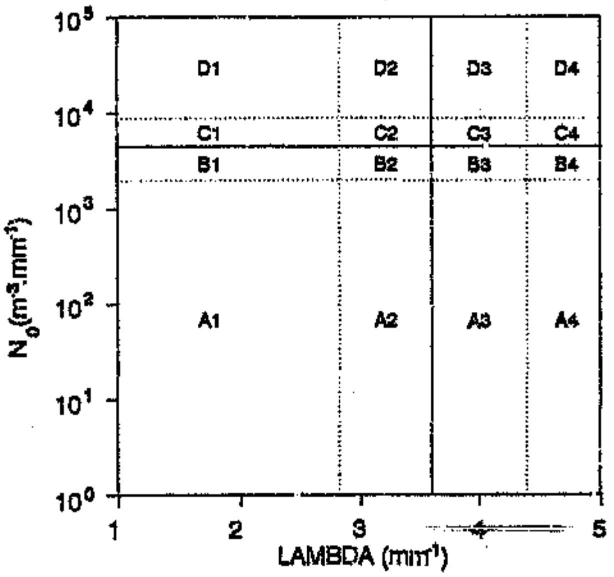

Figure 3.6: All possible combinations of N_0 and Λ for rain rates exceeding 0,01 $mm.h^{-1}$. Solid lines indicate median values, dashed lines the 25 per cent and 75 per cent quartiles respectively.

Table 3.1: DSD characteristics specific to each of the blocks identified in Figure 3.6.

Block	N_o	Λ	Characteristics of the distribution
C2, C3, B2, B3	Median	Median	Equilibrium distribution
C4, B4	Median	Above median	Few large drops. Possible drop break-up effects
C1, B1	Median	Below median	More large drops. Drop coalescence and/or large drops originating at cloud base
D2, D3	Above median	Median	Higher numbers of drops across the spectrum. High rain rates
D4	Above median	Above median	Large numbers of small drops. Considerable drop break-up effects
D1	Above median	Below median	Higher numbers of drops across the spectrum, but with relatively more larger drops
A2, A3	Below Median	Median	Few drops across the entire spectrum.
A4	Below median	Above median	No large drops. Few small drops
A1	Below median	Below median	Scattering of larger drops. Drop-sorting or coalescence effects.

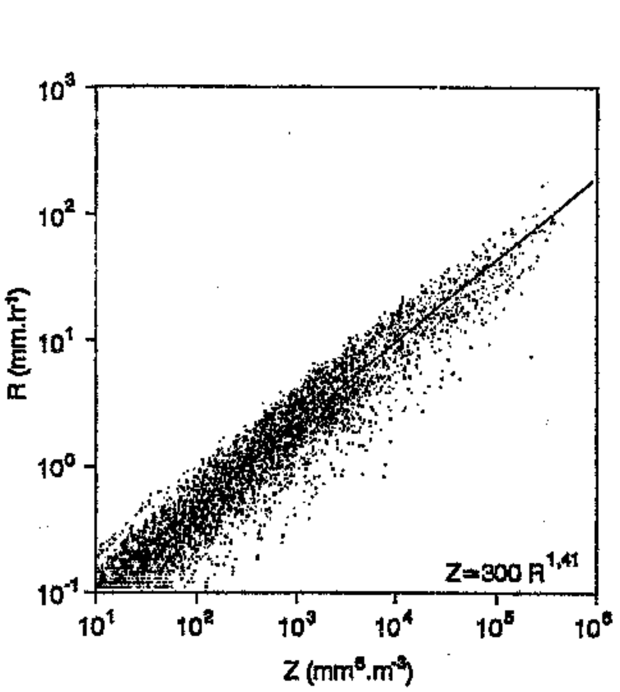

Figure 3.7: Scatter plot of the relationship between Z and R computed from disdrometer data recorded in Pretoria during the 1989/1990 rainfall season.

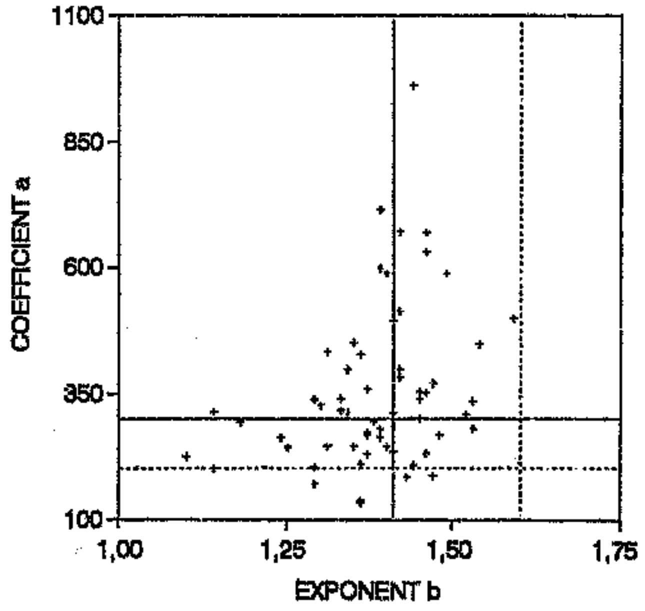

Figure 3.8: Distribution of values for the coefficient a and the exponent b in the relationship $Z = aR^b$ from individual rain episodes between November 1989 and May 1990.

Z-R Relationships

An average Z-R relationship for the 1989/90 season of $Z = 300\ R^{1.41}$ has been determined by least squares linear regression (Fig. 3.7). Z-R relationships calculated for individual rain episodes, however, are seen to vary considerably from storm to storm in response to different suites of DSDs (Fig 3.8). The 16 blocks described in the $N_0 - \Lambda$ plot have been used to categorise each minute of disdrometer data by DSD. Once the data had been categorised in this manner rain rate measured using the disdrometer was compared to rain computed from the average Z-R relationship. The results are summarised in Table 3.2. Positive values in the table indicate the percentage by which the actual rain rate exceeds the rain rate computed using the average Z-R relationship. Similarly negative values indicate the percentage by which rain rate computed from the average Z-R relationship exceeds actual rain rate. The percentage frequency of occurrence of each DSD category is also included in the table.

It can be seen from the table that the maximum rain rate in block A1 (116 mm.h^{-1}) was overestimated by the average Z-R relationship by about 55 per cent. In block D1, on the other hand, the maximum rain rate of 196 mm.h^{-1} was underestimated by 36 per cent using the average Z-R relationship. Similarly in blocks A4 to D3, in which similar rain rates were measured, the average Z-R relationship can both overestimate and underestimate the rain rate depending on the drop-size distribution.

The problem was compounded when an average Z-R relationship of $Z = 220R^{1.41}$ was calculated for the 1990/91 season (Fig. 3.9) and combining the two data sets gave $Z = 245R^{1.4}$. In addition Hodson (1986) contends a single Z-R relationship cannot be used for all rain rates and that above 25 mm.h^{-1} a different Z-R relationship must be used. Using data from a vertically-pointing Doppler radar (Pasqualucci, 1982a, 1982b) Hodson showed that Λ becomes constant once rain rates exceed 25 mm.h^{-1} and, based on this observation, he calculated a Z-R relationship of $Z = 939R$ for rain rates exceeding 25 mm.h^{-1}. $\Lambda - R$ scatter plots were constructed for both seasons (Figs. 3.10). In both plots a tendency towards a constant Λ value is apparent but only at rain rates of about 100 mm.h^{-1}, a finding supported by Willis and Tattleman (1989). Hodson also describes a tendency for Λ to become constant once liquid water values exceed

Table 3.2: Differences between measured rain rate and rain rate computed using an average Z-R relationship of $Z = 300\ R^{1.41}$ Each block refers to the drop-size distribution patterns illustrated in Fig. 3.6 and characterised in Table 3.1. Maximum, minimum and mean differences and relative frequency of occurrence are shown for each DSD category.

Block		1	Frequency of occurrence of DSD category %	2	Frequency of occurrence of DSD category %
A	Mean Min Max	+11,24% -74,00% -54,69%	13,2	-16,67% -71,43% -25,12%	9,6
B	Mean Min Max	+24,00% -65,00% -40,80%	7,6	-3,75% -24,10% -6,4[illegible]%	6,9
C	Mean Min Max	+26,06% +04,23% -12,92%	3,9	+19,77% +3,82% +21,40%	6.6
D	Mean Min Max	+36,66% +19,89% +36,19%	2,3	+39.64% +25.73% +46.30%	5,0
		3		4	
A	Mean Min Max	-17,65% -75,00% -18,33%	9,3	-16,67% -50,00% -15,79%	4,9
B	Mean Min Max	+ 4,00% - 9,09% + 9,09%	6,8	+ 8,33% - 8,33% 11,90%	3,5
C	Mean Min Max	+23,26% +20,20% +23,22%	7,0	+24,00% + 8,33% +28,87%	3,0
D	Mean Min Max	+44,67% +28,71% +53,63%	7,5	+47,77% +32,70% +57,24%	2,8

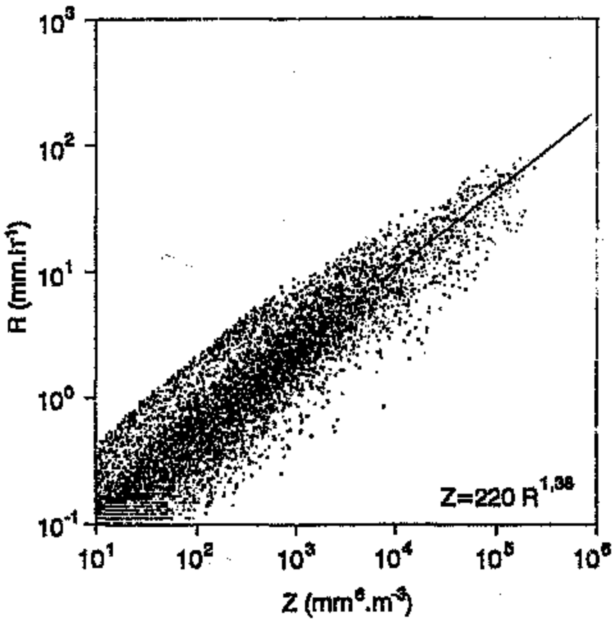

Figure 3.9: Scatter plot of the relationship between Z and R computed from disdrometer data recorded during the 1990/91 rainfall season.

1,2 g.m^{-3} which is reflected in $\Lambda - W$ scatter plots for both rainfall seasons (Fig. 3.11).

In both sets of plots the spread of Λ values is seen to be significantly greater in the 1990/91 season than in the 1989/90 season. Summary statistics for the two rainfall seasons as well as for the two seasons combined are presented in Table 3.3. If the median values are compared to Figure 3.4 it can be seen that the 1990/91 season would have been characterised by DSDs with larger numbers of smaller drops, whereas DSDs in rain events during the 1989/90 season would have had a greater number of large drops. The wide spread of Λ values in the 1990/91 $\Lambda - W$ plot also reflects the presence of drop disintegration effects. Collisional drop breakup reportedly prevails in conditions of high liquid water content (Grosh, 1989).

A quadratic fit Z-R relationship has also been proposed as a means of attaining more accurate estimates of radar derived rainfall (Jones, 1965). It has been argued that when the terminal velocity of falling drops $V_t(D)$ is correctly specified, the Z-R relationship becomes highly non-linear on logarithmic

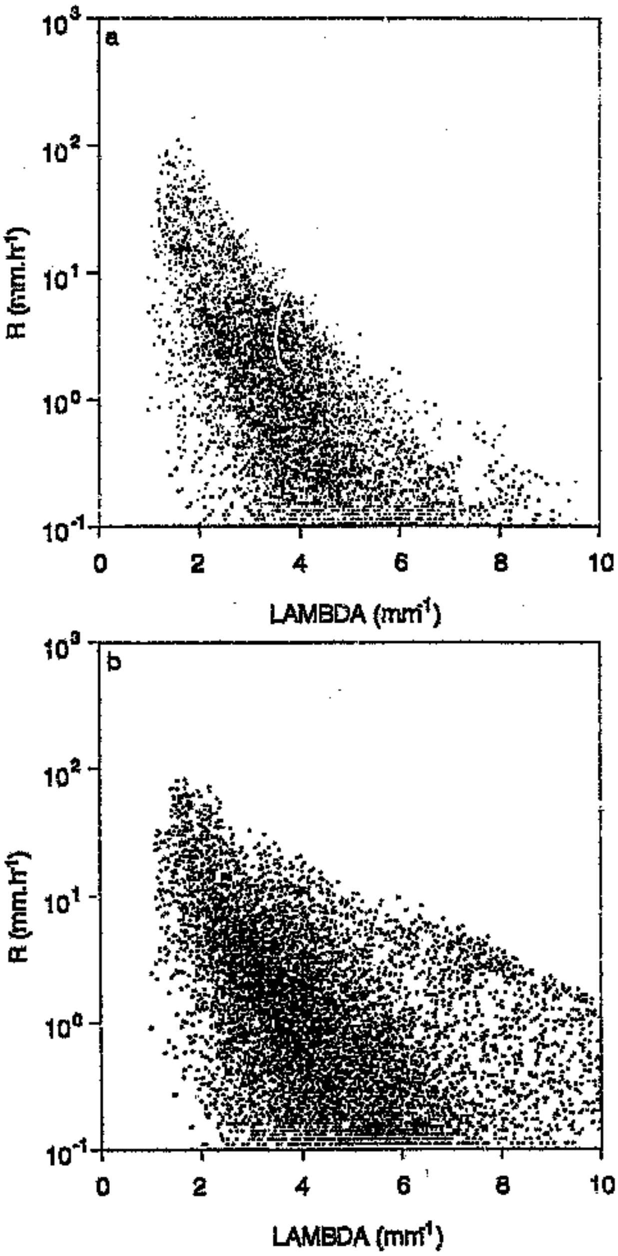

Figure 3.10: Scatter plot of the relationship between Λ and R computed from the disdrometer data.
a) 1989/90 rainfall season.
b) 1990/91 rainfall season.

coordinates and that a quadratic fit Z-R may well be more appropriate than a linear relationship (Grosh, 1989).

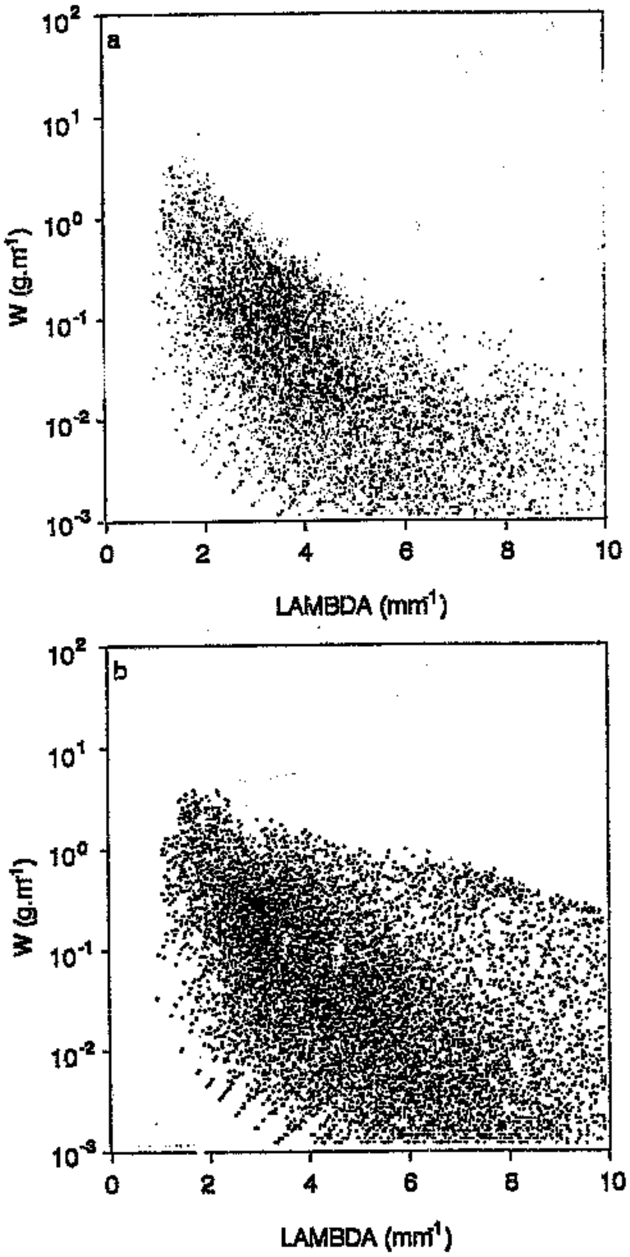

Figure 3.11: Scatter plot of the relationship between Λ and liquid water content computed from the disdrometer data.
a) 1989/90 rainfall season.
b) 1990/91 rainfall season.

Based on the above, selection of a single *Z-R* relationship for radar rainfall measurement in storms occurring on the Transvaal Highveld would be tenuous

Table 3.3: Summary statistics for the 1989/90 and 1990/91 rainfall seasons obtained from the disdrometer data.

Season	Λ (mm^{-1})	N_o ($m^{-3}.mm^{-1}$)
8990	3,56	3859
9091	4,04	5747
Both	3,8	4803

at best. Clearly the only means of properly appraising any *Z-R* relationship is by comparing actual reflectivity values from radar with rainfall measured at the ground. A series of *Z-R* relationships have been determined, therefore, for use in the V-ATI analysis. *Z-R* relationships for all rain rates (hereafter referred to as the linear *Z-R* relationship), for rain rates less than and greater than 25 mm.h $^{-1}$ (hereafter referred to as the 25 mm.h^{-1} *Z-R* relationship) and a quadratic form of the *Z-R* (hereafter referred to as the quadratic *Z-R*relationship) have been calculated. The *Z-R* relationships were calculated for each season individually as well as from the combined data sets. They are summarised in Table 3.4 and plotted graphically in Figure 3.12.

Table 3.4: *Z-R* relationships for two rainfall seasons.
$\times_1$ $Z = a + b(\log R) + c(\log R)^2$ (Grosh, 1989).
$\times_2$ $Z = aR^b$

Type	Rainfall season	a	b	c
QUADRATIC (X_1)	89/90 90/91 Both	2,46 2,30 2,35	1,39 1,34 1,36	0,00 0,11 0,09
R<25 mm.h^{-1} (X_2)	89/90 90/91 Both	298 217 242	1,39 1,36 1,37	NA NA NA
R> = 25 mm.h^{-1} (X_2)	89/90 90/91 Both	638 572 539	1,28 1,26 1,3	NA NA NA
All rain rates LINEAR (X_2)	89/90 90/91 Both	300 220 245	1,41 1,38 1,4	NA NA NA

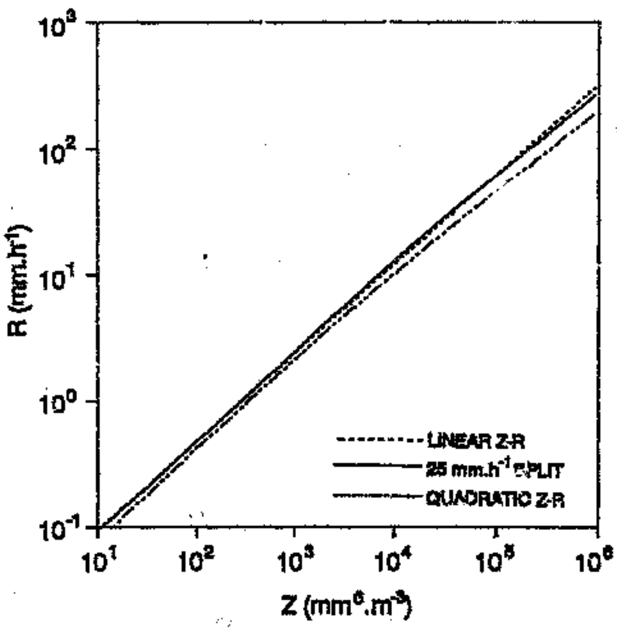

Figure 3.12: Different *Z-R* relationships determined from combined data sets.

Summary

Drop-size distributions (DSDs) which occur in rain from storm systems on the Transvaal Highveld have been considered in this chapter. The analysis has been based on the assumption that any DSD will be described adequately by an exponential distribution. The DSD can be described in turn by the intercept value, N_0, and the slope of the distribution, Λ. In plotting the temporal variation of N_0 and Λ, various kinematic and microphysical processes have been identified and related to evolving DSDs. Drop sorting effects are clearly evident in convective rain with resultant DSDs having relatively fewer smaller drops with higher numbers of large drops. 'Jumps' in the temporal pattern of N_0, which have been described by other authors, have also been identified in the DSD data. Characteristics of the storm in which an N_0 jump was identified suggest that N_0 jumps are related to the rapid collapse of the thunderstorm updraught. DSDs measured in stratiform rain, in the absense of updraughts, appear to represent equilibrium between drop growth and drop disintegration effects. Verification of the above interpretations requires a comprehensive radar analysis of the evolving morphology of the thunderstorm which is beyond the scope of the present study.

Changing DSDs have been shown to influence markedly the accuracy of radar measured rainfall. Radar estimated rainfall can both overestimate and underestimate actual rainfall depending on the DSD. An average *Z-R* relationship of $Z = 245\,R^{1,4}$ has been calculated by least squares linear regression on logarithmic values from disdrometer data collected during 1989/90 and 1990/91. In addition a quadratic fit Z-R relationship of

$$Z = 2{,}35 + 1{,}36(\log R) + 0{,}09(\log R)^2$$

has been calculated and seperate Z-R relationships of $Z = 539\,R^{1,3}$ and $Z = 242\,R^{1,37}$ have been calculated for rain rates greater than and less than 25 mm.h^{-1} respectively. The tendency for Λ to become constant when rain rates approach 100 mm.h $^{-1}$ has been seen in $\Lambda - \bar{R}$ relationships with a similar tendency in $\Lambda - W$ plots. Λ tends towards a constant value when liquid water content values exceed 1,2 g.m^{-3}.

****

Drop-size distributions in convective rain over the Transvaal Highveld have been characterised and analysed to assess the effect of drop size variability on the Z-R relationship. Three Z-R relationships have been derived from these drop size distributions. In the following chapter the derived Z-R relationships will be used in investigating the area-time integral (ATI) method of radar rainfall measurement and to derive a rainfall volume versus area-time integral (V-ATI) relationship.

SECTION III

THE AREA-TIME INTEGRAL METHOD OF RADAR RAINFALL MEASUREMENT

CHAPTER 4

THE AREA-TIME INTEGRAL (ATI) METHOD

Introduction

The area-time integral (ATI) method of radar rainfall measurement is based on the observed relationship between storm area and duration and the rainfall volume produced by that storm. Related theoretical considerations have been discussed in greater detail in Chapter one. Indeed much of the more recent work done on the ATI method has been theoretical and based to some degree on earlier results. The work of Doneaud *et al.* (1981; 1984a,b), Lopez *et al.* (1983) and Chiu (1988a; 1988b) features prominently in these theoretical considerations. Doneaud *et al.* showed that the ATI of the radar echo in excess of a certain threshold would provide an accurate measure of rain volume over the lifetime of the storm, whereas Chiu used the fractional area covered by radar echoes above a preset threshold rain rate to explain 98 per cent of the variance of the instantaneous areawide rainfall.

The work that has been done for this dissertation has been based almost exclusively on the technique developed by Doneaud *et al.* (1981, 1984a, 1984b). In other words the focus has been on establishing a rain volume versus area-time integral (V-ATI) relationship. In this chapter different methods of integrating radar echo area with respect to duration will be considered in order to establish which approach provides the most suitable V-ATI relationship. The different *Z-R* relationships obtained from the disdrometer data (see Chapter 3) will be used in the calculation of radar-estimated rain volume to see how changing *Z-R* relationships effect the V-ATI relationship. The derived V-ATI relationships will be assessed in the light of documented characteristics of Highveld storms and by comparing V-ATI derived rain rates with rain rates measured at the ground using automatic rain gauges and the disdrometer. Comparisons will be made for both seasonal mean rain rates and for average rain rates measured on individual storm days. The chapter will be concluded with some general comments on the accuracy of the ATI technique.

Maximum and Average Hourly Echo Area

The first step in deriving a V-ATI relationship is selecting an appropriate means of echo area integration with respect to time. As mentioned in Chapter 1, Doneaud *et al.* (1981) attempted two approaches to integrating area with respect to time, *viz.* using either the maximum hourly echo area (MHEA) or the average hourly echo area (AHEA) as the ATI. V-ATI relationships have been derived for convective rain over the Transvaal Highveld using both the MHEA and AHEA approaches. The regression parameters are listed in Table 4.1 and Table 4.2 for MHEA and AHEA, respectively. Radar estimated rain volume (hereafter RERV) has been determined using a Z-R relationship of $Z = 300R^{1,41}$. With MHEA the highest correlation coefficient is evident at the 23,3 dBZ threshold. The correlation coefficient decreases from 23,3 to 26,6 dBZ increasing marginally to the 33,3 dBZ threshold. On the strength of the correlation coefficient, 23,3 dBZ would appear to be a suitable reflectivity threshold and therefore for MHEA a V-ATI relationship of the form $V = 3{,}27(ATI)^{1,15}$ at the 23,3 dBZ threshold appears to be most suitable. V-ATI relationships calculated using AHEA show a pattern of decreasing correlation coefficients with increasing threshold (Table 4.2). The higher correlation coefficient in the case of AHEA ($r = 0{,}96$) and the lower standard error of the estimate ($s = 0{,}11$) implies that the AHEA derived V-ATI relationship of $V = 3{,}06\,(ATI)^{1,14}$ is possibly more accurate than the MHEA derived V-ATI.

Scan-by-Scan Echo Area

Both MHEA and AHEA suffer an obvious shortfall in that a minimum tracking time of one hour is needed before volumetric rainfall totals can be estimated. In addition accurately defining storm duration is sometimes problematic since cell clusters that develop early on in the lifetime of the storm as well as the final stages storm decay are not always included in the radar records. Doneaud *et al.* (1984a) ultimately derived their V-ATI relationship using a scan-by-scan integration procedure, summing individual scans over the hour period. A similar approach has been used in V-ATI calculations over the eastern Transvaal Highveld (Mather, *pers. comm.*). The approach that has been used in this study is to measure echo area and calculate an equivalent radar-estimated

Table 4.1: Radar-estimated rain volume versus ATI regression parameters for differing reflectivity thresholds. RERV and ATI are calculated from maximum hourly echo areas (MHEA).

Threshold values in dBZ	23,3	26,6	30,0	33,3
Equivalent rain rate ($Z=300R^{1,41}$) in mm.h^{-1}	0,79	1,35	2,35	3,83
Coefficient K	3,27	10,04	11,85	14,28
Exponent b	1,15	1,03	1,05	1,07
Correlation coefficient	0,95	0,91	0,92	0,93

Table 4.2: Radar-estimated rain volume versus ATI regression parameters for differing reflectivity thresholds. RERV and ATI are calculated from average hourly echo areas (AHEA).

Threshold values in dBZ	23,3	26,6	30,0	33,3
Equivalent rain rate ($Z=300R^{1,41}$) in mm.h^{-1}	0,79	1,35	2,35	3,83
Coefficient K	3,06	8,13	10,21	12,23
Exponent b	1,14	1,05	1,06	1,08
Correlation coefficient	0,96	0,92	0,94	0,94

rain volume for each individual minimum elevation radar scan. Duration has been taken as the time between each radar scan and both ATI and RERV calculated on the basis of that time interval. The approach used here is similar to that described by Chiu (1988a, b), with each scan essentially representing an areawide snapshot of a multiplicity of evolving rain rates. As such the approach requires that all echo within effective radar range be included in deriving a V-ATI relationship to ensure adequate representation of all evolving rain rates (Atlas *et al.*, 1990a).

V-ATI relationships have been derived using the scan-by-scan integration method for each of the nine *Z-R* relationships previously determined from the disdrometer data (see Chapter 3). Regression parameters for each of the different *Z-R* relationships are shown in Table 4.3. Values of the coefficient *K* are seen to be fairly similar across the range of *Z-R* relationships, ranging from a minimum value of 2,88 to a maximum value of 3,89. The values of *K* also

Table 4.3: Radar-estimated rain volume versus ATI (V-ATI) regression parameters for differing Z-R relationships. RERV and ATI are calculated using the scan-by-scan integration technique. The form of the V-ATI equation is $V = K(ATI)^b$.

Z-R	Season	K	b	Correlation coefficient (r)
Linear Z-R	89/90	2,95	1,24	0,95
	90/91	3,63	1,25	0,95
	Both	3,31	1,25	0,95
25 mm.h^{-1} split Z-R	89/90	2,88	1,25	0,95
	90/91	3,89	1,23	0,96
	Both	3,47	1,23	0,95
Quadratic Z-R	89/90	2,88	1,23	0,96
	90/91	3,47	1,22	0,97
	Both	3,31	1,22	0,96

compare favourably with K in the V-ATI relationship of $V = 3,7\,(ATI)^{1,08}$ computed for convective storms over North Dakota (Doneaud *et al.*, 1984a).

Slopes of the different V-ATI relationships derived for the Transvaal Highveld are seen to be similar. V-ATI relationships derived using the linear Z-R and the 25 mm.h^{-1} split Z-R are seen to have the steepest slopes while those derived using the quadratic Z-R relationship have slightly flatter slopes. All the slopes are noticeably steeper than the slope of the North Dakota V-ATI relationship. The fact that these slopes are steeper indicates that smaller, short-lived storms over the Transvaal Highveld have lower average rain rates than similar storms over North Dakota, whereas larger, long-lived storms have higher average rain rates than equivalent North Dakota storms. Assessing whether these V-ATI implied characteristics of Highveld storms were consistent with known characteristics of Highveld storms, therefore, became the first step in evaluating the derived V-ATI relationship.

Documented Characteristics of Highveld Storms

Many of the documented studies of Highveld storms have been based on data from the Houtkoppen weather radar (see Fig. 2.1). Most of these studies have emphasised hail-producing versus non hail-producing features of Highveld storms (Carte, 1979, 1981; Held, 1980; Held and Carte, 1979; Held and van den Berg, 1977; O'Beirne, 1988). Tracking routines have also been developed in order to assess Highveld storm climatologies (Mader, 1979; Mader *et al.*, 1985). If the outer limit of a storm is defined by the 30 dBZ reflectivity contour, areas of 100 km² are attained by a mere 23 per cent of storms with only 8 per cent lasting longer than an hour. Average storm lifetime is 24 minutes with an average area of 86 km². Longer-lived storms average lifetimes of 86 minutes attaining areas of about 196 km². Unfortunately little reference has been made in these studies to the rain produced by the storm systems described. Similar characteristics were obtained from a C-Band weather radar situated at Bethlehem in the northeastern Orange Free State. The majority of storms were seen to be short-lived making them inefficient rain-producing systems. The bulk of the rainfall received in the area was produced by storms which developed into large complexes. These larger storm systems often develop as a result of merging of smaller cells or cell clusters. Merged storm complexes resulted in larger, more intense storms with increases in storm lifetimes, maximum vertical depth, maximum height and average and maximum growth rate (Steyn and Bruintjies, 1990).

Several radar-derived properties of continental, convective clouds have been compared for the South African Highveld and Israel to determine which played a significant role in altering the storm rain volume yield (Rosenfeld and Gagin, 1989). The radar-derived variables included the depth of the cell above freezing level, the depth of the convective layer, the size of the total convective complex and the absolute humidity at cloud base. The synergistic effect on rain volume yield brought about by merging was also highlighted with clusters containing at least 32 individual cells producing seven times more rain volume than the combined volumes of the separate cells. Merged cell complexes were also seen to live between 50 to 70 per cent longer than individual cells. Of greatest importance to the V-ATI relationships is that changes in the size of a cluster housing an individual cell, while other independent properties remained constant, may cause a threefold increase in rain volume yield from that cell. Half of this increase in rain volume yield would be generated by an increase in the area and about 20 per cent by the increase in the duration of the storm, with the remaining 30 per cent being generated by increases in the rain intensity. The concluding factor is that the short lifetime of continental convective clouds is a major limiting factor in precipitation efficiency (Rosenfeld and Gagin, 1989).

In a similar vein instantaneous area average rain rates have been determined by measuring the ratio of the area of rain intensity above a given threshold to total echo area (Fr) and comparing it to areal rain intensity (R) (Rosenfeld *et al.*, 1990). A comparison of $R - Fr$ relationships between South Africa, Texas, Australia (Darwin) and data from the GATE experiment showed the steepest $R - Fr$ slope for convective storms over South Africa at rain rate thresholds above 6 and 8 $mm.h^{-1}$ respectively. At rain rate thresholds of 2 and 4 $mm.h^{-1}$ slopes from Texas rainfall were found to be steeper. The slope of the $R - Fr$ relationship $S(r)$ was also shown to decrease in a regular manner from South Africa to Texas, to GATE, to Darwin in opposing order to the mean cloud base temperatures of 8°, 16°, 23° and 24° respectively. The many light convectional showers that cover a large fractional area such as in GATE and Darwin imply smaller average area rain rates. In areas where warm rain processes are dominant, there will be an increased frequency of small showers characterised by light rainfall (Rosenfeld *et al.*, 1990). Convective rain over central South Africa is initiated through ice-phase mechanisms with no evidence of any significant warm rain processes (Kraus and Bruintjies, 1985).

A V-ATI derived relationship has been derived for the eastern Transvaal Highveld using a gauge network in a manner similar to that first proposed by Doneaud *et al.* (1981). A coverage area is calculated for each of the rain gauges in the rain gauge network. Rainfall over each of consecutive five minute period is then summed over an hour. The rainfall measurement is irrelevant in determining ATI, all that is needed is whether rain fell or not in any given five minute period. Rain volume is then ascertained from the rain gauge data and regressed against the derived ATI values. In this manner a V-ATI relationship of $V = 3{,}06\,(ATI)^{1,18}$ with a correlation coefficient of 0,97 was derived (NPRP Seasonal Report, 1990/91). Not only is the relationship quite similar to those derived in this study but the slope of the relationship strengthens the argument that average rain rates from convective rain storms over the Transvaal Highveld are likely to increase with increasing area and duration.

Average Rain Rates

Much of the interest in the ATI technique of radar rainfall measurement has been generated by the extremely high correlation coefficients between ATI and radar estimated rain volume. The good correlation coefficients are obtained in part by construction, however, since both are computed from the same reflectivity field (Raghaven and Chandrasekar, 1991). While the significance of the good correlations should not be overlooked a more suitable means is needed to appraise the accuracy of a given V-ATI relationship. One approach is to calculate average rain rates from the V-ATI relationship as shown in equation 1.15 (where ATI is taken as the mean ATI of either a rainfall season or an individual storm as appropriate) and to compare these rain rates to average rain rates measured at the ground (hereafter referred to as gauge rain rates). V-ATI derived average rain rates (hereafter referred to as V-ATI rain rates) have been calculated for each of the four dBZ thresholds used in the MHEA and the AHEA V-ATI calculations. These rain rates are listed in Table 4.4. Unfortunately ground-based rainfall data from the area covered by the radar is rather sparse. Time resolved rainfall data is available for only four automatic rain gauges (see Fig. 2.1) and the disdrometer. Although inadequate, this data is all that is available for the present study. In order to effect comparisons between gauge rain rates and V-ATI rain rates, average rain rates have been calculated for each of the three automatic rain gauge sites and for the disdrometer site. Average rain rates have also been calculated for each rain rate equivalent of the dBZ thresholds used in the V-ATI calculations (Table 4.5).

A comparison of V-ATI and gauge rain rates for the Transvaal Highveld shows that gauge rain rates are considerably less than V-ATI rain rates. If the V-ATI rain rates are compared to gauge rain rates which have been averaged above the equivalent rain rate thresholds a significant improvement is noted. One possible reason for the large discrepancy between V-ATI and gauge average rain rates is that radar operations (from which the V-ATI relationship has been derived) are aimed specifically at understanding the processes in convective storms. The rain gauge record on the other hand is likely to include rain from low intensity echoes which were either not detected by radar or were deemed not to warrant radar operations. What cannot be ignored, however, is the suggestion

Table 4.4: Rain rates derived from the maximum hourly echo area (MHEA) and the average hourly echo area (AHEA) V-ATI relationships.

Threshold values in dBZ	23,3	26,6	30,0	33,3
MHEA ($mm.h^{-1}$)	9,58	12,4	16,58	22,3
AHEA ($mm.h^{-1}$)	7,95	10,8	13,44	19,69

that even using the 23,3 dBZ reflectivity contour as the V-ATI threshold may lead to an overestimate of rain at the ground.

Average rain rates derived from rain gauges, the disdrometer and all the V-ATI relationships are portrayed graphically in Figure 4.1. The V-ATI relationship computed by Doneaud *etal.* (1984a), using a 25 dBZ threshold, gave an average rain rate for convective storm systems over North Dakota of 4,0 $mm.h^{-1}$ with a standard deviation of 1,55 $mm.h^{-1}$ (Doneaud *et al.*, 1984b). A 20 per cent increase in average rain rate was found for a subsequent, wetter rainfall season. The V-ATI rain rate of 7,95 $mm.h^{-1}$ for AHEA (23,3 dBZ threshold) is more realistic than the 9,58 $mm.h^{-1}$ for MHEA but the closest estimate of rain rates measured at the ground is given by the 1989/90 quadratic *Z-R* relationship with a measurement error of some 23 per cent. The 1987/88 seasonal average is overestimated by about 37 per cent. Assuming, however, that the V-ATI relationship has been derived only from *convective* storm echoes then a good comparison is evident between the average rain rates measured using the disdrometer during the predominantly convective 1989/90 rainfall season. In this case the V-ATI rain rate overestimates the disdrometer-derived rain rate, averaged above the equivalent rain rate threshold by four per cent.

Average Rain Rates for Individual Storms

Seasonal average rain rates do not provide an adequate assessment of the accuracy of V-ATI rain rate estimates for individual storm days. Initially it was hoped that individual clusters could be tracked and assessed as individual storms, but applying such an approach operationally would be virtually impossible. Average ATI was determined, therefore, for twenty individual storm days from

Table 4.5: Mean rain rates calculated for the area scanned by the radar
a: Automatic rain gauge data from the Forum Building, Pretoria (SAWB), the weather station at Irene and Jan Smuts airport for four rainfall seasons and stratified by the minimum equivalent rain rate threshold. b: Disdrometer data (CSIR Campus, Pretoria) for two rainfall seasons and stratified by the four equivalent rain rate thresholds.

a Season	THRESHOLD LEVELS				
	$0,1\ mm.h^{-1}$	$0,79\ mm.h^{-1}$	$1,35\ mm.h^{-1}$	$2,35\ mm.h^{-1}$	$3,83\ mm.h^{-1}$
89/90	4,43	7,33	8,91	11,3	15,14
90/91	3,16	5,34	6,65	8,65	11,69
Mean	3,80	6,34	7,78	9,98	13,42

b Station	ALL RAIN RATES				
	86/87	87/88	88/89	89/90	Mean
Forum Building	4,69	3,89	3,19	4,25	4,01
Irene	5,23	3,88	4,24	4,73	4,4
Jan Smuts	4,1	4,77	3,85	6,56	4,82
Mean	4,67	4,01	[illegible]76	5,18	4,41
RAIN RATES ABOVE MINIMUM THRESHOLD					
Forum Building	6,64	5,21	5,23	5,72	5,7
Irene	7,87	4,69	5,8	6,77	6,28
Jan Smuts	5,9	6,69	5,47	8,23	6,57
Mean	6,8	5,53	5,5	6,91	6,19

the 1987/88 rainfall season and V-ATI rain rates compared to the average gauge rain rates (which were averaged above $0,79\ mm.h^{-1}$ rain rate threshold) for the appropriate days. The approach implicitly assumes that average rain rates for the three gauges will reflect average rain rates for the entire areal coverage of the storm systems traversing the radar coverage area. This is clearly an assumption prone to considerable potential error but rain gauge data does not permit otherwise. V-ATI and gauge rain rates have been plotted on a histogram for the twenty selected storm days (Fig. 4.2).

Although the V-ATI derived rain rate averaged over the entire season is remarkably close to the average rain rate for the automatic rain gauges, individual storms are seen to vary quite considerably. Most noticeable is the

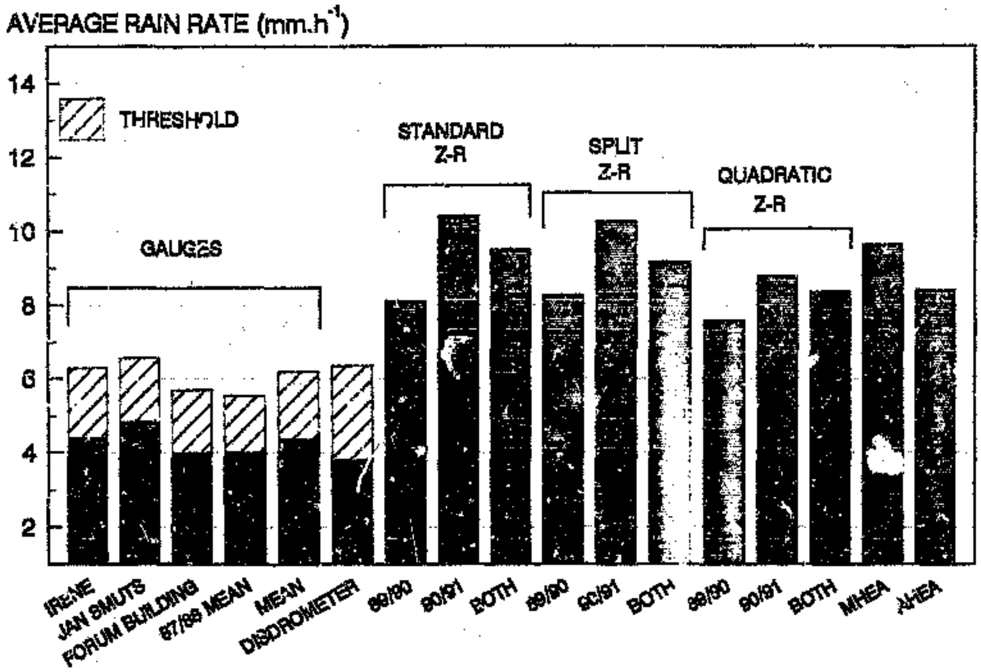

Figure 4.1: Comparison of average rain rates measured at the ground and those derived from the V-ATI relationship. Where both rainfall seasons have been used in the derivation of the Z-R relationship BOTH is indicated on the X axis. MHEA and AHEA refers to maximum hourly echo area and average hourly echo area respectively.

large disparity between the gauge measured rainfall average and the V-ATI average rainfall on 17 December 1987 (Fig. 4.2). In this case rain was registered at the Forum gauge only. Rain lasted for some 45 minutes during which time a rain rate peak of 135 mm.h^{-1} was registered at the gauge. The gauge measurements for 17 December 1987 would appear to represent a high intensity portion of the storm, rather than average rain rates for the total area of the storm.

Conversely average rain rates for the three gauges are significantly less than the V-ATI derived rain rates for a storm that occurred on 24 November 1987. Two PPI (Plan Position Indicator) scans from radar data for 24 November 1987 are shown in Figure 4.3. The Jan Smuts gauge, which registered light rainfall from 17:14 is situated beneath the outer edge of the storm in the 17:16 PPI (Fig. 4.3a). The Irene gauge is seen to be slightly ahead of the main echo area but not in the path of significant cell development to the north of the radar in

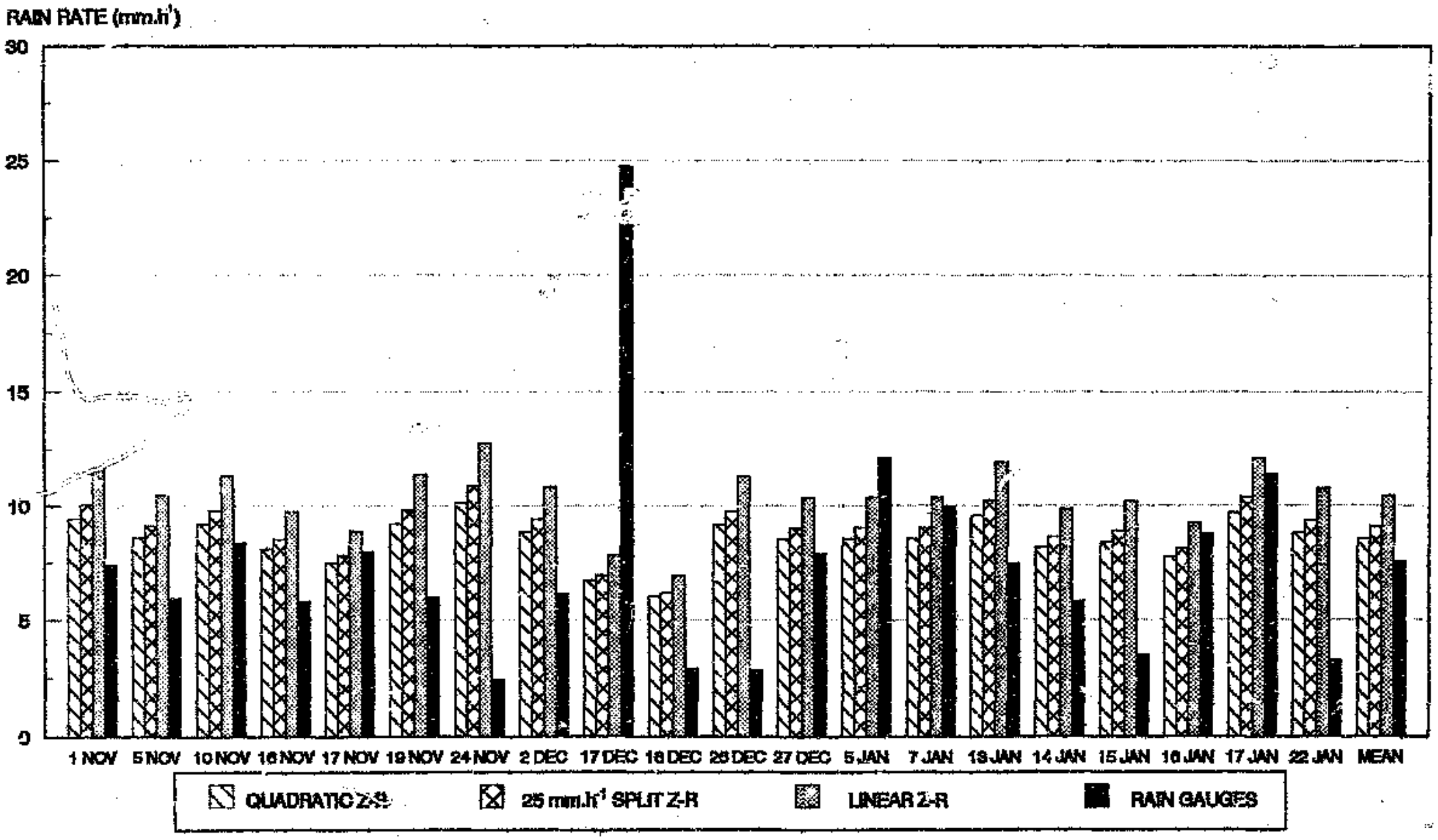

Figure 4.2: Histogram of gauge and V-ATI rain rates for twenty storms selected from the 1987/88 rainfall season to illustrate the sensitivity of the V-ATI relationship to different Z-R relationships.

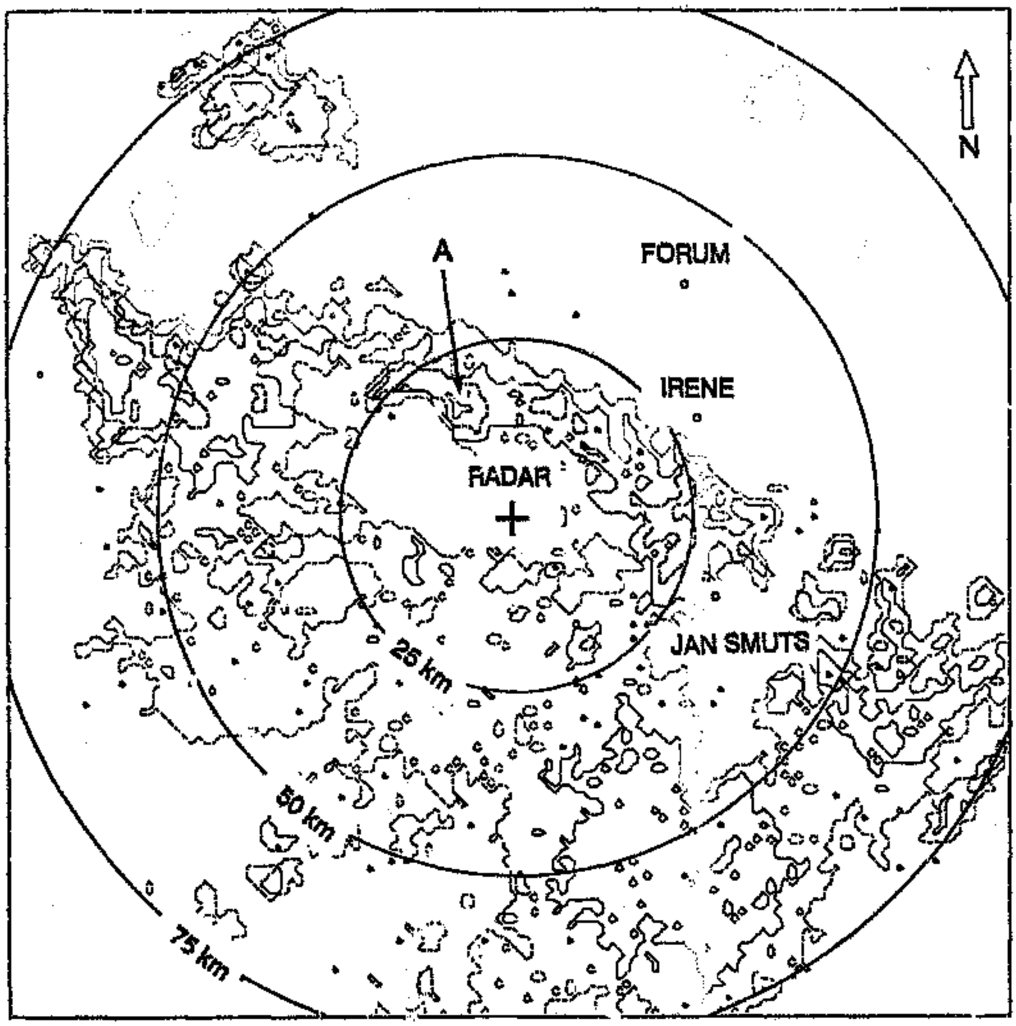

Figure 4.3a: PPI radar scans a. minimum elevation angle showing the storm of 24 November 1987 a. 17:16. The position of the radar is demarcated by a cross, open circles indicate automatic rain gauges. Isolines indicate reflectivity levels of 23,3, 30,0, 40,0, 50,0 and 60,0 dBZ respectively. Radar range rings are at 25 km intervals.

which a 40 dBz cell area with a 50 dBz core is evident (marked 'A' in Fig. 4.3a). Although a region of high intensity echo is evident to the southwest of the Forum gauge (marked 'B' in Fig. 4.3b), rain from this echo area was not manifested in the rain gauge data with the rain gauge data showing a maximum rain rate of 2 mm.h^{-1}. Only light rain rates were recorded at the rain gauges despite much higher rain intensities being evident in the radar echo pattern.

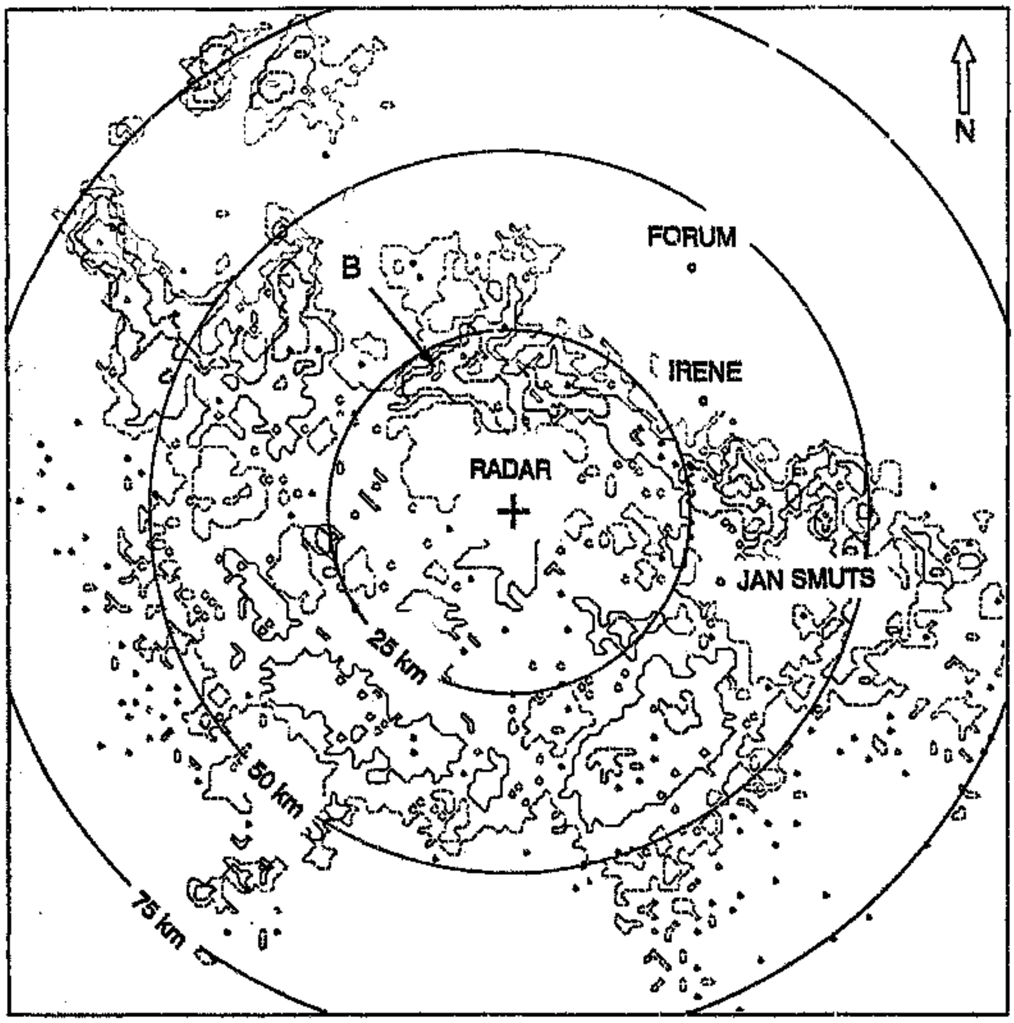

Figure 4.3b: PPI radar scans at minimum elevation angle showing the storm of 24 November 1987 at 17:26. The position of the radar is demarcated by a cross, open circles indicate automatic rain gauges. Isolines indicate reflectivity levels of 23,3, 30,0, 40,0, 50,0 and 60,0 dBZ respectively. Radar range rings are at 25 km intervals.

The 26 December 1987 shows one of the highest discrepancies between gauge rain rates and V-ATI rain rates. Even the best V-ATI estimate was some 190 per cent higher than the gauge rain rates. Rainfall was registered at the Forum gauge only, and appears to have originated from an echo cluster that developed initially as two separate clusters to the east and southeast of the Forum Building gauge (Clusters A and B in Fig. 4.4a). The two clusters subsequently merged while moving in a westerly direction just north of the Forum gauge (Cluster C in

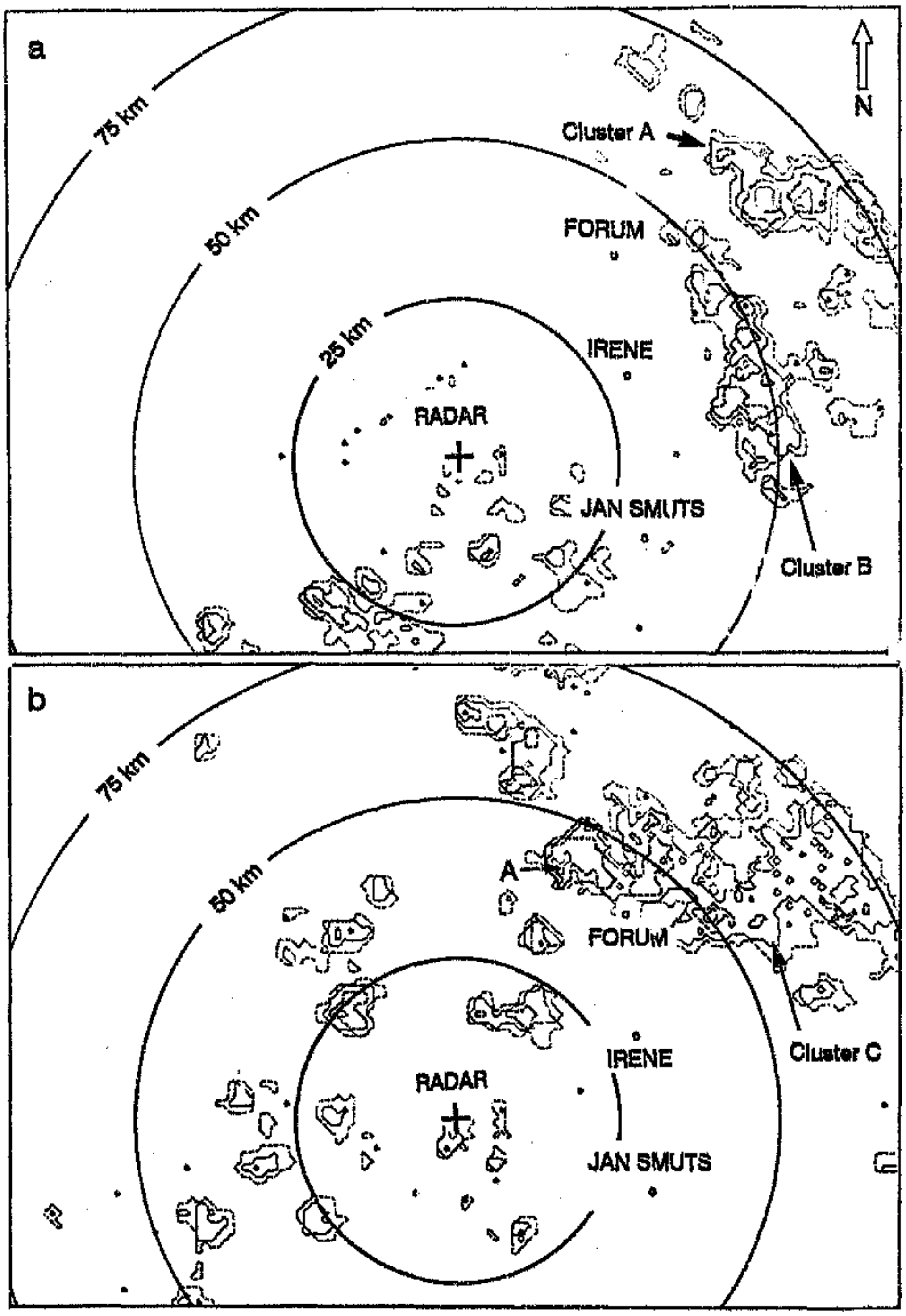

Figure 4.4: PPI radar scans at minimum elevation angle showing the storm of 26 December 1987. The position of the radar is demarcated by a cross, open circles indicate automatic rain gauges. Isolines indicate reflectivity levels of 23,3, 30,0, 40,0, 50,0 and 60,0 dBZ respectively. Radar range rings are at 25 km intervals.
a: 14:29; b: 15:27

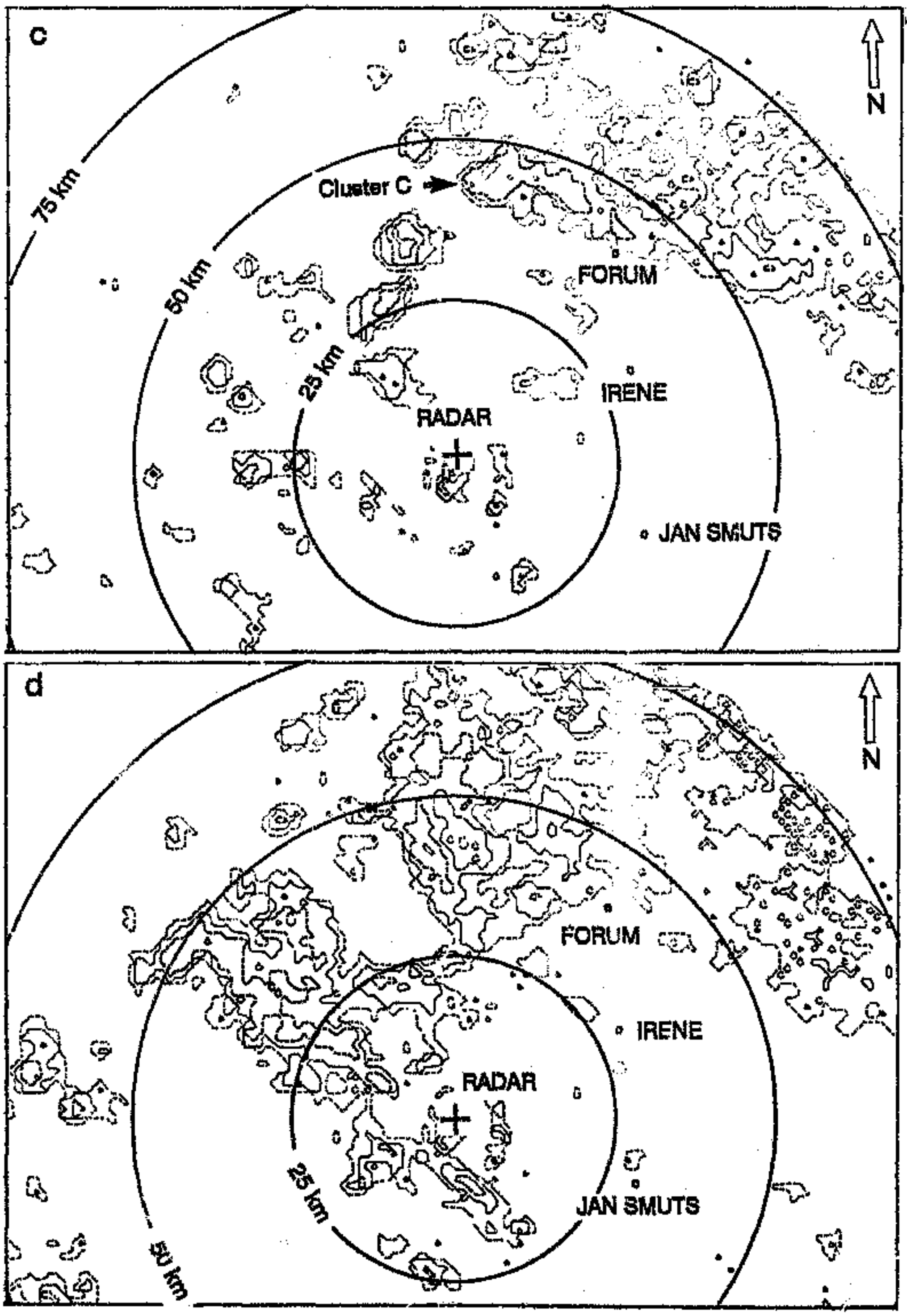

Figure 4.4: PPI radar scans at minimum elevation angle showing the storm of 26 December 1987. The position of the radar is demarcated by a cross, open circles indicate automatic rain gauges. Isolines indicate reflectivity levels of 23,3, 30,0, 40,0, 50,0 and 60,0 dBZ respectively. Radar range rings are at 25 km intervals.
c: 15:41, d: 16:25

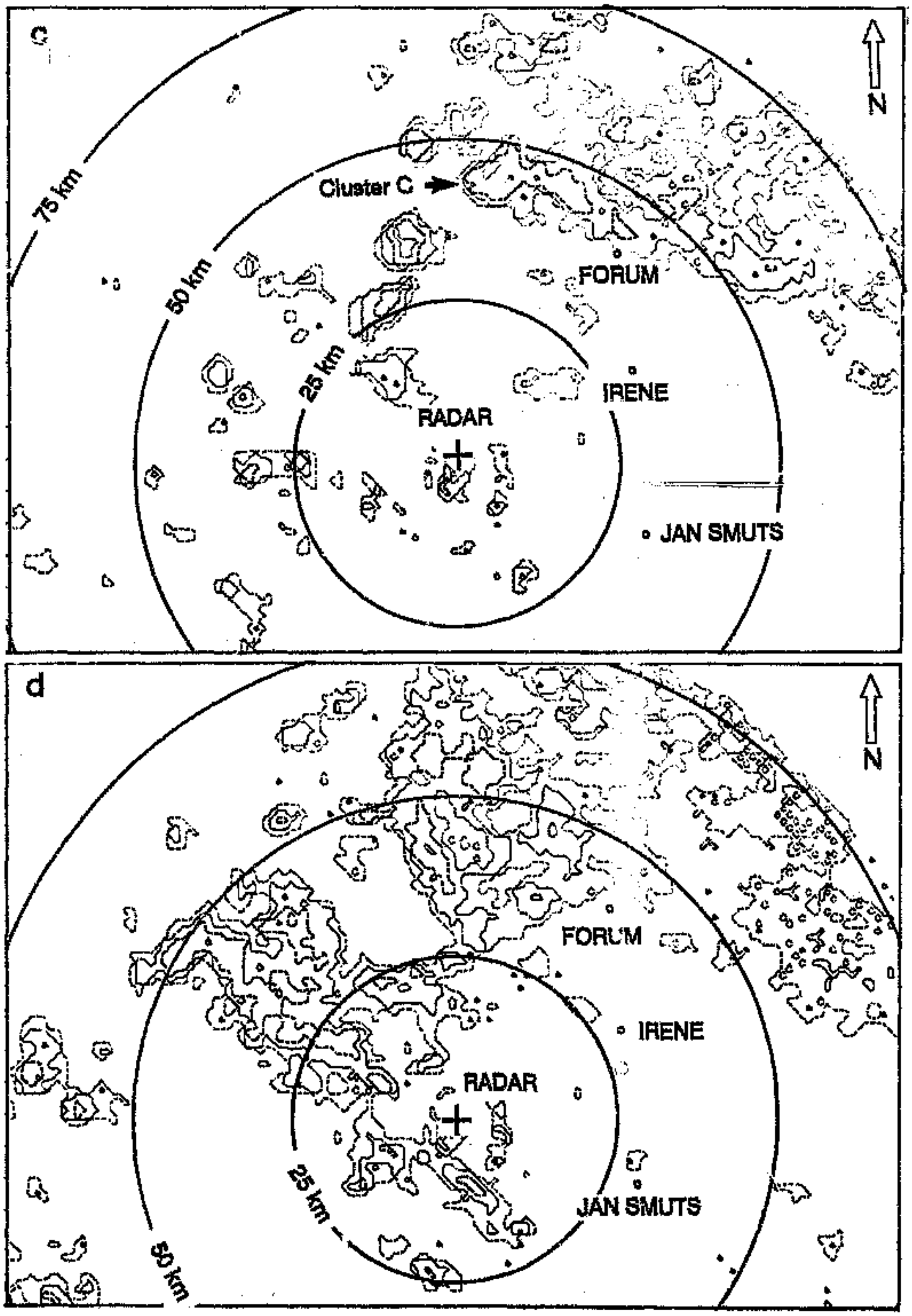

Figure 4.4: PPI radar scans at minimum elevation angle show[illegible] the storm of 26 December 1987. The position of the radar is [illegible]ated by a cross, open circles indicate automatic rain gauges. Is[illegible] indicate reflectivity levels of 23,3, 30,0, 40,0, 50,0 and 60,0 dBZ res[illegible]ctively. Radar range rings are at 25 km intervals.
c: 15:41, d: 16:25

Fig. 4.4b). The rain rate peak of 18 $mm.h^{-1}$ was measured at the gauge at 15:30 at which time a 50,0 dBZ core is evident to the northeast of the Forum gauge (marked 'A' in Fig. 4.4b). Cluster C continued to grow as several smaller clusters developed ahead, and ultimately merged with cluster C (Fig. 4.4c, d). By 16:25 (Fig. 4.4d) the storm had developed into a large multicellular complex with an area of approximately 3000 km^2. At this stage most of the echo area was concentrated to the northwest of the radar. Again the discrepancy between the V-ATI and gauge rain rates appears to be related to the fact that the gauge registered only low intensity sections of the storm rather than the average rain rates in the storm as a whole.

The V-ATI rain rate was better matched with the gauge rain rate for a storm that occurred on 27 December 1987. This storm has been previously described in some detail emphasising the synergistic effects of cloud merging (Gomes *et al.*, 1989). There appears to have been a considerable degree of convective activity on the afternoon of 27 December 1987 with the development of at least two major storm systems. Radar operations only commenced at 17:00 by which time hail reports received from a network of voluntary observers indicated that a storm system had already traversed the radar coverage area. This first storm system is evident in the rain gauge records with first rains being registered at the Jan Smuts gauge at 15:32. The second storm system began to develop in the late afternoon and became apparent by 18:00 as several cell clusters in the southwestern quadrant of the radar coverage area (Fig. 4.5a). By 18:33 these clusters had merged to form three distinct cell groupings (Fig 4.5b). The Jan Smuts gauge first began registering rain at 18:33 at which time a large cell grouping (marked 'Cluster B' in Fig. 4.5b) is seen to have been just west of the gauge. By 19:40 (Fig. 4.5c) the cell cluster had traversed the Jan Smuts gauge at which an average rain rate of 13,62 $mm.h^{-1}$ was measured. This cell cluster did not appear to produce the rain measured at the Irene gauge, which was generated by a cluster that developed in the wake of the other three later in the afternoon (Cluster D in Fig. 4.5d). Similarly the rain registered at the Forum gauge was produced by a separate cell cluster (cluster 'E' in Fig. 4.5d). This is an important point because average gauge rain rates compare well with average V-ATI rain rates. Each gauge, however, appeared to have registered rain from a different cell cluster and it is only by averaging rain rates from the three gauges that the V-ATI rain rate is matched.

Fig. 4.4b). The rain rate peak of 18 mm.h^{-1} was measured at the gauge at 15:30 at which time a 50,0 dBZ core is evident to the northeast of the Forum gauge (marked 'A' in Fig. 4.4b). Cluster C continued to grow as several smaller clusters developed ahead, and ultimately merged with cluster C (Fig. 4.4c, d). By 16:25 (Fig. 4.4d) the storm had developed into a large multicellular complex with an area of approximately 3000 km^2. At this stage most of the echo area was concentrated to the northwest of the radar. Again the discrepancy between the V-ATI and gauge rain rates appears to be related to the fact that the gauge registered only low intensity sections of the storm rather than the average rain rates in the storm as a whole.

The V-ATI rain rate was better matched with the gauge rain rate for a storm that occurred on 27 December 1987. This storm has been previously described in some detail emphasising the synergistic effects of cloud merging (Gomes *et al.*, 1989). There appears to have been a considerable degree of convective activity on the afternoon of 27 December 1987 with the development of at least two major storm systems. Radar operations only commenced at 17:00 by which time hail reports received from a network of voluntary observers indicated that a storm system had already traversed the radar coverage area. This first storm system is evident in the rain gauge records with first rains being registered at the Jan Smuts gauge at 15:32. The second storm system began to develop in the late afternoon and became apparent by 18:00 as several cell clusters in the southwestern quadrant of the radar coverage area (Fig. 4.5a). By 18:33 these clusters had merged to form three distinct cell groupings (Fig 4.5b). The Jan Smuts gauge first began registering rain at 18:33 at which time a large cell grouping (marked 'Cluster B' in Fig. 4.5b) is seen to have been just west of the gauge. By 19:40 (Fig. 4.5c) the cell cluster had traversed the Jan Smuts gauge at which an average rain rate of 13,62 mm.h^{-1} was measured. This cell cluster did not appear to produce the rain measured at the Irene gauge, which was generated by a cluster that developed in the wake of the other three later in the afternoon (Cluster D in Fig. 4.5d). Similarly the rain registered at the Forum gauge was produced by a separate cell cluster (cluster 'E' in Fig. 4.5d). This is an important point because average gauge rain rates compare well with average V-ATI rain rates. Each gauge, however, appeared to have registered rain from a different cell cluster and it is only by averaging rain rates from the three gauges that the V-ATI rain rate is matched.

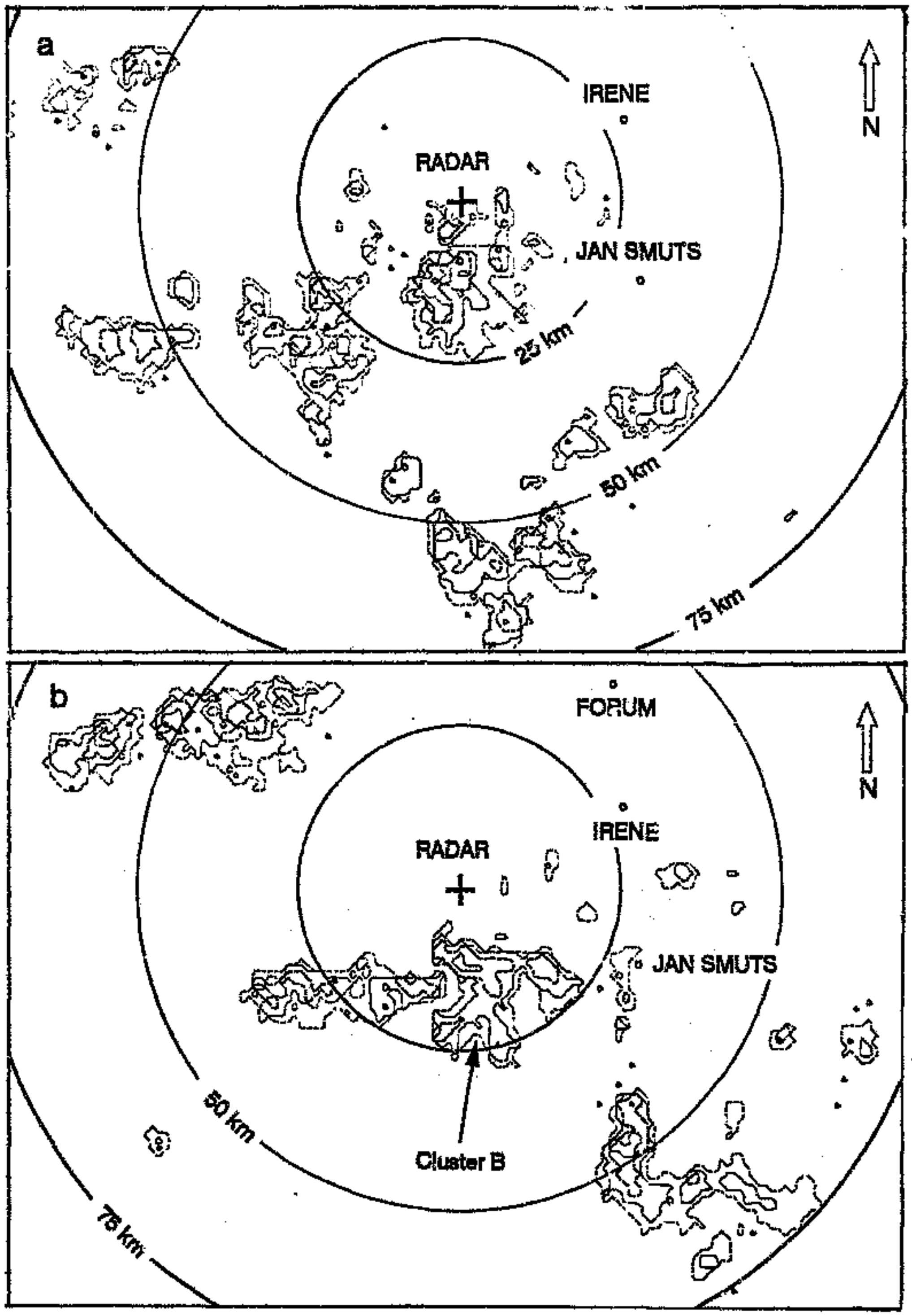

Figure 4.5: PPI radar scans at minimum elevation angle showing the storm of 27 December 1987. The position of the radar is demarcated by a cross, open circles indicate automatic rain gauges. Isolines indicate reflectivity levels of 23,3, 30,0, 40,0, 50,0 and 60,0 dBZ respectively. Radar range rings are at 25 km intervals.
a: 18:00; b: 18:33

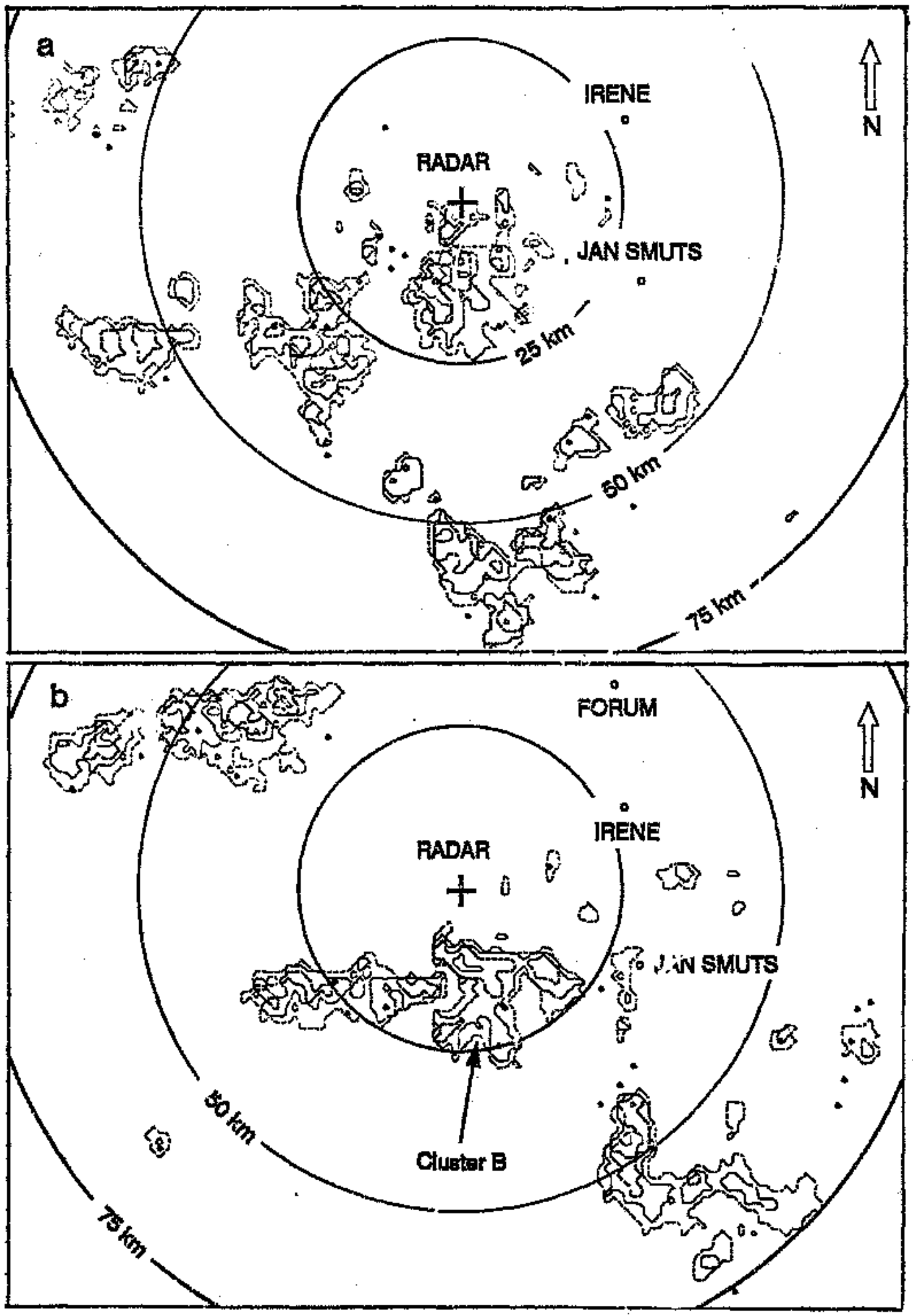

Figure 4.5: PPI radar scans at minimum elevation angle showing the storm of 27 December 1987. The position of the radar is demarcated by a cross, open circles indicate automatic rain gauges. Isolines indicate reflectivity levels of 23,3, 30,0, 40,0, 50,0 and 60,0 dBZ respectively. Radar range rings are at 25 km intervals.
a: 18:00; b: 18:33

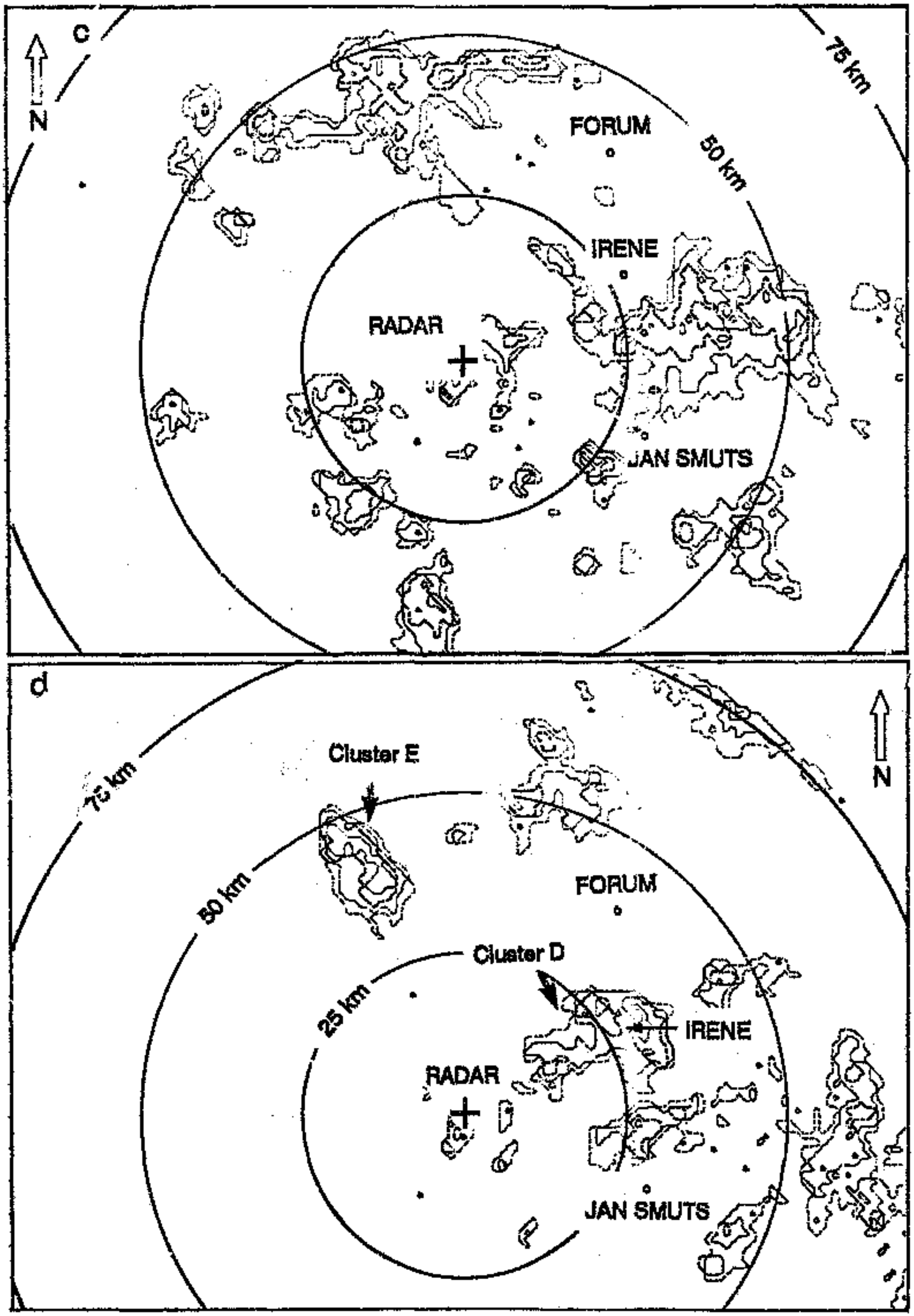

Figure 4.6: PPI radar scans at minimum elevation angle showing the storm of 27 December 1987. The position of the radar is demarcated by a cross, open circles indicate automatic rain gauges. Isolines indicate reflectivity levels of 23,3, 30,0, 40,0, 50,0 and 60,0 dBZ respectively. Radar range rings are at 25 km intervals.
c: 19:40; d: 20:51

The best comparison between gauge rain rates and V-ATI rain rates is evident for a storm system that occurred on 10 November 1987. The measurement error obtained using the quadratic *Z-R* V-ATI relationship was some 2 per cent. The storm on 10 November 1987 displayed characteristics of a squall line storm exhibiting a large areal coverage and producing rain and hail over a widespread area (Gomes and Held, 1988). The areal coverage exceeded 3000 km² at stages during the lifetime of the storm. The relationship between the gauge rain rates and the V-ATI rain rates is significant both from the measurement accuracy point of view but also from the fact that rain measured at each of the gauges originated from the same storm system. Thus each gauge indicates rain rates evolving during different stages of the storm lifetime. The position of the storm is shown is shown for four half-hourly intervals from 15:05 to 16:35 as a series of PPI scans (Fig. 4.6a, b).

The results from the storm of 10 November 1987 provide encouraging results but no concrete verification of the accuracy of the ATI technique. In fact it seems likely that all the storms in the series of twenty could have been analysed in a similar way and appropriate reasons shown as to why the V-ATI rain rates are either good or a poor estimates of gauge rain rates. The most unambiguous verification would appear to be the V-ATI - gauge rain rate comparisons for the season as a whole. This suggests in turn, that the assessment of seasonal rainfall volumes is possibly the best application of ATI based radar rainfall measurement. In addition the approach would adequately serve the purpose of assessing global changes in rainfall patterns using spaceborne radar as proposed for TRMM (Rosenfeld, 1990). For operational measurement of rainfall there is not sufficient evidence to suggest that the ATI approach will offer a more accurate means of radar rainfall measurement than the conventional *Z-R* approach.

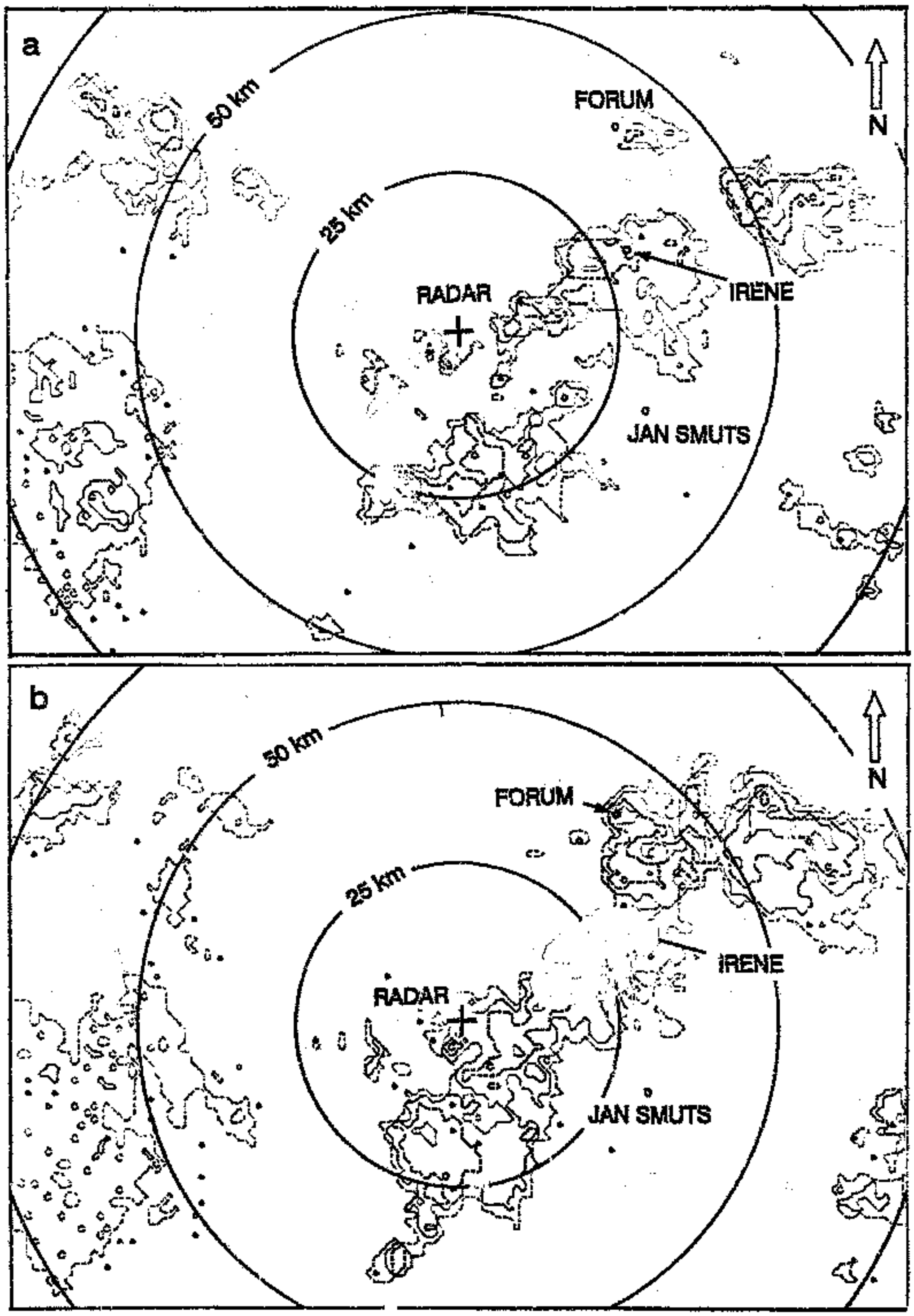

Figure 4.6: PPI radar scans at minimum elevation angle showing the storm of 10 November 1987. The position of the radar is demarcated by a cross, open circles indicate automatic rain gauges. Isolines indicate reflectivity levels of 23,3, 30,0, 40,0, 50,0 and 60,0 dBZ respectively. Radar range rings are at 25 km intervals.
a: 15:05; b: 15:34

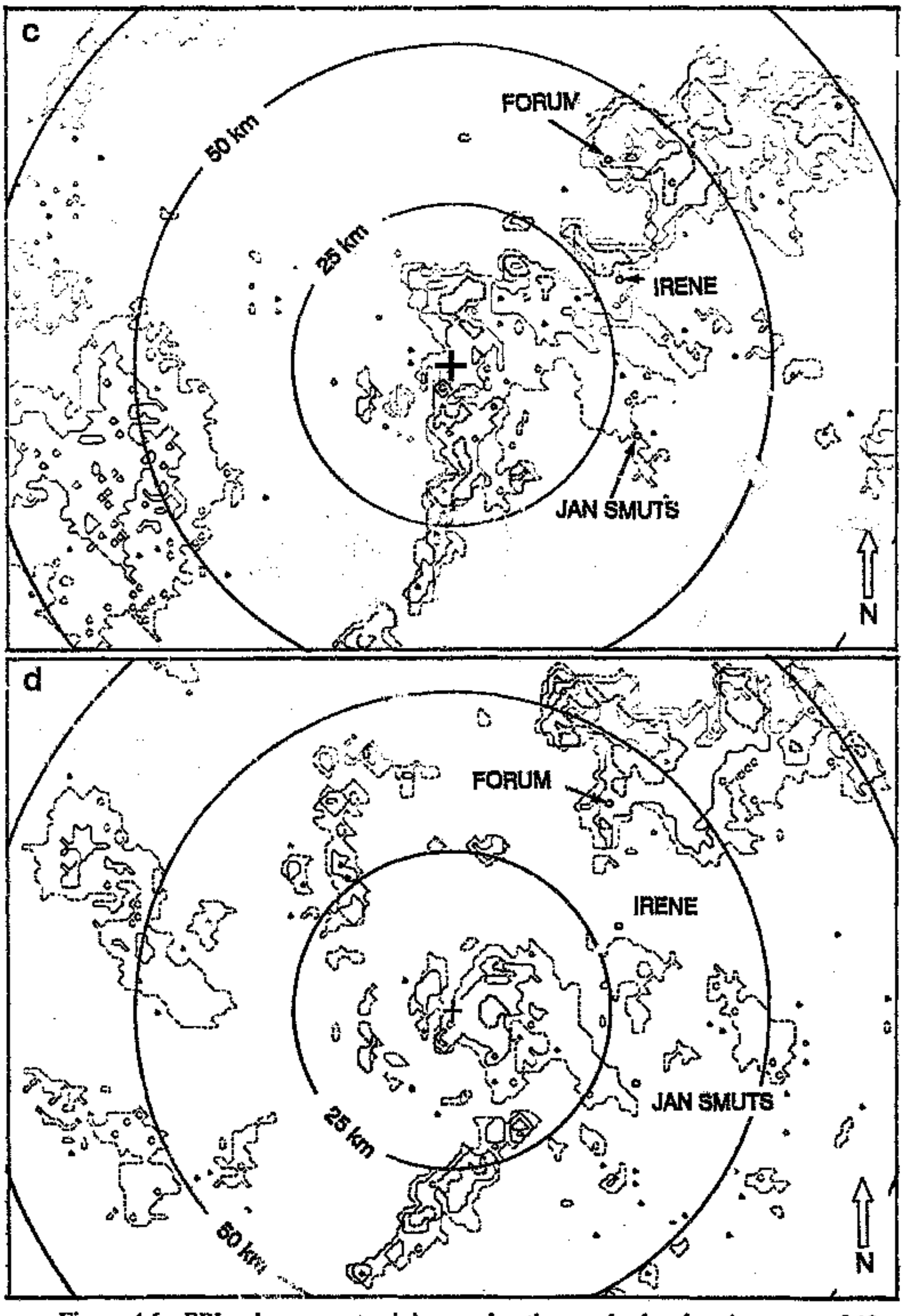

Figure 4.6: PPI radar scans at minimum elevation angle showing the storm of 10 November 1987. The position of the radar is demarcated by a cross, open circles indicate automatic rain gauges. Isolines indicate reflectivity levels of 23,3, 30,0, 40,0, 50,0 and 60,0 dBZ respectively. Radar range rings are at 25 km intervals.
c: 16:05; d: 16:35

Summary

In this chapter the ATI method of radar rainfall measurement has been investigated. Various V-ATI relationships have been determined using radar data from an S-Band weather radar. Different methods of area time integration were investigated and, on the basis of both practical considerations and the fact that the approach provided the most reasonable estimate of average ground-based rain rates, the scan by scan method of area time integration has been deemed optimal. The sensitivity of the V-ATI relationship to changes in the Z-R relationship has also been considered with changes in the Z-R relationship having been seen to introduce varying degrees of measurement error. The quadratic Z-R relationship appears to be most appropriate in determining radar estimated rain volume because the increase in equivalent rain rate with increasing dBZ is far less dramatic when using the quadratic Z-R than for either the linear Z-R or for the 25 $mm.h^{-1}$ split Z-R relationship.

V-ATI rain rates have also been compared to gauge rain rates for twenty selected storms days in an attempt to verify the validity of the derived V-ATI relationship. While the average rain rate values (calculated using the equivalent rain rate thresholds) were well estimated by average V-ATI rain rates, severe discrepancies were evident for individual storm days. An attempt was made to explain some of the discrepancies by showing how rain gauges failed to adequately reflect average rain rates over the entire areal coverage of the storm but this was hindered by very limited ground truth data. The need to average ground-based rainfall measurements above the equivalent rain rate threshold in order to match the V-ATI rain rate estimates indicated the need for optimisation of the ATI approach. In the following chapter the possibility of optimising the V-ATI relationship will be investigated.

****

The area-time integral (ATI) method of radar rainfall measurement has been investigated in this chapter. The scan-by-scan approach to integrating area with respect to time has been used to derive a radar estimated rain volume versus ATI (V-ATI) relationship. Comparisons between ATI derived rain rates and those measured at the ground for twenty selected storms indicate the need to optimise the V-ATI relationship. Several approaches to optimising the V-ATI relationship will be investigated in the following chapter.

CHAPTER 5

OPTIMISING THE V-ATI RELATIONSHIP

Introduction

It was shown in the previous chapter that relatively good agreement can be reached between seasonally averaged rain rates derived from the V-ATI relationship and rain rates measured at the ground, provided the ground-based rain rate measurements are averaged above the equivalent rain rate threshold. The implications of having to adjust ground-based rain measurements to match those measured by radar immediately render the ATI technique inaccurate and inhibit any potential operational applicability. Documented results of other ATI studies do not include comparisons between V-ATI derived rain rates and those measured at the ground. This study suggests that in spite of a strong correlation between radar estimated rain volume and the ATI, significant discrepancies may exist between V-ATI rainfall estimates and those measured at the ground.

There have been several attempts at 'fine-tuning' the average *Z-R* relationship in various radar rainfall measurement studies. These studies suggest that a similar approach could be used to refine the V-ATI relationship. In this chapter the possibility of optimising the V-ATI relationship will be considered. Firstly, the role of thresholds will be examined to determine how different threshold specifications may alter the V-ATI relationship, and secondly a probability matching method similar to that used in refining *Z-R* relationships will be investigated as an additional means of V-ATI optimisation.

The Role of Thresholds

The choice of 'most appropriate reflectivity threshold (MART)' received considerable attention in early V-ATI studies for storm systems over North Dakota. Several qualitative considerations in selecting MART have already been discussed in Chapter 1. It stands to reason that quantitative criteria in establishing a MART should be simply that threshold generating the most accurate estimates of rainfall volume. It was argued for V-ATI studies over North Dakota that 'most appropriate' should in fact mean most independent with respect to $\overline{R}$ (Doneaud *et al.*, 1984b). In this study, however, 'most appropriate' has been interpreted to mean that which most accurately estimates average rain rate at the ground, rain volume notwithstanding.

Criteria on which to base MART selection have also been addressed in V-ATI studies for the eastern Transvaal. An increasing threshold implies a decreasing storm area, but as the storm area decreases the value of the coefficient K in the V-ATI relationship must increase to maintain the rainfall volume. In the event of K increasing too rapidly, determination of the threshold level becomes critical, demanding precise radar calibrations. In effect this nullifies one of the major appeals of the ATI approach, *viz.* that it can be used to make accurate rainfall estimates even with a poorly calibrated radar (NPRP, Draft Seasonal Report, 1990/91).

In the North Dakota V-ATI studies the threshold value was defined as the echo value above which total echo area is integrated for ATI. It is important to note that this definition effectively means that only the ATI should be determined above a given threshold whereas RERV will always be determined using the minimum radar reflectivity value. If the V-ATI relationship is viewed graphically, it becomes evident that measuring the echo area above a given threshold will lead to a reduction in ATI i.e. ATI will move closer to 1 (Fig. 5.1). The RERV will not change so the overall effect will be to steepen the slope of the V-ATI relationship. If the V-ATI relationship overestimates rain rates, therefore, introducing a threshold into RERV calculations rather than ATI will lead to lower V-ATI derived rain rates. This view is supported by a conclusion that was drawn from a rain storm model study, that increasing ATI thresholds would lead to inaccuracies in the ATI technique because of the increasing dependence of *average* rain rate on *maximum* rain rate as higher thresholds are used to define the echo area (Rogers, 1989).

For this reason it was decided to experiment with threshold values, introducing a threshold to the ATI measurements and then into RERV. The results of these two approaches are compared as functions of ATI and RERV (Fig. 5.2). If the curves are considered below the point at which the three curves intersect it can be seen that for a given ATI the lowest corresponding rain volume is associated with the curve representing the RERV threshold. In other words at an ATI value of 10 $km^2.h$ the corresponding ATI derived average rain rates

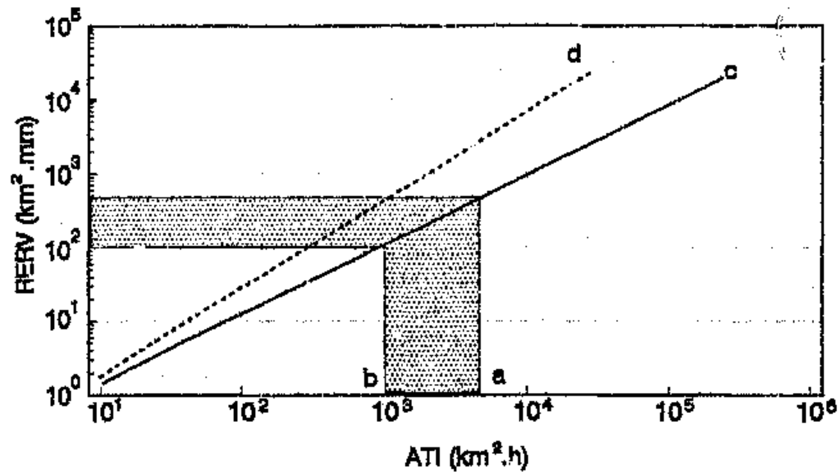

Figure 5.1: Schematic illustration of the effect of introducing a threshold into the ATI in deriving a V-ATI relationship.

lower for the rain volume threshold curve. Above the point of intersection the situation is reversed. The mean ATI is just below this point of intersection and generates lower average rain rates in conjunction with the V-ATI curve derived from RERV values above a given threshold. In line with the criteria set for MART by Doneaud *et al.* (1984b) introducing a threshold into the ATI measurements does indeed lead to $\overline{R}$ becoming independent but at an unrealistically high $\overline{R}$. Not only are average rain rates overestimated using this approach but the low slope values imply that V-ATI derived rain rates will change only marginally even with significant changes in ATI. Gauge derived rain rates from the twenty selected storm days discussed in the previous chapter are compared to different V-ATI derived rain rates on a histogram (Fig. 5.3). The V-ATI rain rates have been derived from data in which firstly thresholds were specified for ATI, then RERV and finally in which no thresholds were specified. It is immediately apparent from the graph that introducing a threshold into the ATI cause rain rate estimations to become virtually independent of the value of the ATI. This is reflected in the fact that rain rates for the individual storms remain virtually unchanged despite significant changes in the ATI (Fig. 5.3). With thresholds introduced into the RERV calculations, the V-ATI derived rain rates are more sensitive to changes in the ATI and to actual rain rates measured at the ground.

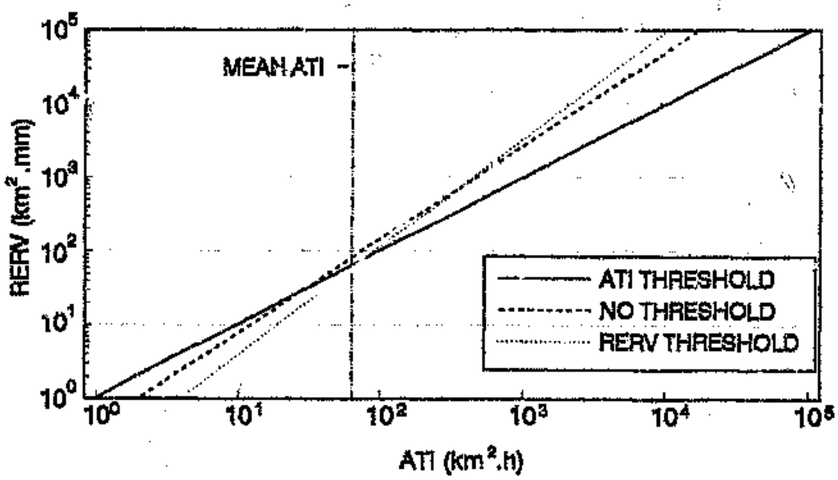

Figure 5.2: Comparison of V-ATI relationships illustrating the effects of introducing a threshold into either ATI or RERV.

The V-ATI derived rain rates when averaged over the twenty storms are remarkably close to the equivalent gauge-derived average rain rates. The V-ATI relationship derived from data in which a threshold was specified for the RERV calculations is seen to marginally underestimate the average gauge rain rate whereas the V-ATI relationship derived from data in which no thresholds were set marginally overestimates the gauge average. This would suggest that the ATI should always be derived from all the information available above the minimum detectable radar signal and that some scope exists in manipulating the threshold used in the RERV calculation for improving the accuracy of the V-ATI relationship. By the same token there are limitations in setting thresholds for the RERV calculations. It is not possible to simply set higher and higher threshold values for RERV until V-ATI derived rain rates match those measured at the ground as significant information will be lost on the areal extent of the rainfall field. Although the selection of a suitable RERV threshold may improve V-ATI estimates of rain rates measured at the ground this approach would not appear to be the best way of optimising the V-ATI relationship.

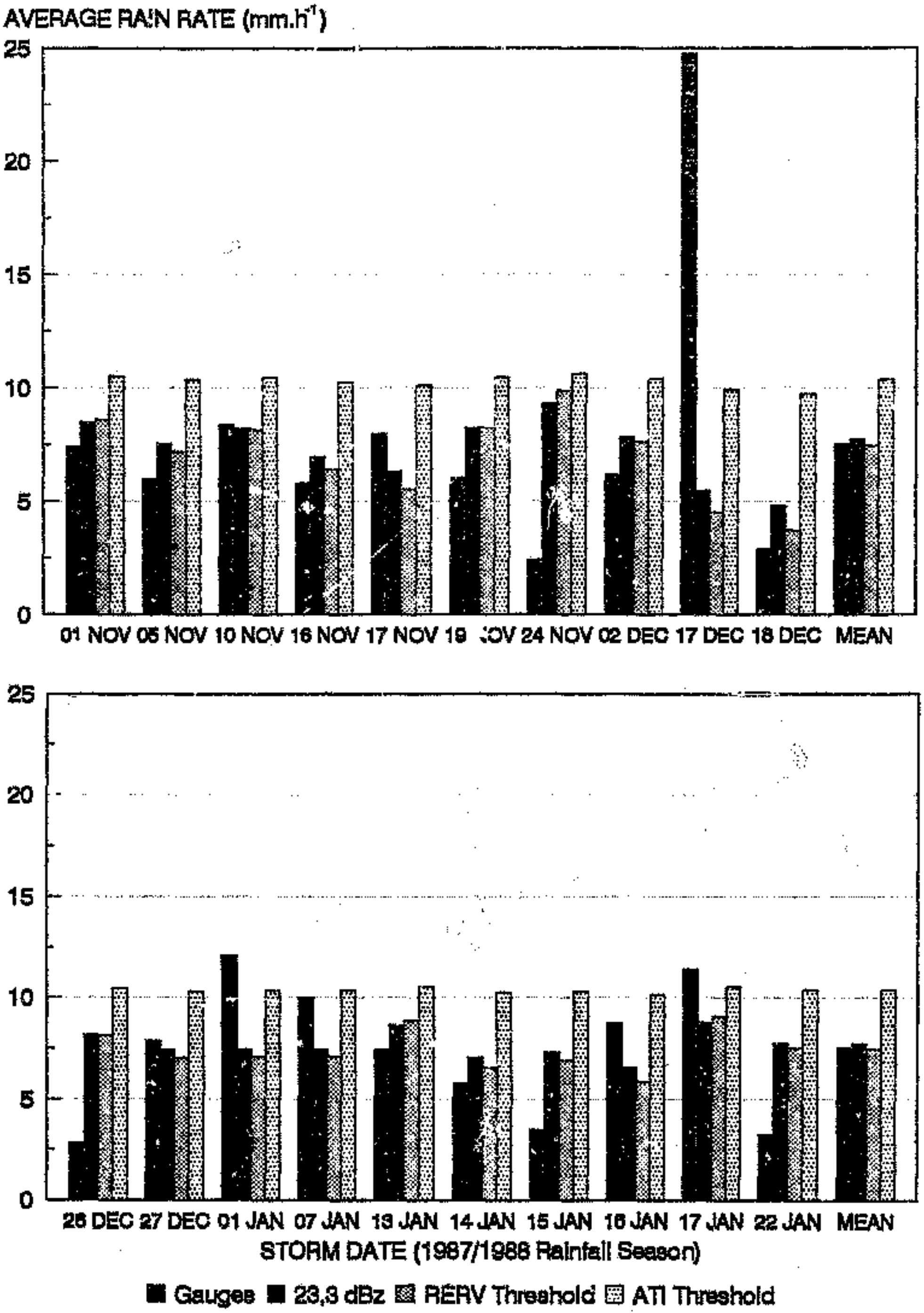

Figure 5.3: Histogram of gauge and V-ATI rain rates for twenty storms selected from the 1987/88 rainfall season to illustrate the V-ATI relationship to thresholds introduced into either the ATI measurements or the RERV calculations or specifying no threshold at all.

A Probability Matching Method for Optimising the V-ATI Relationship

It has been argued earlier that the fundamental basis of the success of the ATI approach is the fact that rain rate probability functions (pdf's) are essentially constant. Comparative gauge and radar derived rain rate pdf's would appear to be a useful analytical tool, therefore, in identifying reasons for the observed discrepancies between gauge and V-ATI rain rates. Rain rate pdf's have been estimated by calculating the percentage frequency of occurrence for different rain rate classes. Rain rate classes were determined by using the rain rate equivalents (derived from the quadratic Z-R relationship) of the respective radar iso echoes. The percentage contribution of each iso echo area to the total storm area has been determined and used as an estimate of the radar-derived pdf (Fig. 5.4). Ground-based rain rate pdf's were then determined for both the disdrometer and the rain gauge data (Fig. 5.5a, b). Although the 1986/87, the 1987/88 and the 1988/89 rainfall season pdf's are seen to be very similar the 1989/90 rainfall season pdf differs fairly markedly, especially in the lower rain rate classes. Similar discrepancies are not evident, however, in the disdrometer data (Fig. 4.11b). The major difference between the two disdrometer derived pdf's is in the higher rain rate classes where a maximum rain rate of 196 mm.h^{-1} was recorded during the 1989/90 season. A maximum rain rate of only 86 mm.h^{-1} was recorded during the subsequent rainfall season.

Average gauge-derived, radar-derived and disdrometer-derived pdf's were then compared. The most obvious difference between the radar derived and the ground-based rain rate pdf's is that there is no equivalent rain rate class for the radar data between 0,1 and 0,96 mm.h^{-1}. This is because the lowest radar signal is 23,3 dBZ with an equivalent rain rate of 0,96 mm.h^{-1}. In addition, the radar pdf has a markedly higher frequency of occurrence in all the other rain rate classes extending to the rain rate class of 320 mm.h^{-1}.

The most likely cause of the significant difference between the radar and the ground-based rain rate pdf's is rain drop evaporation between the height of the radar beam and the ground. Evaporation as a function of height and rain intensity at cloud base has been investigated in storm systems over the northern Orange Free State, by comparing area and time integrated rain volumes at cloud

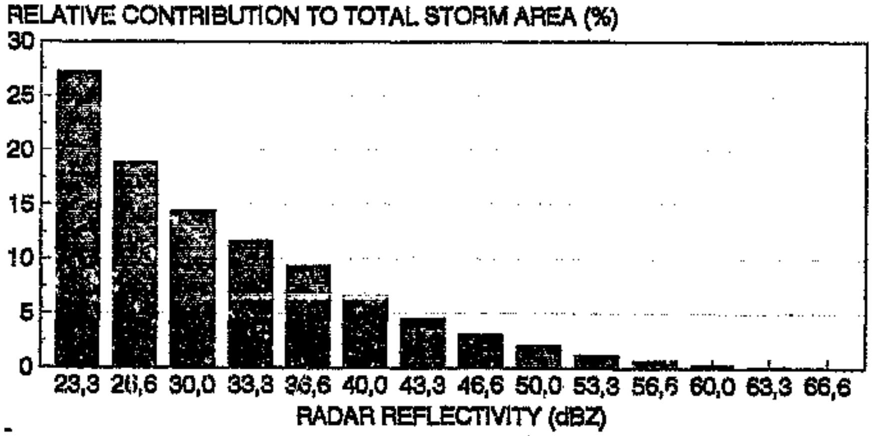

Figure 5.4: Relative percentage contributions of iso echo areas to total storm area derived for all storm days used in establishing the V-ATI relationship.

base with those derived at lower levels. Findings showed that about 50 per cent of rain with a small lifetime peak intensity (1,0 mm.h^{-1}) will be evaporated over a fall distance of 1 km, with all the rain being evaporated over a fall distance of 1,6 km; about 25 per cent will be evaporated for a rain rate peak of 10 mm.h^{-1} over a fall distance of 1 km with 50 per cent being evaporated over a fall distance of 1,6 km and about 15 per cent for a rain rate peak of 80 mm.h^{-1} over a fall distance of 1 km, 30 per cent over a fall distance of 1,6 km (Rosenfeld and Mintz, 1988). At a minimum elevation angle of 1,9° the height of the radar beam above the rain gauges varies between 1 (over the Irene gauge) and 1.6 km (over the Forum gauge) implying a substantial difference between rain measured at the height of the radar beam and rain measured at the ground and providing some explanation for observed differences in the radar-derived and gauge-derived rain rate pdf's.

Probability matching methods have been employed by several authors in deriving 'climatologically tuned' *Z-R* relationships (Calheiros and Zawadzki, 1988; Atlas *et al.*, 1990b; Rosenfeld, 1991). The *Z-R* relationship is essentially tuned by having the reflectivity probability distribution *P*(*Z*) replicate *R* over a predetermined space-time climatic domain (Atlas *et al.*, 1990b). This work suggests that a similar probability matching approach could be applied to the V-ATI relationship. The V-ATI approach differs somewhat in that instead of matching percentile pairs as has been done in fine tuning *Z-R* relationships, rain

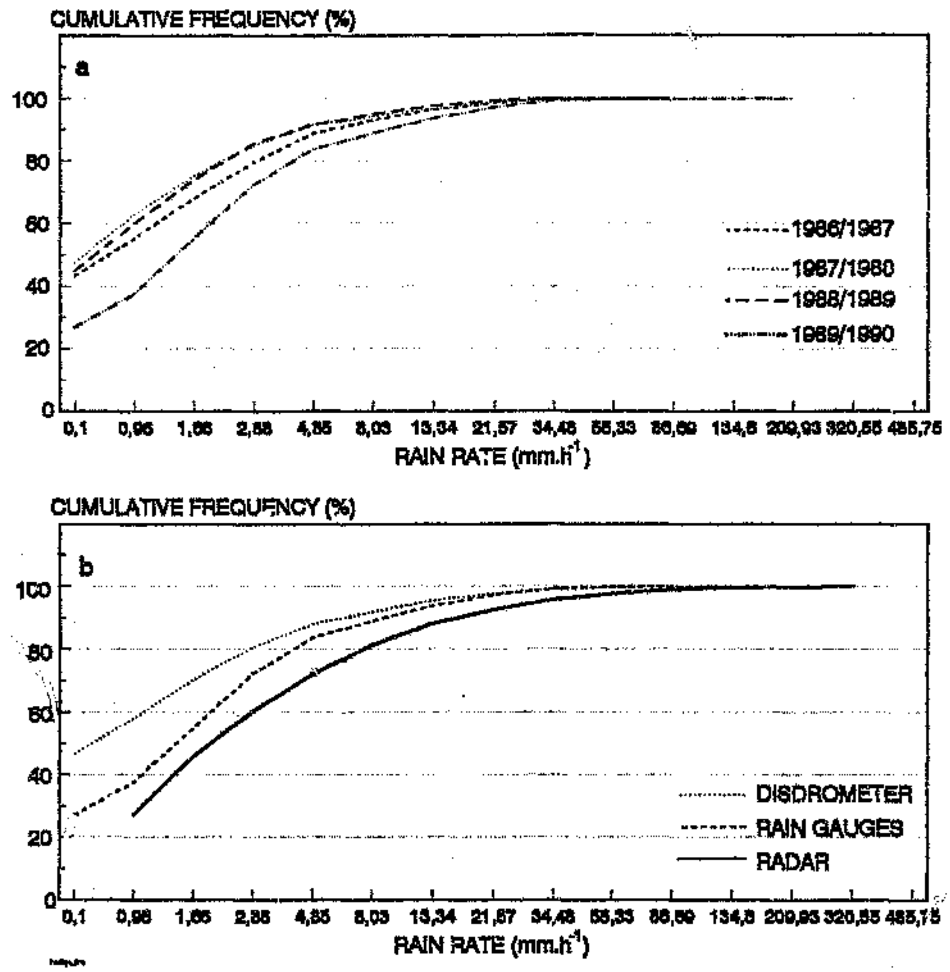

Figure 5.5: Estimates of rain rate probability density functions derived from:
a: Automatic rain gauge data
b: Disdrometer data, mean rain gauge data and radar data

rate class pairs have been matched. The rain rate class pairs have been matched by building a weighting factor into the derivation of the V-ATI relationship. Thus if the percentage difference between the gauge-derived and the radar-derived rain rate is say five per cent, the weighting factor will reduce (increase) the radar derived pdf to match that of the gauge-derived pdf. As there is no frequency representation in the first rain rate class for the radar-derived pdf, the relative frequencies of the first two gauge classes were summed and then the radar pdf weighted according to the combined gauge values.

The V-ATI relationship was then optimised by incorporating the weighting factor in each rain class interval. In other words, instead of simply taking the area of the radar echo and multiplying it by time and equivalent rain rate to get rainfall volume, the product was also multiplied by the appropriate weighting factor. An optimised V-ATI relationship has been derived using the quadratic *Z-R* relationship and weighting the relative contributions of each echo area according to the pdf correction factor. The regression parameters are shown in Table 5.1. A significant improvement is evident in the correlation coefficient ($r = 0.99$) and the V-ATI rain rate of 3,31 mm.h^{-1} gives a measurement error of about 24 per cent when compared to the seasonal average rain rates in Table 4.5 (Chapter 4).

The V-ATI relationship derived using the above probability matching approach still suffers a serious shortfall. There has already been a long discussion of storm characteristics in which the conclusion was drawn that the steeper slopes of the earlier derived V-ATI relationships were in fact appropriate to storms that developed over the Transvaal Highveld. In addition it can be seen from Figure 5.2 that the closer the slope is to unity the less dependent average rain rate will be on storm area. In fact average rain rate will only change by some 1,5 mm.h^{-1} with a change in ATI of 1000 km^2.mm. The reason for this flattening of the slope would appear to be related to the fact that higher rain intensity areas (in excess of 56,6 dBz) will be weighted to 0 by virtue of the fact that they do not appear in the gauge derived pdf's. It appears, therefore, that the weighting factor should be constant for all rain rate classes so that the exponential increase of rain rate with increasing dBZ is reflected in the V-ATI relationship.

The average discrepancy between the radar-derived and the gauge-derived pdf's is 48,5 per cent. Using this as a standard weighting factor in all the rain rate classes a V-ATI relationship was determined. Regression parameters are given in Table 5.2. The slight reduction noted in the correlation coefficient ($r = 0,96$) suggests that much of the variance in the V-ATI relationship is introduced by the higher intensity radar echo areas. The moderately steeper slope of 1,2 is consistent with earlier theoretical considerations and implies that the V-ATI relationship is sensitive to and will reflect changes in the ATI. The V-ATI rain rate of 4,11 mm.h^{-1} gives a measurement error of some six per cent when compared to the seasonal mean rain rate. This suggest that an optimised V-ATI

Table 5.1: Regression parameters for a V-ATI relationship derived from probability-weighted RERV calculations in different rain rate class intervals.

K	b	Correlation coefficient (r)	V-ATI derived average rain rate $mm.h^{-1}$
2,67	1,06	0,99	3,31

relationship of $V = 1{,}77\,(ATI)^{1,2}$ would provide the most accurate estimate of rain volumes from convective storms over the Transvaal Highveld (Fig 5.6).

Concluding Remarks

Validating the V-ATI relationship has proven to be the most difficult part of this study. While encouraging results have been obtained from the comparisons between ATI and gauge rain rates, the study has been severely limited by a lack of ground truth data. The conclusions that can be drawn from the study are that the ATI approach offers a useful and potentially accurate means of assessing the volume of rain that falls within the effective rainfall measurement range of the radar for the duration of a rainfall season. In light of the objectives set for the Tropical Rain Measuring Mission (TRMM) this finding should be seen as encouraging. Results obtained from the spaceborne radar that will be used in TRMM will be used to assess whether climatic change is being manifested in seasonal and spatial changes in rainfall patterns. The precise calibrations normally required in effecting accurate radar rainfall measurements will not be possible on the TRMM radar. The results of this study suggest that the radar rainfall measurement technique that has been proposed for TRMM, which is based on the principle of the ATI technique, may generate accurate rainfall estimates regardless.

It has been suggested that V-ATI relationships may well change from season to season. As mentioned in Chapter 1, these changes offer academic interest regarding changes in the efficiency of rain-producing storm systems. It would make an interesting and useful study to investigate changes in the V-ATI relationship from season to season and to relate these changes to observed changes in meteorological variables. By the same token the robustness of a given

Table 5.2: Regression parameters for a V-ATI relationship derived from a standard probability-weighting derivation of RERV across all the rain rate class intervals

K	b	Correlation coefficient (r)	V-ATI derived average rain rate mm.h^{-1}
1,77	1,2	0,96	4,11

V-ATI relationship in measuring rainfall from one season to the next also requires investigation. Suggestions are that an acceptable experimental approach would be to define a rain gauge network that did not necessarily cover every spatial variation in rainfall over the radar coverage area but simply ensured that the pdf of a host of different rain rates were accurately recorded. Under these circumstances information from sparse rain gauge networks could be used effectively in enhancing the accuracy of radar-derived rainfall estimates.

Finally the operational applicability of the ATI technique as a radar rainfall measurement technique needs to be considered. The question simply cannot be answered with available information. The spatial resolution of the ground-based rainfall measurements meant that it was not possible to distinguish an individual storm cluster and assess the accuracy of the ATI in determining the rainfall yield from that cluster. The approach that was used in this study, namely to determine the V-ATI relationship on the basis of a scan-by-scan integration technique requires that all radar echo within the effective rainfall measurement range of the radar be included in the ATI. This does not readily facilitate using the ATI technique to measure rainfall over a given geographical area such as a catchment. The conventional *Z-R* approach would probably be a better approach under such circumstance. There is nothing to suggest, however, that the ATI technique cannot be used to assess the rainfall volume within the effective rainfall measurement range of the radar on any given storm day. Information available for this study was simply insufficient in validating the accuracy of such an approach.

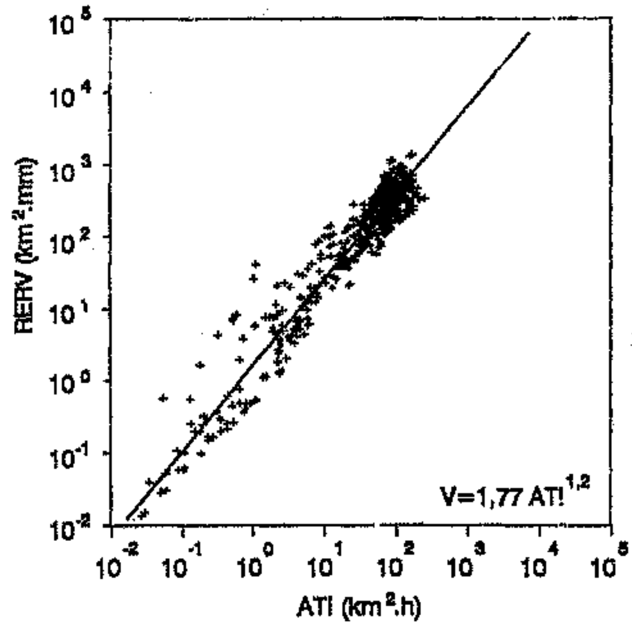

Figure 5.6: Optimised V-ATI relationship for radar-based convective rain measurement over the Transvaal Highveld.

Summary

In this chapter different methods of optimising the V-ATI relationship have been investigated. The intorduction of thresholds into either ATI or RERV in determining V-ATI relationships was also investigated to identify the most appropriate reflectivity threshold (MART). It has been argued that introducing a threshold to the ATI at iso levels above the 23,3 dBZ echo essentially defeats the object of the exercise because the slope of the V-ATI relationship is consequently reduced to near unity. As soon as the slope is near unity, average rain rate calculations become independent of the ATI. Theoretical considerations based on documented characteristics of Highveld convective storms suggest that larger, longer lived storms are likely to have larger rainfall volumes than smaller, short duration storms. Steeply-sloped V-ATI relationships for convective storms over the Transvaal Highveld are thus consistent with documented storm characteristics. Introducing a threshold to RERV causes the slope of the V-ATI curve to steepen and ensures that average rain rate estimations are sufficiently sensitive to changes in the ATI.

Finally the V-ATI relationship has been optimised by matching radar-derived and gauge-derived probability density functions. The optimisation process made use of an averaging weighting factor in each rain rate class. An optimised V-ATI relationship of $V = 1,77\,(ATI)^{1,2}$ has been determined for convective storms over the Transvaal Highveld which when compared to the average seasonal rain rate gave a measurement error of about 6 per cent.

****

The V-ATI relationship has been optimised in this chapter. Introducing equivalent rain rate thresholds into ATI and RERV respectively, was initially investigated as a means of V-ATI optimisation. As this method proved to be an unsatisfactory approach a probability matching method based on comparing rain gauge and radar-derived rain rate pdf's was used to optimise the V-ATI relationship. In the final chapter the conclusions drawn in each of the chapters will be consolidated to conclude the study as a whole.

SECTION IV

CONCLUSIONS

CHAPTER 6

CONCLUSIONS

The measurement of convective rainfall using a conventional S-Band weather radar has been examined in this dissertation. The dissertation has been divided into two main sections, each examining a different aspect of radar rainfall measurement. The first of these sections has been a study of drop size distributions that occur in convective rain over the Transvaal Highveld and the second an investigation of a particular technique of radar rainfall measurement known as the area-time integral (ATI). Radar rainfall measurement is dependant on the use of a *Z-R* relationship which empirically relates the strength of the return signal on the radar to rain rate intensity. The main aim of the first section has been to establish an average *Z-R* relationship for convective rain over the Transvaal Highveld and to develop an understanding of the way changing drop size distributions effect the *Z-R* relationship. The aim of the second section has been to derive an appropriate *V-ATI* relationship for convective rainfall over the Transvaal Highveld and to verify and refine the accuracy of that relationship.

1. Drop-Size Distributions

1.1. Drop-size distributions (DSDs) have been measured using a Joss-Waldvogel raindrop disdrometer, an electro-mechanical device that counts the numbers of drops in a range of size distributions impacting on a styrofoam body. The disdrometer has been operated for two consecutive rainfall seasons in conjunction with a tipping bucket rain gauge. Rainfall totals measured by the tipping bucket have been compared to those measured by the disdrometer indicating a tendency for the disdrometer to underestimate rainfall totals during periods of very high rain rates. Although the disdrometer is capable of resolving several hundred drops a second there still appears to be instrument 'dead time' when smaller drops are not registered during periods of very high rain rates.

1.2. Due to the importance of assessing temporal variability of DSDs in a study of this nature, Waldvogel's (1974) parameterisation scheme has been used. The parameterisation scheme is based on the assumption that the exponential distribution adequately describes a given DSD. Thus the DSD can be quantified in terms of the intercept value, N_0 and the slope of the distribution, Λ. N_0 and Λ as well as corresponding radar reflectivity factor, rain rate and liquid water content have been calculated from measured DSDs on a minute-by-minute basis. In plotting the temporal variation of N_0 and Lambda various kinematic and microphysical processes have been identified and related to evolving DSDs. Drop sorting effects are clearly evident in convective rain with resultant DSDs having relatively fewer smaller drops with higher numbers of large drops and leading to rain rate overestimates when using the average Z-R relationship.

1.3. 'Jumps' in the temporal pattern of N_0, which have been described by other authors, have also been identified in the DSD data. Characteristics of the storm in which an N_0 jump was identified suggest that N_0 jumps may be related to the rapid collapse of the thunderstorm updraught. DSDs measured in stratiform rain, in the absence of updraughts, appear to represent equilibrium between drop growth and drop disintegration effects generating an underestimate of rain rate when using the average Z-R relationship.

1.4. Changing DSDs have been shown to markedly influence the accuracy of radar measured rainfall. Radar estimated rainfall can both overestimate and underestimate actual rainfall depending on the DSD. An average Z-R relationship of $Z = 245\ R^{1,4}$ has been calculated by least squares linear regression on logarithmic values from disdrometer data collected during 1989/1990 and 1990/1991. In addition a quadratic fit Z-R relationship of $Z = 2,35 + 1,36(\log R) + 0,09(\log R)^2$ has been calculated and separate Z-R relationships of $Z = 539\ R^{1,3}$ and $Z = 242\ R^{1,37}$ have been calculated for rain rates greater than and less than 25 mm.h^{-1} respectively. The tendency for Λ to become constant when rain rates approach 100 mm.h^{-1} has been seen in $\Lambda - R$ relationships with a similar tendency in $\Lambda - W$ plots. Λ tends towards a constant value when liquid water content values exceed 1,2 g.m^3.

2. The ATI Method of Radar Rainfall Measurement

The ATI method of radar rainfall measurement proposed by Doneaud *et al.* (1981, 1984a, 1984b, 1987, 1988) has been the focus of the applied radar rainfall measurement section of the dissertation. The ATI approach is based on correlations between the areal coverage of a storm and its duration and the rainfall volume produced by that storm. Various *V-ATI* (rainfall volume versus area time integral) relationships have been determined for convective rain over the Transvaal Highveld using radar data from an S-Band weather radar.

2.1. Different methods of area time integration have been investigated and, on the basis of both practical considerations and the fact that the approach provided the most reasonable estimate of average ground-based rain rates, the scan by scan method of area time integration has been deemed optimal. The sensitivity of the *V-ATI* relationship to changes in the *Z-R* relationship has also been considered with changes in the *Z-R* relationship having been seen to introduce varying degrees of measurement error. The quadratic *Z-R* relationship appears to be most appropriate in determining radar estimated rain volume because the increase in equivalent rain rate with increasing dBZ is far less dramatic when using the quadratic *Z-R* than for either the linear *Z-R* or for the 25 $mm.h^{-1}$ split *Z-R* relationship.

2.2. Introducing thresholds into either ATI or RERV in determining *V-ATI* relationships was also investigated to identify the most appropriate reflectivity threshold (MART). It has been argued that introducing thresholds into ATI at iso levels above the 23,3 dBZ echo essentially defeats the purpose of the exercise because the slope of the *V-ATI* relationship is thereby reduced to to near unity. As soon as the slope is near unity average rain rate calculations become independent of the ATI. Theoretical considerations based on documented characteristics of Highveld convective storms suggest that larger, longer lived storms are likely to have larger rainfall volumes than smaller, short duration storms. Steeply-sloped *V-ATI* relationships for convective storms over the Transvaal Highveld are thus consistent with documented storm characteristics. Thresholding the RERV steepened the slope of the *V-ATI* still further, making average rain rate estimations far more sensitive to changes in the ATI.

2.3. V-ATI rain rates have also been compared to gauge rain rates for twenty selected storms days in an attempt to verify the validity of the derived *V-ATI* relationship. While the average rain rate values (calculated using the equivalent rain rate thresholds) were well estimated by average *V-ATI* rain rates, severe discrepancies were evident for individual storm days. An attempt has been made to explain some of the discrepancies by showing how rain gauges failed to adequately reflect average rain rates over the entire areal coverage of the storm, but the analysis in general was hindered by limited ground truth data. A conclusion that could be drawn from this section of the study, however, was that the quadratic *Z-R* relationship is probably the most suitable for use in ATI studies. Both the linear *Z-R* and the 25 mm.h^{-1} split *Z-R* generate what appear to be excessive estimates of rain rates at the higher radar reflectivity levels. To illustrate this point consider that the standard *Z-R* relationship estimates an equivalent rain rate for 63,3 dBZ of 652,08 mm.h^{-1}, the 25 mm.h^{-1} estimates an equivalent rain rate of 764,21 mm.h^{-1} and the quadratic *Z-R* estimates an equivalent rain rate of 320,55 mm.h^{-1}. On the other hand the highest rain rate recorded at the ground during the four rainfall seasons was 196 mm.h^{-1} measured by disdrometer during the 1989/1990 rainfall season with a maximum value of 210 mm.h^{-1} during the same rainfall season at one of the gauges within the rain gauge network.

2.4. Finally the *V-ATI* relationship has been optimised by matching radar-derived and gauge-derived probability density functions. The optimisation process made use of an average weighting factor in each rain rate class. Although not explicitly investigated the optimisation procedure used suggests that measurement errors introduced by use of an inappropriate *Z-R* could be lessened or even nullified by optimisation of the *V-ATI* relationship. An optimised *V-ATI* relationship of $V = 1{,}77\,(ATI)^{1,2}$ has been determined for convective storms over the Transvaal Highveld which, when compared to the average seasonal rain rate, gave a measurement error of approximately six per cent.

It has been shown in the course of this study that the ATI technique is a viable approach in effecting the measurement of rainfall using a conventional S-Band weather radar. The operational applicability of the technique could not be properly assessed due to inadequate ground-based rain rate measurements. For this reason conclusions regarding the advantages of the ATI technique over conventional *Z-R* techniques cannot be drawn. Nevertheless the fact that an optimised V-ATI relationship could be used to estimate seasonal average rain rates with a measurement error of only six per cent indicates great promise for the potential application of the ATI technique in measuring convective rainfall volumes over the Transvaal Highveld.

REFERENCES

Atlas, 1964: Advances in radar meteorology, *Advances in Geophysics*, Vol 10, Academic Press, New York.

Atlas, D. and Bell, T.L., 1991: The relation of radar to cloud area-time integrals and implications for rain measurements from space, *25th Conference on Radar Meteorology*, Paris, American Meteorological Society.

Atlas, D., Rosenfeld, D. and Short, D.A., 1990a: The estimation of convective rainfall by area integrals 1. The theoretical and empirical Basis, *Journal of Geophysical Research*, 95, 2153-2160.

Atlas, D., Rosenfeld, D. and Wolff, D.B., 1990b: Climatological tuned reflectivity-rain rate relations and links to area-time integrals, *Journal of Applied Meteorology*, 29, 1120-1135.

Austin, P.M., 1981: On deducing rainfall from radar reflectivity measurements, *Preprints, 20th Conference on Radar Meteorology*, , American Meteorological Society, 200-207.

Austin, P.M. and Geotis, S, 1979: Raindrop sizes and related parameters for GATE, *Journal of Applied Meteorology*,, 569-575.

Battan, L.J., 1973: *Radar Observations of the Atmosphere*, University of Chicago Press, Chicago.

Breuer, L.J. and Kreuels, R.K., 1976: Seasonal variation of precipitation parameters and a new hydrological field experiment in Western Germany, *Preprints: 17th Conference on Radar Meteorology*, American Meteorological Society, Boston, 432-437.

Byers, H.R., 1948: The use of radar in determining the amount of rain falling over a small area, *Transactions of the American Geophysical Union*, 29, 118-132.

Calheiros, R.V. and Zawadski, I., 1987: Reflectivity-rain rate relationships for radar hydrology in Brazil, *Journal of Climate and Applied Meteorology*, 26, 118-132.

Carbone, R.E. and Nelson, L.D., 1978: The evolution of raindrop spectra in warm-based convective clouds as observed and numerically modelled, *Journal of the Atmospheric Sciences*, 35, 2302-2314.

Carte, A.E., 1979: Sustained storms on the Transvaal Highveld, *South African Geographical Journal*, 61, 39-56.

Carte, A.E., 1981: Morphology of persistent in the Transvaal on 16/17 October 1978, *Beitrage zur Physik der Atmosfare*, 54, 86-100.

Caton, P.G.F., 1966: Raindrop-size distributions in the free atmosphere, *Quarterly Journal of the Royal Meteorological Society*, 92, 15-30.

Chisholm, A.J. and Renick, J.H., 1972: The kinematics of multicell and supercell Alberta hailstorms, *Alberta Hail Studies*, Research Council of Alberta, Report No. 72-2, Red Deer, Alberta, Canada, 24-31.

Chiu, L.S., 1988a: Estimating areal rainfall from rain area, in J.S. Theon and N. Fugono (eds), *Tropical Rainfall Measurements*, Deepak, Hampton, Va, 361-367.

Chiu, L.S., 1988b: Rain estimation from satellites: Areal rainfall-rain area relation, *paper presented at the 3rd Conference on Satellite Meteorology and Oceanography*, American Meteorological Society, Anaheim, California.

Doneaud, A.A., Smith, P.L., Dennis, A.S. and Sengupta, S., 1981: A simple method for estimating convective rain volume over an area, *Water Resources Research*, 17, 1676-1682.

Doneaud, A.A., Ionescu-Niscov, S., Priegnitz, D.L. and Smith, P.L., 1984a: The area-time integral as an indicator for convective rain volumes, *Journal of Climate and Applied Meteorology*, 23, 555-561.

Doneaud, A.A., Ionescu-Niscov, S. and Miller, J.R. (Jnr), 1984b: Convective rain rates and their evolution during storms in a semiarid climate, *Monthly Weather Review*, 112, 1602-1612.

Doneaud, A.A., Miller, J.R. (Jnr) and Johnson, L.R, 1987: The area-time integral technique to estimate convective rain volumes over areas applied to satellite data - a preliminary investigation, *Journal of Climate and Applied Meteorology*, 26, 156-169.

Doneaud, A.A., Makarau, A. and Johnson, L.R, 1988: A modified ATI technique for nowcasting convective rain volumes over areas, *Journal of Applied Meteorology*, 27, 491-502.

Doviak, R.J. and Zrnic, D.S., 1984: *Doppler Radar and Weather Observations*, Academic Press, Orlando.

Geotis, S.G., 1991: Relationship between echo area and rain flux in tropical rains, *25th Conference on Radar Meteorology*, Paris, American Meteorological Society.

Goddard, J.W.F., Cherry, S.M. and Bringi, V.N., 1982: Comparison of dual-polarisation radar measurements of rain with ground-based disdrometer measurements, *Journal of Applied Meteorology*, 21, 252-256.

Gomes, A.M. and Held, G., 1988: First progress report: Precipitation and airflow (PRAI) project, *CSIR Report EMA-C 8885*, Pretoria.

Gomes, A.M., O'Beirne, S. and Held, G., 1989: Second progress report: Precipitation and airflow (PRAI) project, *CSIR Report EMA-C 89126*, Pretoria.

Gomes, A.M. and Held, G., 1990: Final report: Precipitation and airflow (PRAI) project and Doppler radar data processing (DOPDATE) project, *CSIR Report EMA-C 90181*, Pretoria.

Gomes, A.M. and Held, G., 1991: First results from the CSIR dual-doppler radar system, *CSIR Internal Report EMA-I 9135*, Pretoria.

Held, G., 1980: Radar observations of an unusual cloud burst in South Africa, *Meteorologische Rundschau*, 33, 37-42.

Held, G. and Carte, A.E., 1980: Hailstorms in the Transvaal during January, 1975, in South Africa, *South African Geographical Journal* 61, 128-142.

Held, G. and van den Berg, H.J.C., 1977: A pre-frontal squall line on 14 November, 1975, *Archiv fur Meterologie, Geophysik und Bioklimatologie* Ser A, 26, 361-379.

Grosh, 1989: The highly non-linear aspects of Z-R and Vt-Z caused by raindrop terminal fall speeds, *Preprints of the 24 Conference on Radar Meteorology*, Florida, American Meteorological Society, 676-681.

Hardy, K.R., 1963: The development of raindrop size distributions and implications related to the physics of precipitation, *Journal of the Atmospheric Sciences*, 20, 299-312.

Harrold, T.W., English, E.J. and Nicholass, C.A., 1974: The accuracy of radar-derived rainfall measurements in hilly terrain, *Quarterly Journal of the Royal Meteorological Society*, 100, 331-350.

Heimbach, J.A. (Jnr) and Super, A.B., 1980: Rain gauge network requirements from a simulated convective complex weather modification experiment, *Journal of Applied Meteorology*, 19, 1176-1183.

Hill, F.F., Browning, K.A. and Bader, M.J. 1974: Radar and rain gauge observations of orographic rain over south Wales, *Quarterly Journal of the Royal Meteorological Society*, 107, 643-670.

Hodson, M.C., 1986: Raindrop-size distributions, *Journal of Climate and Applied Meteorology*, 25, 585-591.

Jones, D.M.A, 1956: Rainfall drop-size distribution and radar reflectivity, *Res. Rep. No. 6, Illinois State Water Survey*, Urbana.

Joss, J. and Gori, E.G., 1978: Shapes of raindrop size distributions, *Journal of Applied Meteorology*, 17, 1054-1061.

Joss, J. and Waldvogel, A., 1967: Ein spektrograph fur Niederschlagstropfen mit automatischer Auswertung, *Pure and Applied Geophysics*, 68, 682-688.

Joss, J. and Waldvogel, A., 1988: Precipitation measurement and hydrology, in Atlas, D., (ed), *Radar in Meteorology*, American Meteorological Society, Boston, 557-606.

Joss, J. and Waldvogel, A., 1989: Precipitation estimates and vertical reflectivity profile corrections, *Preprints: 24 Conference on Radar Meteorology*, Florida, American Meteorological Society, 682-688.

Kinnel, P.I.A., 1976: Some observations of the Joss-Waldvogel rainfall disdrometer, *Journal of Applied Meteorology*, 15, 499-502.

Kozu, T. and Nakamura, K., 1991: Rainfall parameter estimation from dual-radar measurements combining reflectivity profile and path-integrated attenuation, *Journal of Atmospheric and Oceanic Technology*, 8, 259-270.

Krauss, T.W. and Bruintjies, R.T., 1985: Physical properties of summertime convective clouds in the Bethlehem region of South Africa, *Preprints, Fourth World Meteorological Organisation Conference on Weather Modification*, Honolulu, World Meteorological Organisation.

List, R., 1988: A linear radar reflectivity-rain rate relationship for steady tropical rain, *Journal of the Atmospheric Sciences*, 45, 3564-3572.

List, R. and Gillespie, J.R., 1976: Evolution of raindrop spectra with collision-induced break-up, *Journal of the Atmospheric Sciences*, 33, 2007-2013.

List, R., Donaldson, N.R. and Stewart, R.E., 1987: Temporal evolution of drop spectra to collisional equilibrium in steady and pulsating rain, *Journal of the Atmospheric Sciences*, 44, 362-372.

Lopez, R.E., Atlas, D., Rosenfeld, D, Thomas, J.L., Blanchard, D.O. and Holle, R.L., 1988: Estimation of areal rainfall using the radar echo area time integral, *Journal of Applied Meteorology*, 28, 1162-1175.

Low, T.B. and List, R., 1982: Collision, coalescence and breakup of raindrops. Part 1: Experimentally established coalescence efficiencies and fragment size distributions in breakup, *Journal of the Atmospheric Sciences*, 39, 1591-1606.

Mader, G.N., 1979: Numerical study of storms in the Transvaal, *South African Geographical Journal*, 61, 85-98.

Mader, G.N., Neishlos, H., Saunders, M.W. and Carte, A.E., 1985: Some characteristics of storms on the Transvaal Highveld, *Journal of Climate*, 173-182.

Marshall, J.S and Palmer, W.McK., 1948: The distribution of raindrops with size, *Journal of Meteorology*, 5, 165-166.

Mason, B.J. and Andrews, J.B. 1960: Drop-size distributions for various types of rain, *Quarterly Journal of the Royal Meteorological Society*, 86, 346-353.

Neff, E.L., 1977: How much rain does a rain gauge gauge?, *Journal of Hydrology*, 35, 213-220.

NPRP, Draft Seasonal Report 1990/1991, submitted to the WRC.

O'Beirne, S. 1988: A case study of a squall line storm over the Transvaal Highveld, Unpublished Honours project, University of the Witwatersrand, Johannesburg.

Pasqualucci, F., 1982a: Drop-size distribution measurements in convective storms with a vertically-pointing 35 GHz doppler radar. Multi-parameter measurements of precipitation, *URSI Open Symposium*, Bournmouth, UK, URSI and IEE, 139-144.

Pasqualucci, F., 1982b: The variation of drop size distributions in convective storms: A comparison between theory and measurement, *Geophysical Research Letters*, 9, 839-841.

Preston-Whyte, R.A. and Tyson, P.D., 1988: *The Atmosphere and Weather of Southern Africa*, Oxford University Press, Cape Town.

Probert-Jones, J.R., 1962: The radar equation in meteorology, *Quarterly Journal of the Royal Meteorological Society*, 88, 485-494.

Raghaven, R. and Chandrasekar, V., 1991: Self consistent assessment of area time integral (ATI) technique for rainfall estimates using multi-parameter radar, *25th Conference on Radar Meteorology*, American Meteorological Society.

Richards, W.G. and Crozier, C.L., 1983: Precipitation measurements with a C-Band weather radar in southern Ontario, *Atmosphere-Ocean*, 21, 125-137.

Rogers, R.R., 1989: Average rain rate in a model rain storm, *Proceedings, 24th Conference on Radar Meteorology*, Miami, American Meteorological Society, 652-653.

Rosenfeld, D., 1991: Method to relate observed radar reflectivity to surface rainfall based on intensity distributions, *25th Conference on Radar Meteorology*, American Meteorological Society.

Rosenfeld, D. and Gagin, A., 1989: Factors governing the total rainfall yield from continental convective clouds, *Journal of Applied Meteorology*, 28, 1015-1030.

Rosenfeld, D. Atlas, D. and Short, D.A., 1990: The estimation of convective rainfall by area integrals 2. The height-area rainfall threshold (HART) method, *Journal of Geophysical Research*, 95, 2161-2176.

Rosenfeld, D. and Mintz, Y. , 1988: Evaporation of rain falling from convective clouds as derived from radar measurements, *Journal of Applied Meteorology*, 27, 209-215.

Sekhon, R.S. and Srivastava, R.C., 1971: Doppler radar observations of drop-size distributions in a thunderstorm, *Journal of the Atmospheric Sciences*, 28, 983-994.

Seliga, T.A. and Bringi, V.N., 1976: Potential use of radar differential reflectivity measurements at orthogonal polarisations for measuring precipitation, *Journal of Applied Meteorology*, [illegible], 69-76.

Seliga, T.A., Bringi, V.N. and Al-Khatib, H.H., 1981: A preliminary study of comparative measurements of rainfall rate using the differential reflectivity radar technique and a rain gauge network, *Journal of Applied Meteorology*, 20, 1362-1368.

Silver, S., 1951: *Microwave Antenna Theory and Design*, McGraw Hill, New York.

Srivastava, R.C., 1967: On the role of coalescence between raindrops in shaping their size distribution, *Journal of the Atmospheric Sciences*, 24, 287-292.

Srivastava, R.C., 1971: Size distributions of raindrops generated by their break-up and coalescence, *Journal of the Atmospheric Sciences*, 28, 410-415.

Srivastava, R.C., 1978: Parameterisation of raindrop size distributions, *Journal of the Atmospheric Sciences*, 35, 108-117

Steyn, P.C.L. and Bruintjies, R.T., 1990: Convective cloud characteristics for the Bethlehem area, *Water SA*, 16, 115-118.

Stout, G.E. and Mueller, E.A., 1968: Survey of the relationships between rainfall rate and radar reflectivity in the measurement of precipitation, *Journal of Applied Meteorology*, 7, 465-474.

Twomey, S., 1953: On the measurement of precipitation intensity by radar, *Journal of Meteorology*, 10, 66-67.

Waldvogel, A., 1974: The N_0 jump of raindrop spectra, *Journal of the Atmospheric Sciences*, 31, 1067-1078.

Wexler, R. and Atlas, D., 1963: Radar reflectivity and attenuation of rain, *Journal of Applied Meteorology*, 2, 276-280.

Wiesner, J., 1895: Beitrage zur Kenntnis des tropischen Regens, *Bericht Math. Nat. Kl.*, Wien, 104.

Willis, P.T. and Tattleman, P., 1989: Drop-size distributions associated with intense rainfall, *Journal of Applied Meteorology*, 28, 3-15.

Wilson, J.W., 1970: Integration of radar and rain gauge data for improved rainfall measurement, *Journal of Applied Meteorology*, 9, 489-497.

Wilson, J.W. and Brandes, E.A., 1979: Radar measurement of rainfall - a summary, *Bulletin of the American Meteorological Society*, 60, 1048-1058.

Woodley, W., Olsen, A.R., Herndon, A. and Wiggert, V., 1975: Comparison of gauge and radar methods of convective rain measurement, *Journal of Applied Meteorology*, 14, 909-928.

Wys, J., Williams, E.R. and Bas, R.L., 1989: Radar rainfall measurements and streamflow estimations in New England drainage basins, *Preprints, 24th Conference on Radar Meteorology*, Florida, American Meteorological Society, 654-659.

Young, K.C., 1975: The evolution of drop spectra due to condensation, coalescence and break-up, *Journal of the Atmospheric Sciences*, 32, 965-973.

Zawadski, I., 1984: Factors affecting the precision of radar measurements of rain, *Preprints, 22nd Conference on Radar Meteorology*, Zurich, American Meteorological Society.

Zawadski, I. and de Agostinho Antonio, M., 1986: Equilibrium raindrop-size distributions in tropical rain, *Journal of the Atmospheric Sciences*, 45, 3452-3459.